UNIVERSITY OF CALIFORNIA

Los Angeles

The host-pathogen interactions of the innate immune system

A dissertation submitted in partial satisfaction of the

requirements for the degree Doctor of Philosophy

in Molecular Biology

by

Elliot Woong Kim

2018

ABSTRACT OF THE DISSERTATION

Host-pathogen interactions of the innate immune system

by

Elliot Woong Kim

Doctor of Philosophy in Molecular Biology

University of California, Los Angeles, 2018

Professor Robert L. Modlin, Chair

Understanding host-pathogen interactions between microbes and the innate immune system will provide insight into the host defense pathways and microbial virulence factors. The macrophage (MΦ) is a sentinel of the innate immune system and serves as the first line of defense against microbial infection. The MΦ provides protection to the host by i) rapidly recognizing harmful pathogens, ii) internalizing pathogens to contain the infection and iii) clearing the pathogen from the host before the onset of disease. Here, we study effector pathways of the MΦ that combat invading pathogens in the host and determine their effects on the invading pathogen.

MΦ are a phenotypically heterogeneous immune subset that provides different functions in host defense. Previous studies in our laboratory have found that interleukin-15 (IL-15) induces a MΦ differentiation program in primary human monocytes (IL-15

MΦ) that express the vitamin D metabolism pathway. Vitamin D supplementation to these specialized immune subsets exhibited an antimicrobial response against mycobacteria *in vitro*. However, clinical trials that supplemented tuberculosis (TB) patients with vitamin D as an adjuvant have largely been unsuccessful *in vivo.* Therefore, we investigate whether vitamin D status prior to the onset of microbial infection would contribute to host defense. Our data demonstrates that vitamin D status during IL-15 MΦ differentiation bestows the capacity to mount an antimicrobial response against *Mycobacterium leprae*. These data suggest that future clinical trials that assess the relationship between vitamin D supplementation to mycobacterial infection will determine if vitamin D can provide prophylactic effects that are therapeutically beneficial.

Similarly to vitamin D, the bioactive form of vitamin A, all-trans retinoic acid (ATRA), triggers an antimicrobial responses against *M. tuberculosis in vitro.* However, high ATRA levels in humans' results in severe or even fatal side effects *in vivo.* Therefore, we investigate how the immune system regulates ATRA production at the site of TB disease. Our data demonstrates that dendritic cells express the vitamin A metabolism pathway, which converts the circulatory form of vitamin A, retinol, into ATRA. The dendritic cells subsequently release ATRA and induce vitamin A-dependent antimicrobial responses in neighboring monocytes and MΦ. Interestingly, this immune model has provided insight into the site of TB disease by showing that the dendritic cell-mediated retinol metabolism pathway is significantly diminished in the lung of active TB patients relative to normal lung. These data demonstrate a novel transcellular effector

pathway between dendritic cells and MΦ that contributes to the host defense against microbial infection.

Toxoplasma gondii is capable of infecting any nucleated cell *in vitro,* but MΦ are the first immune subset infected by *T. gondii* in mice *in vivo.* It is well known that both interferon-gamma-induced responses and MΦ functions are critical to controlling *T. gondii* infections in mice *in vivo.* Interferon-gamma induces the expression of two different families of immune loading proteins called the immunity-related GTPases (IRGs) and guanylate binding proteins (GBPs) that function to clear the parasite from the MΦ. However, *T. gondii* is equipped with secretory organelles called the rhoptries that inject ROP proteins into MΦ to modulate host cell functions. We have found a novel rhoptry pseudokinase effector, ROP54. Disruption of ROP54 demonstrates a 100-fold decrease in virulence in mice *in vivo* and increased GBP2 protein loading onto the parasite containing vacuole *in vitro*. Immunoprecipitation of ROP54 demonstrates that none of the known ROP effector proteins formed a complex with the pseudokinase, which suggests it may be a divergent effector protein. Collectively these data show that ROP54 is a novel virulence factor that evades a IFN-gamma-mediated immune response in MΦ and may be a potential drug target for the development of novel therapeutics.

The data presented in this thesis evaluates the efficiency of immune pathways against disease causing pathogens. The host-pathogen interaction from these models provides insight into microbial infection, which may help in the development of novel therapeutics and identification of drug targets. These data contributes to the importance of micronutrient supplementation and how it can help contain the spread of

mycobacterial-related diseases. Additionally we found a novel ROP effector protein that may be a potential drug target in toxoplasma infection.

The dissertation of Elliot Woong Kim is approved.

Lili Yang

John S. Adams

Marcus Horwitz

Kent L. Hill

Robert L. Modlin, Committee Chair

University of California, Los Angeles

2018

Dedication

First, I would to give my deepest thanks and gratitude to my mentor Robert L. Modlin. From the day I have joined the laboratory I have grown in every aspect of a scientist from writing, critical thinking to strategically planning experiments. I appreciate the freedom to explore the world of biological sciences with no restrictions, and providing me the opportunity to learn from my numerous mistakes. Thank you for opening the doors to your laboratory and allowing me to become a member of the Modlin research team. Deciding to be part of this laboratory was the best decision I have ever made!

Next, I would like to thank Dr. Philip T. Liu for being one of the most influential persons in my life. All the encouragement and assistance during my 9-year tenure at UCLA has given me a belief in myself that I never knew I had. I appreciate how you helped me develop my craft, achieve my goals as a scientist and even share a good laugh. My graduate career has truly been a memorable experience and would not be possible without all your support through the most difficult times.

Thank you Allan L. Chen for being my friend, basketball teammate and supervisor all at the same time. Your selflessness has been an inspiration and has been contagious in all the researchers you have trained. I wish you the best in all your future endeavors and all the happiness with Audrey!

Finally, I would like to give a special thanks to my mother. Your guidance has led me to live a life full of passion and excitement with everything I do. Thank you for being the most positive and motivating force in my life, and providing me with the constant love and care that has helped me become the man I am today. I do not know

how my future as a scientist will unfold, but I do know that as long as you are by my side I will never give up and strive to become the best that I can be.

TABLE OF CONTENTS

LIST OF FIGURES

Acknowledgements

Chapter 2 is a version of a manuscript that has been submitted. Rosane Teles generated confocal microscopy images. Salem Haile performed image flow cytometry.

Chapter 3 is a version of a manuscript that has been submitted. Avelino De Leon, Zhichun Jiang and Roxana Radu conducted experiments and acquired data. Adrian R. Martineau provided clinical samples, acquired and analyzed data. Edward D. Chan, Xiyuan Bai and Wen Lin Su provided clinical materials. Dennis Montoya analyzed bioinformatics data. Robert L. Modlin designed experiments. Philip T. Liu designed studies, analyzed data and wrote the manuscript.

Chapter 3 is a reprint of an article titled "The Rhoptry Pseudokinase ROP54 Modulates Toxoplasma gondii Virulence and Host GBP2 Loading" published in mSphere pii: e00045-16, 2016. Santhosh M. Nadipuram, Ashley L. Tetlow, William D. Barshop, Philip T. Liu, James A. Wohlschlegel were co-authors in this study.

All of the work described in the dissertation was directed by Robert L. Modlin.
This work was supported by the Philip Whitcome training grant (2015-2016).

VITA

2004-2009	**B.S Biology** **Ohio State University, Columbus** **Columbus, Ohio**
2009-2011	**Laboratory Assistant(Paul D. Benya)** **Orthopaedic Hospital Research Center, UCLA** **Los Angeles, CA**
2011-2013	**Laboratory Assistant(Philip T. Liu)** **Orthopaedic Hospital Research Center, UCLA** **Los Angeles, CA**
2011-2018	**Graduate Student Researcher(Robert L. Modlin)** **Molecular Biology Institute** **Los Angeles, CA**

Publications

Kim EW, Teles RMB, Haile S, Liu PT, Modlin RL (2018) Vitamin D status contributes to the antimicrobial activity of macrophages against *Mycobacterium leprae*. PLoS Negl Trop Dis 12(7): e0006608. https://doi.org/10.1371/journal.pntd.0006608

Wheelwright, M*., **Kim, E.W***., Inkeles, M.S., De Leon, A., Pellegrini, M., Krutzik, S.R., and Liu, P.T. (2014). All-trans retinoic acid-triggered antimicrobial activity against Mycobacterium tuberculosis is dependent on NPC2. J Immunol *192*, 2280-2290.

Kim, E.W., Nadipuram, S.M., Tetlow, A.L., Barshop, W.D., Liu, P.T., Wohlschlegel, J.A., and Bradley, P.J. (2016). The Rhoptry Pseudokinase ROP54 Modulates Toxoplasma gondii Virulence and Host GBP2 Loading. mSphere *1*.

Chen, A.L., **Kim, E.W**., Toh, J.Y., Vashisht, A.A., Rashoff, A.Q., Van, C., Huang, A.S., Moon, A.S., Bell, H.N., Bentolila, L.A*., et al.* (2015). Novel components of the Toxoplasma inner membrane complex revealed by BioID. MBio *6*, e02357-02314.

Beck, J.R., Chen, A.L., **Kim, E.W**., and Bradley, P.J. (2014). RON5 is critical for organization and function of the Toxoplasma moving junction complex. PLoS Pathog *10*, e1004025.

Nadipuram, S.M., **Kim, E.W**., Vashisht, A.A., Lin, A.H., Bell, H.N., Coppens, I., Wohlschlegel, J.A., and Bradley, P.J. (2016). In Vivo Biotinylation of the Toxoplasma Parasitophorous Vacuole Reveals Novel Dense Granule Proteins Important for Parasite Growth and Pathogenesis. MBio *7*.

Chen, A.L., Moon, A.S., Bell, H.N., Huang, A.S., Vashisht, A.A., Toh, J.Y., Lin, A.H., Nadipuram, S.M., **Kim, E.W**., Choi, C.P.*, et al.* (2017). Novel insights into the composition and function of the Toxoplasma IMC sutures. Cell Microbiol *19*.

Lee, Y.S., Hsu, T., Chiu, W.C., Sarkozy, H., Kulber, D.A., Choi, A., **Kim, E.W**., Benya, P.D., and Tuan, T.L. (2016). Keloid-derived, plasma/fibrin-based skin equivalents generate de novo dermal and epidermal pathology of keloid fibrosis in a mouse model. Wound Repair Regen *24*, 302-316.

Poster Presentations

Molecular Biology Institute (MBI) retreat 2016-2017
Dendritic cell metabolism of vitamin A triggers an innate antimicrobial response in *Mycobacterium tuberculosis*-infected macrophages

Molecular Biology Institute (MBI) retreat 2015-2016
The Rhoptry Pseudokinase ROP54 Modulates *Toxoplasma gondii* Virulence and Host GBP2 Loading.

Southern California Eukaryotic Pathogen Symposium (SCEP 2015)-2016
The Rhoptry Pseudokinase ROP54 Modulates *Toxoplasma gondii* Virulence and Host GBP2 Loading.

Seminar Presentations

2017 Pacific Tuberculosis Pathogenesis and Host-Response Research Retreat (PacTB)
Dendritic cell metabolism of vitamin A triggers an innate antimicrobial response in *Mycobacterium tuberculosis*-infected macrophages

Parasitology meeting (2016)
The Rhoptry Pseudokinase ROP54 Modulates *Toxoplasma gondii* Virulence and Host GBP2 Loading.

CHAPTER 1

Introduction

Host-pathogen interactions of the innate immune system

The two arms of the human immune system are the innate and adaptive immune systems. The innate immune system serves as the first line of defense against invading pathogens. The adaptive immune system provides a secondary antigen specific immune response and the development of memory. Host-pathogen interactions between the immune system and commensal flora have developed metabolic and homeostatic functions in the host. However, pathogenic relationships between the immune system and invading microbes have evolved defense mechanisms to protect the host from infection and disease. The immune system employs an array of host defense mechanisms that serve to rapidly recognize and clear harmful deleterious microbes from the host *in vivo*. This thesis will focus on understanding host-pathogen interactions of the innate immune system and deleterious microbes.

The innate immune system consists of multiple different immune subsets that collaborate together to eliminate invading microbes. These subsets are a conglomerate of highly evolved network of cells that cooperate to clear pathogens from the host. This network consists of dendritic cells, MΦ, neutrophils, eosinophils and keratinocytes in which each has distinct functions in host defense. Both primary human MΦ and dendritic cells reside within tissues throughout the body and respond immediately to the onset of infection. However, additional MΦ and dendritic cells can be derived at the site of infection from primary human monocytes that circulate in the blood and infiltrate the area. The differentiation and function of these immune subsets are determined by the cytokine profile of the microenvironment at the site of infection. The work of this thesis will investigate the immune responses of MΦ and dendritic cells and determine their effect against invading microbes.

This introductory chapter outlines previously established innate immune models that detail the link between pattern recognition receptor (PRR) activation and the differentiation of immune subsets and their functions. We will describe how the activation of TLR2/1 and NOD2 has revealed direct and indirect effector pathways of the immune response at the site of infection. In contrast, we will also describe how the activation of TLR2/1 has also been shown to inhibit immune responses against *M. leprae*. The observations from these studies led to the investigation of divergent MΦ phenotypes and functional profiles that correlate with the prognosis of leprosy patients.

These innate immune models have led to the investigation of host-pathogen interactions between MΦ/dendritic cells and harmful microbes. Here, we study the link between micronutrient metabolism pathways in immune subsets that contribute to the host defense against mycobacteria. We investigate how vitamin D status affects the differentiation and function of antimicrobial MΦ. Provide evidence that the transcellular metabolism of vitamin A by dendritic cells triggers an antimicrobial response in monocytes and MΦ against *M. tuberculosis*. Then we evaluated the status of vitamin A-mediated transcellular metabolism in the lung of active TB patients. Finally, we investigate the role of a novel effector protein of *T. gondii* that evades an immune loading protein in the MΦ. Despite the current knowledge of host-pathogen interactions, how innate immune effector pathways are regulated in the context of microbial infection remains unknown.

Pathogens

Mycobacterium tuberculosis

M. tuberculosis, the causative agent of TB, is the one of leading causes of death by a single infectious agent worldwide. Currently one-third of the world's population is infected and according to the Centers for Disease Control and Prevention (CDC) 10.4 million new *M. tuberculosis* infections occurs each year [1]. However only 10% of the infected population succumbs to active TB disease. TB is an easily transmissible disease because it spreads from person to person in aerosolized saliva droplets that contain the bacteria. *M. tuberculosis* infects the alveolar MΦ in the lung and is and an extremely virulent bacteria; as little as a single bacterium is sufficient to establish either latent or active disease. Latent TB patients do not present active disease and develop granulomas, which is a tight gathering of activated and inactivated MΦ, tissue-like MΦ, multinucleated giant cells and lymphocytes that surround the bacteria to contain the infection within the host [2]. Active TB patients present a spectrum of clinical manifestations that range from pulmonary cavitation to disseminated disease. Tuberculin skin tests and IFN-gamma release assays are used to determine whether someone is infected with *M. tuberculosis,* but these tests do not reveal the severity of the disease [3-5]. Additionally, the antibiotic regimen for active TB patients is expensive and requires 6-9 months of treatment. The emergence of drug resistant and totally drug resistant strains of *M. tuberculosis* has been found, which calls for the need for more research to find new treatments against the pathogen and disease [6,7].

We model the interactions between the host innate immune system and *M. tuberculosis* to gain insight into infection and disease. The vast majority of TB exposed individuals i) do not exhibit any form of the disease [8], ii) HIV+TB+ rapidly succumb to

disease [9,10] and iii) PET imaging shows that lymph nodes are different sizes in *M. tuberculosis* individuals [11], which collectively indicates that the immune system plays a significant role in regulating *M. tuberculosis* infection. Therefore, we are interested in the factors that influence MΦ function against *M. tuberculosis*. Mycobacteria reside in a phagosome within MΦ isolated from the cytoplasm [12]. Therefore, investigating the antimicrobial mechanisms against *M. tuberculosis* in the MΦ will provide insight into how the immune system controls *M. tuberculosis* infection. In contrast, understanding the evasion mechanisms of the bacteria in the MΦ will recapitulate the outcome of disease. The knowledge gained from these host-pathogen interactions will help in the development of effective therapies that may treat and prevent the spread of disease.

Mycobacterium leprae

Leprosy is a disease that primarily affects the skin and the causative agent of the disease is *M. leprae*. Leprosy is a dynamic condition that provides an opportunity to investigate mechanisms of the innate immune system that contribute to the host defense and pathogenesis of disease. Similarly to TB, the disease presents a spectrum of clinical manifestations and immunological responses that correlate with the prognosis of the patient. The two ends the clinical spectrum of leprosy disease are tuberculoid leprosy (T-Lep) and lepromatous leprosy (L-lep) [13]. T-lep patients represent the resistant end of the spectrum and present organized granulomas that localize around the bacilli to either restrict the growth or kill the bacteria [14-17]. The lesions in T-lep patients contain a small number of bacilli, but a strong cell-mediated immune response that is mediated by a Th1 cytokine and type II interferon. In contrast, L-Lep patients present the disseminated and

progressive form of the disease, which reflects a susceptibility to *M. leprae* infection. L-lep lesions contain a large number of skin lesions/bacilli, tissue damage and nerve damage. The lesions of L-lep patients show a humoral immune response in combination with a Th2 cytokine and type 1 interferon. Leprosy patients that demonstrate reversal reactions are showing an upgrade in L-lep patients towards the T-lep pole, which represents the process of *M. leprae* clearance from host [18]. The immune models found in leprosy have provided useful paradigms that contribute insight into the human immune response against mycobacteria infection.

Toxoplasma gondii

Toxoplasma gondii is an intracellular parasite and is a member of the phylum Apicomplexa [19]. The lifecycle of *T. gondii* can be briefly described as two different components: a sexual component that occurs in cats and an asexual component that occurs in any warm-blooded animal, also known as intermediate hosts. The ingestion of unwashed vegetables or cleaning the litter box of an infected cat is the mode of transmission to intermediate hosts [20]. These vehicles are contaminated with bradyzoites, the cyst form of the parasite, which have rigid cyst walls that allows the parasite to survive outside of the host and bypass the acidic nature of the stomach [20,21]. To establish infection, the bradyzoites convert into tachyzoites to initiate the acute infection. The tachyzoites infect the cells in the intestinal epithelium and spreads throughout the body by the blood stream [22]. The infection of intermediate hosts is usually asymptomatic, but severe disease only occurs in immunocompromised individuals. This suggests that the immune system is sufficient in containing the disease in check. However, once the

immune system is attenuated the clinical manifestations of toxoplasmosis ranges from encephalitis to fatal illness [19].

Tachyzoites are armed with secretory organelles that secrete proteins into target cells that evade the immune response of the host and to establish infection. The secretory organelles are the micronemes, rhoptries and dense granules and each serve distinct functions in either invasion of host cells or modulation of host cell functions [23]. The micronemes are located towards the apical end of the parasite and secrete adhesion proteins that attach parasite to target cells [24]. The rhoptries are bulb-shaped organelles that contain two types of proteins called the ROPs and RONs. The ROPs are positioned in the bulbous-end of the rhoptries and RONs are located towards the neck of the rhoptries. After the micronemes attach the parasite to the cell, the RONs are injected into the host-cell membrane and assemble the invasion machinery and initiate formation of the parasitophorous vacuole (PV) [25]. Simultaneously, the ROPs are injected into the host cytosol where they transit either to the host nucleus to alter host cell functions or to the outside of the PV to evade immune loading proteins that kill the parasite. The dense granule organelle constitutively secretes dense granule proteins (GRAs) into the milieu between the parasite and host cell to maintain the PV [26]. The GRAs have been associated with other functions such as acquiring nutrients and modulating the immune response of the host cell. The role of the parasite organelles has been established, but the proteins involved in *T. gondii* virulence remains largely unknown.

Innate immune models of mycobacteria

The main challenge of studying the dynamics of active TB is that infection and disease occurs in the lung. The lack of an animal model that fully recapitulates the human immune response and the difficulty in acquiring lung biopsies from active and latent TB patients has led us to use leprosy as a model to study the immune response against mycobacteria [27]. We will highlight the immune models developed from leprosy and how they project into immune models of TB disease.

Pattern Recognition Receptors (PRRs)

The role of innate immune system is to provide a variety of defense mechanisms that serve to protect the host from harmful pathogens. The immune response by PRRs is one mechanism by which the biochemical properties of invading pathogens can be recognized and trigger antimicrobial responses. The role of PRRs was discovered in drosophila where mutations in *toll* made the host more susceptible to fungal infections [28]. Later work then demonstrated that mutations in the expression of antimicrobial peptides made flies susceptible to bacterial infections [29]. Recently, activation of human PRRs has been described to trigger a variety of immune responses such as secreting cytokines to initiate the differentiation of immune subsets [30], triggering the expression of antimicrobial peptides [31,32], and inducing the formation of reactive oxygen species [33,34]. Here, we will describe the human PRR-mediated immune responses using mycobacteria as a model pathogen.

Toll-like receptor 2/1 in leprosy

Studies have shown that activation of different TLRs have demonstrated different immune responses by the innate immune system [35]. However, the differences in TLR activation between human and murine immune responses are unclear. Our laboratory research shows that TLR2/1 activation induced antimicrobial activity against *M. tuberculosis* in murine MΦ, human monocytes and human alveolar MΦ [36]. However, murine MΦ demonstrated that the antimicrobial response was dependent on nitric oxide (NO), but human monocytes/MΦ triggered an antimicrobial response that was independent of NO. The difference in immunological response between humans and mice corresponds with the different pathologies observed in TB disease [37-39].

To determine if the activation and regulation of TLR2 and TLR1 was critical to the human innate immune system, we took advantage of immunological spectrum observed in leprosy disease. Previous work from our laboratory found that heat-killed *M. leprae* robustly activated HEK293 cells expressing the TLR2/1 heterodimer [40]. The presence of the Th1 cytokines during TLR2/1 activation of primary human monocytes amplified the degree of pro-inflammatory cytokine release. In contrast, the presence of Th2 cytokines decreased TLR2 surface expression on primary human monocytes. Although the monocytes of T-lep and L-lep patients equally express TLR2 on the surface, only T-lep lesions sustained high levels of TLR2 and TLR1 protein levels at the site of disease. These data indicate that the activation and regulation of both TLR2 and TLR1 are influenced by the cytokine profile in the skin lesion. Therefore a more in-depth understanding the immune responses by TLR2/1 will provide insight into designing therapeutics that regulate TLR expression.

Since the expression of TLR2 and TLR1 correlates with the resistant form of leprosy disease, we hypothesized that activation of these PRRs triggered essential immune responses that contribute to the host defense. TLR activation has been characterized to regulate direct effector pathways such as phagocytosis, expression of antimicrobial peptides and release cytokines that activate the adaptive immune system [30,36,41-44]. However, how indirect effector immune pathways such as cellular differentiation have been associated with direct effector pathways is unknown. Previously established immune models demonstrate that an indirect effector pathway mediated by TLR2/1 activation, which induced the expression of IL-15 and granulocyte-macrophage colony-stimulating factor (GM-CSF) with their respective receptors [45,46]. Primary human monocytes treated with IL-15 differentiate into CD209+ phagocytic MΦ. In contrast, primary human monocytes treated with GM-CSF differentiated into CD1b+ dendritic cells (GM-DC), which secrete pro-inflammatory cytokines and activate naïve T-cells. Using leprosy as a model we found that in T-lep lesions both CD209+ and CD1b+ positive cells were present, but in L-lep lesions only CD209+ cells were detected. These data indicate that DC status is critical to host defense and the outcome of disease in leprosy.

One potential mechanism in which leprosy prevents DC differentiation and inhibits DC function in L-lep lesions is through leukocyte Ig-like receptor A2 (LILRA2) [47,48]. LILRA2 is expressed on monocytes and MΦ, which have been demonstrated to alter the innate and adaptive immune responses [49-51]. Interestingly, LILRA2 is highly expressed in L-lep lesions and absent in T-lep lesions, but LILRA2-activated monocytes treated with GM-CSF differentiate into CD14+ and CD40+ cells (data not shown). This

suggests that LILRA2 induces an aberrant GM-DC differentiation pathway that promotes the differentiation of alternative MΦ, which correlates with the progressive form of the disease. Therefore, recapitulating the differentiation pathways of immune subsets may provide insight into how *M. leprae* infection causes disease.

The cytokine profile of the microenvironment at the site of infection strongly influences the effector functions of MΦ. IL-10 is a Th2 cytokine that is present in L-lep lesions, secreted in response to TLR2/1 activation [45,52], and described to inhibit the differentiation and function of Th1 subsets [53,54]. Primary human monocytes that are treated with IL-10 differentiate into CD209+CD163+ macrophages (IL-10 MΦ), which demonstrate increased phagocytic function relative to IL-15 MΦ and resemble a foam cell [27]. IL-10 MΦ express scavenger receptors (scavenger receptor A and CD36) on the cellular surface that is critical to acquiring oxidized low-density lipoprotein (oxLDL) [27,55]. The IL-10 MΦ becomes a foam cell once the influx of oxLDL out competes the efflux of lipids [39]. The pathogenesis of several different microbes has been shown to thrive in lipid rich environments such as *M. tuberculosis* [38,56], *Chlamydia* [57], and *Toxoplasama* [58,59] that foam cells provide. Therefore, understanding the virulence factors and the immune modulation mechanisms that pathogens employ to create foam cells warrants further investigation.

Nucleotide-binding oligomerization domain 2 (NOD2)

Several studies have indicated that several PRRs activated with their respective ligands trigger overlapping immune responses [30,43]. However, recent research has revealed that NOD2 and TLR2 appear to initiate distinct immune responses against

microbial infection [60]. Clinical studies have shown that mutations in NOD2 demonstrate increased susceptibility to mycobacteria-related diseases [61,62] and have been associated with Crohn's disease [63,64]. These data suggest that NOD2 activation may serve a role in host defense against microbial pathogens. Previous studies in our laboratory have found that NOD2 activation induces an indirect effector pathway that is distinct from TLR2/1 activation.

NOD2 is an intracellular PRR that recognizes the pathogen associated molecular pattern (PAMP) muramyl dipeptide (MDP). Activation of NOD2 by either MDP or *M. leprae* triggered the release of IL-32 in which induced monocytes to differentiate into CD1b+ DCs independent of GM-CSF receptor [54]. We used leprosy as a model to associate where the NOD2 and IL-32 differentiation axis related with the immune response. Both NOD2 and IL-32 was only detected in T-lep lesions, but absent in the progressive form of the disease. In addition, monocytes treated with IL-32 demonstrated the ability to express a functional vitamin D-dependent antimicrobial pathway against *M. tuberculosis* [65]. These experiments provide evidence that IL-32-derived DCs are involved in the cell-mediated response against *M. leprae*.

CD1b+ DCs are classically known to be pathogen sensing and antigen-presenting cells that are central to the initiation and regulation of adaptive immune response [66]. However, the heterogeneity of DC subsets displays unique phenotypes and distinct functional properties [67]. Primary human monocytes titrated with IL-32 differentiated into CD1b+ DCs in a dose-dependent manner. The phenotype of IL-32-derived CD1b+ DCs was assessed, and increased protein abundance in HLA-ABC and CD86 was observed relative to GM-CSF-derived CD1b+ DCs [54]. Given the differences in MHC class-I

expression on IL-32-derived DCs versus GM-CSF-derived DCs, antigen presentation was investigated to determine a functional difference in naïve T-cell activation. Both DC subsets equally presented antigen and activated CD4+ T-cells. However, IL-32-derived CD1b+ DCs showed significantly higher levels of CD8+ T-cell proliferation and IFN-gamma release relative to GM-CSF derived DCs. Therefore, IL-32-derived DCs demonstrated the capacity to effectively cross-present antigen via MHC class-I to CD8+ T cells.

Micronutrients in disease

Although evidence indicates that the immune system is sufficient in containing the *M. tuberculosis* infection, the disease remains one of leading causes of death by a single infectious agent. Epidemiological studies have revealed that malnutrition is frequently observed in active TB patients [68]. Here, we will investigate the mechanisms of vitamin A and vitamin D in the innate immune system and how each provides host defense against mycobacteria.

Vitamin D

Vitamin D is a fat-soluble nutrient that humans primarily acquire through skin exposure to ultraviolet B from sunlight [69]. In the skin there are copious amounts of 7-dehydrocholesterol, and once exposed to light between 270-300 nanometers it is converted into vitamin D3 [70]. Vitamin D3 is converted by liver into the major circulatory form of the nutrient, 25-hydroxyvitamin D (25D3) bound to a chaperone known as vitamin D-binding protein (DBP) [71]. 25D3 is then metabolized in the liver by an enzyme

1-alpha-vitamin D hydroxylase (CYP27B1) into 1,25 dihydroxyvitamin D (1,25D3) the biologically active, hormonal form of the micronutrient. The metabolism of 25D3 into 1,25D3 is tightly regulated and known to have a significant role in maintaining calcium and phosphorus levels, which influence bone structure [72]. In humans, 25D deficiency has been associated with bone dysplasia diseases such as rickets [73]. The mechanisms and function of vitamin D in the human immune system will be addressed in this section and in Chapter 2.

Human epidemiological studies have correlated low vitamin D levels with susceptibility to TB disease [74,75]. TB patients in the pre-antibiotic era were treated in sanatoriums. At this facility patients were exposed to plenty of sunlight and were provided with micronutrient rich meals such as fish oils with cod livers [76-79]. With the absence of scientific data from this era, historical anecdotal evidence has only implied that vitamin D may have contributing effects against TB. However, the link between vitamin D and immune function was recently discovered [80].

Vitamin D and Antimicrobial Activity

TLR activation mediates effector functions of the innate immune system to provide host defense against *M. tubeculosis* infection [43]. Previous studies show that primary human monocytes treated with TLR2/1L, a triacylated lipopeptide (19kD), spontaneously release the pro-inflammatory cytokine IL-15 [45]. IL-15 treated primary human monocytes differentiate into CD209+ MΦ and demonstrate the capacity to phagocytose and contain *M. tuberculosis*, and express the vitamin D pathway.

A key observation of TLR activation was the decrease in *M. tuberculosis* viability in both human and murine innate immune systems [8,43,81]. However, the main difference in the murine immune response is that the antimicrobial activity was NO dependent. To determine the antimicrobial mechanism of human TLR2/1 activation against *M. tuberculosis*, previous work from our laboratory analyzed the expression profile of primary human monocytes treated with 19kD via microarray [80]. Investigation of this expression profile led to the finding that monocytes treated with 19kD demonstrated a significant increase in CYP27B1 mRNA and vitamin D receptor (VDR) mRNA [80,82]. Supplementing either 25D3 or 1,25D3 to monocytes treated with 19kD demonstrated the functional status of the vitamin D metabolism pathway. The genes CAMP mRNA, which encodes the antimicrobial peptide cathelicidin, and CYP24A1 were measured by qPCR and were dependent on 25D3 supplementation. In addition, monocytes infected with *M. tuberculosis* and then treated with 1,25D3 demonstrated that the bacteria co-localized with cathelicidin in which coincided with decrease bacteria viability. Other studies have confirmed that cathelicidin demonstrates direct antimicrobial effects against invading pathogens including *M. tuberculosis* [83,84]. Collectively these data indicate that human monocytes treated with 19kD demonstrate a vitamin D-dependent antimicrobial response against *M. tuberculosis*.

The essential function of the MΦ is to rapidly recognize an invading pathogen and effectively clear the microbe from the host. TLR2/1 activation revealed an indirect effector pathway which revealed that primary human monocytes treated with IL-15 differentiated into CD209+ MΦ that express the vitamin-D dependent antimicrobial pathway [46]. The expression of the vitamin D pathway in monocytes treated with 19kD is

dependent on IL-15. The supplementation of 25D3 to IL-15 MΦ has demonstrated that the vitamin D pathway is functional by i) the bioconversion of 25D3 into 1,25D3, ii) activating VDR by triggering the expression of CAMP mRNA and iii) significantly decreasing *M. tuberculosis* viability. However, the caveat to all these experiments is that IL-15 MΦ were differentiated in vitamin D deficient conditions. Therefore in Chapter 2 we will address how primary human monocytes treated with IL-15 in the presence of vitamin D influences MΦ differentiation and function.

Vitamin A

According to the World Health Organization (WHO) vitamin A deficiency (VAD) is associated with blindness in children, increased risk of maternal mortality and high risk of disease and death. Epidemiological studies have shown that TB burden is high in low-income countries where malnutrition and VAD is common [85]. However, clinical trials where active TB patients are supplemented with retinol are largely unsuccessful *in vivo* [86-89]. In contrast, the bioactive form of vitamin A, all-trans retinoic acid (ATRA), induces an antimicrobial response against *M. tuberculosis in vitro* [56,90,91].

Laboratory research has revealed that ATRA induces several different effector pathways in the innate immune response [90,92]. Monocytes and MΦ treated with ATRA induce the expression of NPC2, which decreases cholesterol content in the cell and *M. tuberculosis* viability [56]. Decreasing cholesterol content is critical to antimicrobial response against *M. tuberculosis* because bacteria persistence correlates with high cellular cholesterol content [93]. In addition, ATRA induces indirect effector pathways by inducing the differentiation of CD209+ MΦ [94] and tissue-like MΦ that sustain the

formation of granulomas [95]. In contrast, ATRA has been characterized to promote wound healing properties by decreasing TLR2 and CD14 surface expression on primary human monocytes [83] and homeostasis by inducing the differentiation regulatory T-cells [96]. Despite the pleiotropic functions ATRA provides the innate immune system, the levels must be tightly regulated in humans *in vivo* because it can cause harmful side effects. Therefore, in Chapter 3 we will investigate vitamin A metabolism by the innate immune system and project it into TB disease.

Evasion mechanisms of microbes

The host immune response has demonstrated the ability to defend against microbial infection and limit the progression of disease. However, pathogens have co-evolved with the immune system and developed evasion mechanisms, which advance the infection towards disease. A variety of factors are associated with host susceptibility to disease such as host genetic mutations, host micronutrient status and modulation of immune response [97]. Identifying the mechanisms of microbial persistence is central to the ability to develop novel approaches to therapeutics and treatments for infectious diseases.

Mycobacteria

Work in our laboratory has demonstrated that *M. leprae* infection modulates the immune response, which contributes to the pathogenesis of disease. Previously, we described that 25D3 supplementation to immune subsets that express the vitamin D pathway triggers a direct antimicrobial response against mycobacteria [27,46,80]. However,

the bacteria have evolved evasion mechanisms that combat this antimicrobial response. We have identified that *M. leprae* infection induces the expression of microRNA-21 (mir-21), which downregulates the mRNA expression of (TLR2/1)-induced *CYP27B1* and *IL-1B* mRNA and upregulates the mRNA expression of IL-10 mRNA.[82] These changes in TLR2/1 activation by mir-21 demonstrate a decreased mRNA expression of vitamin D dependent antimicrobial peptides, cathelicidin and DEFB4. The expression of DEFB4, which encodes beta defensin 2, is dependent on VDR activation and IL-1B to clear mycobacteria in the MΦ [98]. IL-10 induces the differentiation of phagocytic MΦ that resemble foam cells [27] and inhibits the differentiation of IL-32 derived DCs [54]. Additionally, *M. leprae* infection induces the expression of Type-1 interferon, which blocks autophagy (data not shown) and also inhibits the mRNA expression of the vitamin D-dependent antimicrobial peptides [17]. Mycobacteria infection induces TACO (tryptophan -containing coat protein), which localizes to the phagosome and prolongs the bacteria survival within MΦ [99]. Therapeutic interventions that block these immune modulation mechanisms may be an effective strategy against mycobacterial related diseases.

Genetic studies have revealed that mutations in TLR2 [100], NOD2 [62,101] and VDR [101] are associated with increased susceptibility to mycobacteria related diseases. These mutations have facilitated in identifying the roles of PRRs and micronutrient levels in the human immune system. Subsequent, epidemiological studies demonstrate that active TB patients demonstrate low sera retinol and 25D levels [75,86]. Low micronutrient levels in humans are linked to decreased host defense mechanisms such as the expression of antimicrobial peptides [80,102-104], autophagy [103], cholesterol efflux [56] and the differentiation

of immune subsets [105]. However, clinical trials that provide micronutrient supplementation to active TB patients have been largely unsuccessful. Thus, further clinical studies are needed to determine if micronutrient supplementation to healthy subjects prior to microbial infection can prevent the spread of disease.

Toxoplasma gondii

Toxoplasma and related parasites (e.g *Plasmodium faciparum)* invade host cells and hijack host cell functions by a specialized secretory organelle called the rhoptry. During the initial stages of infection, the parasite injects rhoptry neck proteins (RONs) into the host plasma membrane to allow the parasite to penetrate into the intracellular space and form the PV. The rhoptries also secrete rhoptry body proteins (ROPs) into the host cytoplasm to modulate signaling pathways that control immune responses that clear the parasite [106,107]. The rhoptry effector proteins are dominated by a large family of ~40 secreted kinases and pseudokinases that are just beginning to be understood, as well as an array of novel factors of unknown functions [108]. One example of a rhoptry kinase effector is the protein ROP16 that is injected into the host cytoplasm and transits to the host nucleus. ROP16 serves to activate STAT-3 and STAT-6, which results in a decrease in IL-12p40 production thereby dampening the Th1 response to the parasite [109]. Two other members of the ROP kinase family are the kinase ROP18 and pseudokinase ROP5. Both effectors are injected and bind to the cytoplasmic face of the PV [109-111]. This kinase-pseudokinase pair collaborate to phosphorylate and disarm loading of the interferon gamma-dependent immunity-related GTPases (IRGs) which would otherwise lyse the parasite vacuole and clear the parasite [109,110]. Interestingly, the pseudokinase

ROP5 is critical for activating the ROP18 kinase, enabling it to phosphorylate the IRGs, which demonstrates the importance of pseudokinases in parasite virulence. Evading the IRGs clearly involves other players, such as another ROP kinase ROP17 and a secreted dense granule protein GRA7 have been shown to also participate in this response [111,112].

The caveat from all these studies is that the ROP effector proteins were found in the hypervirulent strain Type-1 parasite. While only one type-1 parasite is required to cause morbidity in mice, the majority of human infections are associated with the type II *T. gondii* strain [113]. Additionally, the ROP5/17/18 complex evades interferon–gamma mediated-immune responses in murine MΦ, but not in human MΦ [114]. These studies suggest that virulence factors in the type II parasite line may have evolved to evade the human immune response. In Chapter 4 we have a characterized a novel ROP effector protein, ROP54 that is conserved between the type-I and type-II parasite lines. A decrease in virulence was only observed in mice infected with Δ*rop54* in type II parasites, but Δ*rop54* in type I parasites. Protein alignment between ROP54 and ROP18 protein sequence revealed that the catalytic residues of a functional kinase were absent in ROP54, which suggests that ROP54 could function as a pseudokinase. Collectively these data indicate that ROP54 is a divergent ROP effector protein that may play a role in the evasion of an immune response distinct from the ROP5/17/18 complex.

Going Forward

The focus of this thesis is to understand the host-pathogen interaction between the innate immune system and harmful pathogens such as *M. leprae*, *M. tuberculosis* and *Toxoplasma.* The innate immune system recognizes microbes and rapidly triggers

antimicrobial responses to protect the host from disease. However, pathogens have evolved mechanisms that evade the immune response and allow the microbe to establish infection. We will determine if 25D3 status contributes towards the antimicrobial response in MΦ. Establish a retinol metabolism model by the immune system that provides insight into TB disease. Then conclude with the characterization of a novel effector protein of *Toxoplasma* that is critical to evasion of the immune response and survival of the parasite.

References

1 Houben, R. M. & Dodd, P. J. The Global Burden of Latent Tuberculosis Infection: A Re-estimation Using Mathematical Modelling. *PLoS Med* **13**, e1002152, doi:10.1371/journal.pmed.1002152 (2016).

2 Zahrt, T. C. Molecular mechanisms regulating persistent Mycobacterium tuberculosis infection. *Microbes Infect* **5**, 159-167 (2003).

3 Esmail, H., Barry, C. E., 3rd, Young, D. B. & Wilkinson, R. J. The ongoing challenge of latent tuberculosis. *Philos Trans R Soc Lond B Biol Sci* **369**, 20130437, doi:10.1098/rstb.2013.0437 (2014).

4 LoBue, P. A. & Castro, K. G. Is it time to replace the tuberculin skin test with a blood test? *JAMA* **308**, 241-242, doi:10.1001/jama.2012.7511 (2012).

5 Hornum, M., Mortensen, K. L., Kamper, A. L. & Andersen, A. B. Limitations of the QuantiFERON-TB Gold test in detecting Mycobacterium tuberculosis infection in immunocompromised patients. *Eur J Intern Med* **19**, 137-139, doi:10.1016/j.ejim.2007.03.020 (2008).

6 Frieden, T. R. *et al.* The emergence of drug-resistant tuberculosis in New York City. *N Engl J Med* **328**, 521-526, doi:10.1056/NEJM199302253280801 (1993).

7 Klopper, M. *et al.* Emergence and spread of extensively and totally drug-resistant tuberculosis, South Africa. *Emerg Infect Dis* **19**, 449-455, doi:10.3201/EID1903.12024610.3201//EID1903.120246 (2013).

8 Modlin, R. L. & Bloom, B. R. TB or not TB: that is no longer the question. *Sci Transl Med* **5**, 213sr216, doi:10.1126/scitranslmed.3007402 (2013).

9 Kwan, C. K. & Ernst, J. D. HIV and tuberculosis: a deadly human syndemic. *Clin Microbiol Rev* **24**, 351-376, doi:10.1128/CMR.00042-10 (2011).

10 Getahun, H., Gunneberg, C., Granich, R. & Nunn, P. HIV infection-associated tuberculosis: the epidemiology and the response. *Clin Infect Dis* **50 Suppl 3**, S201-207, doi:10.1086/651492 (2010).

11 Malherbe, S. T. *et al.* Persisting positron emission tomography lesion activity and Mycobacterium tuberculosis mRNA after tuberculosis cure. *Nat Med* **22**, 1094-1100, doi:10.1038/nm.4177 (2016).

12 Clemens, D. L., Lee, B. Y. & Horwitz, M. A. The Mycobacterium tuberculosis phagosome in human macrophages is isolated from the host cell cytoplasm. *Infect Immun* **70**, 5800-5807 (2002).

13 Modlin, R. L. The innate immune response in leprosy. *Curr Opin Immunol* **22**, 48-54, doi:10.1016/j.coi.2009.12.001 (2010).

14 Cooper, C. L. *et al.* Analysis of naturally occurring delayed-type hypersensitivity reactions in leprosy by in situ hybridization. *J Exp Med* **169**, 1565-1581 (1989).

15 Yamamura, M. *et al.* Defining protective responses to pathogens: cytokine profiles in leprosy lesions. *Science* **254**, 277-279 (1991).

16 Yamamura, M. *et al.* Cytokine patterns of immunologically mediated tissue damage. *J Immunol* **149**, 1470-1475 (1992).

17 Teles, R. M. *et al.* Type I interferon suppresses type II interferon-triggered human anti-mycobacterial responses. *Science* **339**, 1448-1453, doi:10.1126/science.1233665 (2013).

18 Waters, M. F., Turk, J. L. & Wemambu, S. N. Mechanisms of reactions in leprosy. *Int J Lepr Other Mycobact Dis* **39**, 417-428 (1971).

19 Hunter, C. A. & Sibley, L. D. Modulation of innate immunity by Toxoplasma gondii virulence effectors. *Nat Rev Microbiol* **10**, 766-778, doi:10.1038/nrmicro2858 (2012).

20 Jones, J. L. & Dubey, J. P. Foodborne toxoplasmosis. *Clin Infect Dis* **55**, 845-851, doi:10.1093/cid/cis508 (2012).

21 Rigoulet, J. *et al.* Toxoplasmosis in a bar-shouldered dove (Geopelia humeralis) from the Zoo of Cleres, France. *Parasite* **21**, 62, doi:10.1051/parasite/2014062 (2014).

22 Kim, K. & Weiss, L. M. Toxoplasma gondii: the model apicomplexan. *Int J Parasitol* **34**, 423-432, doi:10.1016/j.ijpara.2003.12.009 (2004).

23 Persson, C. M. *et al.* Transmission of Toxoplasma gondii from infected dendritic cells to natural killer cells. *Infect Immun* **77**, 970-976, doi:10.1128/IAI.00833-08 (2009).

24 Brossier, F. & David Sibley, L. Toxoplasma gondii: microneme protein MIC2. *Int J Biochem Cell Biol* **37**, 2266-2272, doi:10.1016/j.biocel.2005.06.006 (2005).

25 Lamarque, M. *et al.* The RON2-AMA1 interaction is a critical step in moving junction-dependent invasion by apicomplexan parasites. *PLoS Pathog* **7**, e1001276, doi:10.1371/journal.ppat.1001276 (2011).

26 Gold, D. A. *et al.* The Toxoplasma Dense Granule Proteins GRA17 and GRA23 Mediate the Movement of Small Molecules between the Host and the

Parasitophorous Vacuole. *Cell Host Microbe* **17**, 642-652, doi:10.1016/j.chom.2015.04.003 (2015).

27 Montoya, D. *et al.* Divergence of macrophage phagocytic and antimicrobial programs in leprosy. *Cell Host Microbe* **6**, 343-353, doi:10.1016/j.chom.2009.09.002 (2009).

28 Tauszig, S., Jouanguy, E., Hoffmann, J. A. & Imler, J. L. Toll-related receptors and the control of antimicrobial peptide expression in Drosophila. *Proc Natl Acad Sci U S A* **97**, 10520-10525, doi:10.1073/pnas.180130797 (2000).

29 Lemaitre, B. *et al.* A recessive mutation, immune deficiency (imd), defines two distinct control pathways in the Drosophila host defense. *Proc Natl Acad Sci U S A* **92**, 9465-9469 (1995).

30 Medzhitov, R., Preston-Hurlburt, P. & Janeway, C. A., Jr. A human homologue of the Drosophila Toll protein signals activation of adaptive immunity. *Nature* **388**, 394-397, doi:10.1038/41131 (1997).

31 Hertz, C. J. *et al.* Activation of Toll-like receptor 2 on human tracheobronchial epithelial cells induces the antimicrobial peptide human beta defensin-2. *J Immunol* **171**, 6820-6826 (2003).

32 Birchler, T. *et al.* Human Toll-like receptor 2 mediates induction of the antimicrobial peptide human beta-defensin 2 in response to bacterial lipoprotein. *Eur J Immunol* **31**, 3131-3137, doi:10.1002/1521-4141(200111)31:11<3131::AID-IMMU3131>3.0.CO;2-G (2001).

33 Henneke, P. *et al.* Cellular activation, phagocytosis, and bactericidal activity against group B streptococcus involve parallel myeloid differentiation factor 88-

dependent and independent signaling pathways. *J Immunol* **169**, 3970-3977 (2002).

34 Aliprantis, A. O., Weiss, D. S. & Zychlinsky, A. Toll-like receptor-2 transduces signals for NF-kappa B activation, apoptosis and reactive oxygen species production. *J Endotoxin Res* **7**, 287-291 (2001).

35 Takeda, K. & Akira, S. Toll-like receptors in innate immunity. *Int Immunol* **17**, 1-14, doi:10.1093/intimm/dxh186 (2005).

36 Thoma-Uszynski, S. *et al.* Induction of direct antimicrobial activity through mammalian toll-like receptors. *Science* **291**, 1544-1547, doi:10.1126/science.291.5508.1544 (2001).

37 Elkington, P. T. *et al.* Mycobacterium tuberculosis up-regulates matrix metalloproteinase-1 secretion from human airway epithelial cells via a p38 MAPK switch. *J Immunol* **175**, 5333-5340 (2005).

38 Kim, M. J. *et al.* Caseation of human tuberculosis granulomas correlates with elevated host lipid metabolism. *EMBO Mol Med* **2**, 258-274, doi:10.1002/emmm.201000079 (2010).

39 Russell, D. G., Cardona, P. J., Kim, M. J., Allain, S. & Altare, F. Foamy macrophages and the progression of the human tuberculosis granuloma. *Nat Immunol* **10**, 943-948, doi:10.1038/ni.1781 (2009).

40 Krutzik, S. R. *et al.* Activation and regulation of Toll-like receptors 2 and 1 in human leprosy. *Nat Med* **9**, 525-532, doi:10.1038/nm864 (2003).

41 Blander, J. M. & Medzhitov, R. Regulation of phagosome maturation by signals from toll-like receptors. *Science* **304**, 1014-1018, doi:10.1126/science.1096158 (2004).

42 Doyle, S. E. *et al.* Toll-like receptors induce a phagocytic gene program through p38. *J Exp Med* **199**, 81-90, doi:10.1084/jem.20031237 (2004).

43 Brightbill, H. D. *et al.* Host defense mechanisms triggered by microbial lipoproteins through toll-like receptors. *Science* **285**, 732-736 (1999).

44 Hertz, C. J. *et al.* Microbial lipopeptides stimulate dendritic cell maturation via Toll-like receptor 2. *J Immunol* **166**, 2444-2450 (2001).

45 Krutzik, S. R. *et al.* TLR activation triggers the rapid differentiation of monocytes into macrophages and dendritic cells. *Nat Med* **11**, 653-660, doi:10.1038/nm1246 (2005).

46 Krutzik, S. R. *et al.* IL-15 links TLR2/1-induced macrophage differentiation to the vitamin D-dependent antimicrobial pathway. *J Immunol* **181**, 7115-7120 (2008).

47 Lee, D. J. *et al.* LILRA2 activation inhibits dendritic cell differentiation and antigen presentation to T cells. *J Immunol* **179**, 8128-8136 (2007).

48 Beckman, E. M. *et al.* CD1c restricts responses of mycobacteria-specific T cells. Evidence for antigen presentation by a second member of the human CD1 family. *J Immunol* **157**, 2795-2803 (1996).

49 Borges, L. & Cosman, D. LIRs/ILTs/MIRs, inhibitory and stimulatory Ig-superfamily receptors expressed in myeloid and lymphoid cells. *Cytokine Growth Factor Rev* **11**, 209-217 (2000).

50 Arm, J. P., Nwankwo, C. & Austen, K. F. Molecular identification of a novel family of human Ig superfamily members that possess immunoreceptor tyrosine-based inhibition motifs and homology to the mouse gp49B1 inhibitory receptor. *J Immunol* **159**, 2342-2349 (1997).

51 Brown, D., Trowsdale, J. & Allen, R. The LILR family: modulators of innate and adaptive immune pathways in health and disease. *Tissue Antigens* **64**, 215-225, doi:10.1111/j.0001-2815.2004.00290.x (2004).

52 Andrade, E. B. *et al.* TLR2-induced IL-10 production impairs neutrophil recruitment to infected tissues during neonatal bacterial sepsis. *J Immunol* **191**, 4759-4768, doi:10.4049/jimmunol.1301752 (2013).

53 Fiorentino, D. F., Bond, M. W. & Mosmann, T. R. Two types of mouse T helper cell. IV. Th2 clones secrete a factor that inhibits cytokine production by Th1 clones. *J Exp Med* **170**, 2081-2095 (1989).

54 Schenk, M. *et al.* NOD2 triggers an interleukin-32-dependent human dendritic cell program in leprosy. *Nat Med* **18**, 555-563, doi:10.1038/nm.2650 (2012).

55 Galkina, E. & Ley, K. Immune and inflammatory mechanisms of atherosclerosis (*). *Annu Rev Immunol* **27**, 165-197, doi:10.1146/annurev.immunol.021908.132620 (2009).

56 Wheelwright, M. *et al.* All-trans retinoic acid-triggered antimicrobial activity against Mycobacterium tuberculosis is dependent on NPC2. *J Immunol* **192**, 2280-2290, doi:10.4049/jimmunol.1301686 (2014).

57 Kalayoglu, M. V. & Byrne, G. I. Induction of macrophage foam cell formation by Chlamydia pneumoniae. *J Infect Dis* **177**, 725-729 (1998).

58 Nadipuram, S. M. *et al.* In Vivo Biotinylation of the Toxoplasma Parasitophorous Vacuole Reveals Novel Dense Granule Proteins Important for Parasite Growth and Pathogenesis. *MBio* **7**, doi:10.1128/mBio.00808-16 (2016).

59 Portugal, L. R. *et al.* Influence of low-density lipoprotein (LDL) receptor on lipid composition, inflammation and parasitism during Toxoplasma gondii infection. *Microbes Infect* **10**, 276-284, doi:10.1016/j.micinf.2007.12.001 (2008).

60 Ferwerda, G. *et al.* NOD2 and toll-like receptors are nonredundant recognition systems of Mycobacterium tuberculosis. *PLoS Pathog* **1**, 279-285, doi:10.1371/journal.ppat.0010034 (2005).

61 Wang, C. *et al.* NOD2 polymorphisms and pulmonary tuberculosis susceptibility: a systematic review and meta-analysis. *Int J Biol Sci* **10**, 103-108, doi:10.7150/ijbs.7585 (2013).

62 Berrington, W. R. *et al.* Common polymorphisms in the NOD2 gene region are associated with leprosy and its reactive states. *J Infect Dis* **201**, 1422-1435, doi:10.1086/651559 (2010).

63 Hugot, J. P. *et al.* Association of NOD2 leucine-rich repeat variants with susceptibility to Crohn's disease. *Nature* **411**, 599-603, doi:10.1038/35079107 (2001).

64 Ogura, Y. *et al.* A frameshift mutation in NOD2 associated with susceptibility to Crohn's disease. *Nature* **411**, 603-606, doi:10.1038/35079114 (2001).

65 Montoya, D. *et al.* IL-32 is a molecular marker of a host defense network in human tuberculosis. *Sci Transl Med* **6**, 250ra114, doi:10.1126/scitranslmed.3009546 (2014).

66 Schlitzer, A., McGovern, N. & Ginhoux, F. Dendritic cells and monocyte-derived cells: Two complementary and integrated functional systems. *Semin Cell Dev Biol* **41**, 9-22, doi:10.1016/j.semcdb.2015.03.011 (2015).

67 See, P. *et al.* Mapping the human DC lineage through the integration of high-dimensional techniques. *Science* **356**, doi:10.1126/science.aag3009 (2017).

68 Karyadi, E. *et al.* Poor micronutrient status of active pulmonary tuberculosis patients in Indonesia. *J Nutr* **130**, 2953-2958, doi:10.1093/jn/130.12.2953 (2000).

69 Shahriari, M., Kerr, P. E., Slade, K. & Grant-Kels, J. E. Vitamin D and the skin. *Clin Dermatol* **28**, 663-668, doi:10.1016/j.clindermatol.2010.03.030 (2010).

70 Holick, M. F. Vitamin D: a D-Lightful health perspective. *Nutr Rev* **66**, S182-194, doi:10.1111/j.1753-4887.2008.00104.x (2008).

71 Strushkevich, N., Usanov, S. A., Plotnikov, A. N., Jones, G. & Park, H. W. Structural analysis of CYP2R1 in complex with vitamin D3. *J Mol Biol* **380**, 95-106, doi:10.1016/j.jmb.2008.03.065 (2008).

72 Holick, M. F. Vitamin D deficiency. *N Engl J Med* **357**, 266-281, doi:10.1056/NEJMra070553 (2007).

73 Hewison, M. & Adams, J. S. Vitamin D insufficiency and skeletal development in utero. *J Bone Miner Res* **25**, 11-13, doi:10.1002/jbmr.2 (2010).

74 Wejse, C. *et al.* Vitamin D as supplementary treatment for tuberculosis: a double-blind, randomized, placebo-controlled trial. *Am J Respir Crit Care Med* **179**, 843-850, doi:10.1164/rccm.200804-567OC (2009).

75 Martineau, A. R. *et al.* A single dose of vitamin D enhances immunity to mycobacteria. *Am J Respir Crit Care Med* **176**, 208-213, doi:10.1164/rccm.200701-007OC (2007).

76 Ganmaa, D. *et al.* Vitamin D, tuberculin skin test conversion, and latent tuberculosis in Mongolian school-age children: a randomized, double-blind, placebo-controlled feasibility trial. *Am J Clin Nutr* **96**, 391-396, doi:10.3945/ajcn.112.034967 (2012).

77 Dowling, G. B. & Prosser Thomas, E. W. Treatment of lupus vulgaris with calciferol. *Br J Dermatol Syph* **58**, 45-52 (1946).

78 Rook, G. A. The role of vitamin D in tuberculosis. *Am Rev Respir Dis* **138**, 768-770, doi:10.1164/ajrccm/138.4.768 (1988).

79 Ellman, P. & Anderson, K. H. Calciferol in tuberculous peritonitis with disseminated tuberculosis. *Br Med J* **1**, 394 (1948).

80 Liu, P. T. *et al.* Toll-like receptor triggering of a vitamin D-mediated human antimicrobial response. *Science* **311**, 1770-1773, doi:10.1126/science.1123933 (2006).

81 Realegeno, S. *et al.* S100A12 Is Part of the Antimicrobial Network against Mycobacterium leprae in Human Macrophages. *PLoS Pathog* **12**, e1005705, doi:10.1371/journal.ppat.1005705 (2016).

82 Liu, P. T. *et al.* MicroRNA-21 targets the vitamin D-dependent antimicrobial pathway in leprosy. *Nat Med* **18**, 267-273, doi:10.1038/nm.2584 (2012).

83 Liu, P. T., Krutzik, S. R., Kim, J. & Modlin, R. L. Cutting edge: all-trans retinoic acid down-regulates TLR2 expression and function. *J Immunol* **174**, 2467-2470 (2005).

84 Wang, T. T. *et al.* Cutting edge: 1,25-dihydroxyvitamin D3 is a direct inducer of antimicrobial peptide gene expression. *J Immunol* **173**, 2909-2912 (2004).

85 Aibana, O. *et al.* Impact of Vitamin A and Carotenoids on the Risk of Tuberculosis Progression. *Clin Infect Dis* **65**, 900-909, doi:10.1093/cid/cix476 (2017).

86 Karyadi, E. *et al.* A double-blind, placebo-controlled study of vitamin A and zinc supplementation in persons with tuberculosis in Indonesia: effects on clinical response and nutritional status. *Am J Clin Nutr* **75**, 720-727 (2002).

87 Mathur, M. L. Role of vitamin A supplementation in the treatment of tuberculosis. *Natl Med J India* **20**, 16-21 (2007).

88 Pakasi, T. A. *et al.* Zinc and vitamin A supplementation fails to reduce sputum conversion time in severely malnourished pulmonary tuberculosis patients in Indonesia. *Nutr J* **9**, 41, doi:10.1186/1475-2891-9-41 (2010).

89 Range, N. *et al.* The effect of multi-vitamin/mineral supplementation on mortality during treatment of pulmonary tuberculosis: a randomised two-by-two factorial trial in Mwanza, Tanzania. *Br J Nutr* **95**, 762-770 (2006).

90 Anand, P. K. & Kaul, D. Downregulation of TACO gene transcription restricts mycobacterial entry/survival within human macrophages. *FEMS Microbiol Lett* **250**, 137-144, doi:10.1016/j.femsle.2005.06.056 (2005).

91 Crowle, A. J. & Ross, E. J. Inhibition by retinoic acid of multiplication of virulent tubercle bacilli in cultured human macrophages. *Infect Immun* **57**, 840-844 (1989).

92 Coleman, M. M. *et al.* All-trans Retinoic Acid Augments Autophagy during Intracellular Bacterial Infection. *Am J Respir Cell Mol Biol*, doi:10.1165/rcmb.2017-0382OC (2018).

93 Nguyen, L. & Pieters, J. The Trojan horse: survival tactics of pathogenic mycobacteria in macrophages. *Trends Cell Biol* **15**, 269-276, doi:10.1016/j.tcb.2005.03.009 (2005).

94 Liu, P. T. *et al.* CD209(+) macrophages mediate host defense against Propionibacterium acnes. *J Immunol* **180**, 4919-4923 (2008).

95 Gundra, U. M. *et al.* Vitamin A mediates conversion of monocyte-derived macrophages into tissue-resident macrophages during alternative activation. *Nat Immunol* **18**, 642-653, doi:10.1038/ni.3734 (2017).

96 Erkelens, M. N. & Mebius, R. E. Retinoic Acid and Immune Homeostasis: A Balancing Act. *Trends Immunol* **38**, 168-180, doi:10.1016/j.it.2016.12.006 (2017).

97 Henderson, B. & Oyston, P. C. F. *Bacterial evasion of host immune responses*. (Cambridge University Press, 2003).

98 Liu, P. T. *et al.* Convergence of IL-1beta and VDR activation pathways in human TLR2/1-induced antimicrobial responses. *PLoS One* **4**, e5810, doi:10.1371/journal.pone.0005810 (2009).

99 Ferrari, G., Langen, H., Naito, M. & Pieters, J. A coat protein on phagosomes involved in the intracellular survival of mycobacteria. *Cell* **97**, 435-447 (1999).

100 Ben-Ali, M., Barbouche, M. R., Bousnina, S., Chabbou, A. & Dellagi, K. Toll-like receptor 2 Arg677Trp polymorphism is associated with susceptibility to tuberculosis in Tunisian patients. *Clin Diagn Lab Immunol* **11**, 625-626, doi:10.1128/CDLI.11.3.625-626.2004 (2004).

101 Bornman, L. *et al.* Vitamin D receptor polymorphisms and susceptibility to tuberculosis in West Africa: a case-control and family study. *J Infect Dis* **190**, 1631-1641, doi:10.1086/424462 (2004).

102 Fabri, M. & Modlin, R. L. A vitamin for autophagy. *Cell Host Microbe* **6**, 201-203, doi:10.1016/j.chom.2009.08.008 (2009).

103 Fabri, M. *et al.* Vitamin D is required for IFN-gamma-mediated antimicrobial activity of human macrophages. *Sci Transl Med* **3**, 104ra102, doi:10.1126/scitranslmed.3003045 (2011).

104 Adams, J. S. *et al.* Vitamin d-directed rheostatic regulation of monocyte antibacterial responses. *J Immunol* **182**, 4289-4295, doi:10.4049/jimmunol.0803736 (2009).

105 Tanaka, H., Abe, E., Miyaura, C., Shiina, Y. & Suda, T. 1 alpha,25-dihydroxyvitamin D3 induces differentiation of human promyelocytic leukemia cells (HL-60) into monocyte-macrophages, but not into granulocytes. *Biochem Biophys Res Commun* **117**, 86-92 (1983).

106 Bradley, P. J. & Sibley, L. D. Rhoptries: an arsenal of secreted virulence factors. *Curr Opin Microbiol* **10**, 582-587, doi:10.1016/j.mib.2007.09.013 (2007).

107 Boothroyd, J. C. & Dubremetz, J. F. Kiss and spit: the dual roles of Toxoplasma rhoptries. *Nat Rev Microbiol* **6**, 79-88, doi:10.1038/nrmicro1800 (2008).

108 Bradley, P. J. *et al.* Proteomic analysis of rhoptry organelles reveals many novel constituents for host-parasite interactions in Toxoplasma gondii. *J Biol Chem* **280**, 34245-34258, doi:10.1074/jbc.M504158200 (2005).

109 Behnke, M. S. *et al.* The polymorphic pseudokinase ROP5 controls virulence in Toxoplasma gondii by regulating the active kinase ROP18. *PLoS Pathog* **8**, e1002992, doi:10.1371/journal.ppat.1002992 (2012).

110 Reese, M. L. & Boothroyd, J. C. A conserved non-canonical motif in the pseudoactive site of the ROP5 pseudokinase domain mediates its effect on Toxoplasma virulence. *J Biol Chem* **286**, 29366-29375, doi:10.1074/jbc.M111.253435 (2011).

111 Etheridge, R. D. *et al.* The Toxoplasma pseudokinase ROP5 forms complexes with ROP18 and ROP17 kinases that synergize to control acute virulence in mice. *Cell Host Microbe* **15**, 537-550, doi:10.1016/j.chom.2014.04.002 (2014).

112 Alaganan, A., Fentress, S. J., Tang, K., Wang, Q. & Sibley, L. D. Toxoplasma GRA7 effector increases turnover of immunity-related GTPases and contributes to acute virulence in the mouse. *Proc Natl Acad Sci U S A* **111**, 1126-1131, doi:10.1073/pnas.1313501111 (2014).

113 Sibley, L. D. & Boothroyd, J. C. Virulent strains of Toxoplasma gondii comprise a single clonal lineage. *Nature* **359**, 82-85, doi:10.1038/359082a0 (1992).

114 Niedelman, W. *et al.* The rhoptry proteins ROP18 and ROP5 mediate Toxoplasma gondii evasion of the murine, but not the human, interferon-gamma response. *PLoS Pathog* **8**, e1002784, doi:10.1371/journal.ppat.1002784 (2012).

CHAPTER 2

Vitamin D status Contributes to the Antimicrobial Activity of Macrophages against *Mycobacterium leprae*

Abstract

Background

The immune system depends on effector pathways to eliminate invading pathogens from the host *in vivo*. Macrophages (MΦ) of the innate immune system are armed with vitamin D-dependent antimicrobial responses to kill intracellular microbes. However, how the physiological levels of vitamin D during MΦ differentiation affect phenotype and function is unknown.

Methodology/Principal

The human innate immune system consists of divergent MΦ subsets that serve distinct functions *in vivo*. Both IL-15 and IL-10 induce MΦ differentiation, but IL-15 induces primary human monocytes to differentiate into antimicrobial MΦ (IL-15 MΦ) that robustly express the vitamin D pathway. However, how vitamin D status alters IL-15 MΦ phenotype and function is unknown. In this study, we found that adding 25-hydroxyvitamin D3 (25D3) during the IL-15 induced differentiation of monocytes into MΦ increased the expression of the antimicrobial peptide cathelicidin, including both CAMP mRNA and the encoded protein cathelicidin in a dose-dependent manner. The presence of physiological levels of 25D during differentiation of IL-15 MΦ led to a significant vitamin D-dependent antimicrobial response against intracellular *Mycobacterium leprae* but did not change the phenotype or phagocytic function of these MΦ. These data suggest that activation of the vitamin D pathway during IL-15 MΦ differentiation augments the antimicrobial response against *M. leprae* infection.

Conclusions/significance

Our data demonstrates that the presence of vitamin D during MΦ differentiation bestows the capacity to mount an antimicrobial response against *M. leprae*.

Introduction

The MΦ is a sentinel of the innate immune system that serves as the first line of defense to recognize and destroy invading microbes. In human MΦ, activation by a toll-like receptor 2/1 (TLR2/1) ligand or interferon-g (IFN-g) triggers a direct antimicrobial response that depends upon the level of available vitamin D [1-3]. The vitamin D-dependent antimicrobial pathway involves the induction of IL-15 and IL-32, the conversion of 25D3 to bioactive 1,25-dihydroxyvitamin D (1,25D3) and subsequent activation of the vitamin D receptor (VDR) to induce the expression of the antimicrobial peptides including cathelicidin, autophagy and phagolysosomal fusion [2,4-8]. This antimicrobial pathway is not induced in MΦ if the levels of 25D are not sufficient.

Macrophages demonstrate phenotypic heterogeneity which confer distinct functions in the innate immune system [9]. IL-15 MΦ demonstrate a vitamin D-dependent antimicrobial profile which includes the expression of CAMP mRNA [4,10]. In contrast, primary human monocytes treated with IL-10 differentiate into phagocytic macrophages (IL-10 MΦ), which readily take up bacteria but weakly express the vitamin D-dependent antimicrobial pathway [10]. These MΦ subtypes can be identified by a specific cell surface phenotype, both IL-15 MΦ and IL-10 MΦ express CD209 but only IL-10 MΦ express CD163. As such, IL-15 MΦ and IL-10 MΦ are differentially identified in the polar forms of leprosy caused by the intracellular bacterium *M. leprae*, correlating with the different outcomes of infection.

In addition to its role in MΦ antimicrobial function, vitamin D has long been recognized to affect the differentiation of diverse cell types, including cells of the myeloid lineage [11]. Activation of the VDR converts malignant myeloid leukemia cells

into non-proliferating monocytes or MΦ [12-15]. Dendritic cells differentiated in the presence of 25D3 or 1,25D3 demonstrate aberrant differentiation and decreased antigen presentation *in vitro* [16,17]. MΦ differentiated in vitamin D have also demonstrated a change in phenotype and phagocytic function *in vitro* [15,18]. Most of these studies were performed by adding non-physiological concentrations of the bioactive form of 1,25D3, such that the ability of the differentiating cell to utilize physiologic concentrations of 25D3 has not been substantially investigated. Although controversy still exists on the normal concentrations of 25D, we used the Endocrine Society Clinical Practice Guidelines which define vitamin D deficiency as below 20ng/mL (50nM), insufficiency as 21-29 ng/mL (52.5nM-72.5nM), sufficient levels as more that 30ng/mL (75nM) [19]. In humans, 1,25D levels are regulated to be constant, such that the available level of 25D determines the amount of bioactive 1,25D that is generated in an activated MΦ and is therefore key to innate immune function [3]. Therefore, the aim of our work is to study the effects of physiological levels of 25D3 during IL-15 MΦ differentiation, function and antimicrobial response against *M. leprae*.

Results

MΦ phenotype is sustained in SFM independent of 25D3 status

To investigate the effect of 25D3 on MΦ differentiation, we used SFM, allowing us to control the amount of 25D3 in the culture. SFM contains neither 25D3 nor any other vitamin D analogues, such that 25D3 can be added at defined concentrations. Thus, SFM has an advantage over fetal calf sera or human sera that have varying amounts of 25D3. Previously, IL-15 and IL-10 were shown to induce the differentiation of monocytes into distinct MΦ populations, however, these experiments were performed using FCS, which contains low levels of 25D3. Thus, it was unclear whether vitamin D status affects the differentiation of monocytes into IL-15 MΦ and IL-10 MΦ.

All experiments here involve MΦs derived from cytokine treated monocytes as previously reported [10]. Monocytes were cultured with either IL-15 or IL-10 for 48 hours in SFM with or without the addition of 25D3 (10^{-8}M 25D3). This is equivalent to the physiologic concentration in vitamin D sufficient serum of 10^{-7}M 25D3, which is then diluted to 10% serum in cell cultures [1,20]. Both IL-15 and IL-10 induced CD209 expression as assessed by flow cytometry, but only IL-10 induced CD163 expression (Fig 1A), similar to differentiation in FCS [10]. Examining co-expression of CD209 and CD163, we found that IL-15 induced $CD209^{+}CD163^{-}$ MΦ, whereas IL-10 induced $CD209^{+}CD163^{+}$ MΦ, accounting ~80% of cells. We also found that the IL-15 MΦ and IL-10 MΦ derived in SFM express the MΦ specific marker CD16. The average surface expression of CD16 increased in IL-15 MΦ when differentiated in 25D3 to similar levels seen on IL-10 MΦ, but was not significant ($p=0.07$). In addition, we observed that 25D3

status did not significantly alter the surface expression of CD209, CD163, CD16 or the coexpression of $CD209^{+}CD16^{+}$ whether derived using IL-15 or IL-10 (Fig 1A). The frequency of CD14 was expressed on IL-15 MΦ, with a small but significant enhancement by 25D3, to the level expressed on IL-10 MΦ (Fig 1A). This was also reflected in an increase in cellular abundance as measured by the change in mean fluorescence intensity (ΔMFI) for MΦ derived in IL-15 but not IL-10 (Fig 1B). Overall, SFM supported the differentiation of monocytes by IL-15 and IL-10 into divergent MΦ phenotypes, which were generally similar whether differentiated in the presence or absence of 25D3.

25D3 status triggers vitamin D-dependent antimicrobial profile in IL-15 MΦ

Although 25D3 did not dramatically affect the differentiation of MΦ by phenotype, we next investigated whether the presence of 25D3 during differentiation affected MΦ function. The induction of the antimicrobial protein cathelicidin is essential for the vitamin D-dependent antimicrobial response against intracellular mycobacteria in infected MΦ [5,21]. To determine whether 25D3 status during MΦ differentiation results in activation of the vitamin D-dependent antimicrobial pathway, we treated monocytes with IL-15 and IL-10 in the presence of increasing concentrations of 25D3 during differentiation and measured CAMP mRNA levels after 48 hours by qPCR. Conditioning during differentiation of both IL-15 MΦ and IL-10 MΦ in SFM supplemented with increasing level of 25D3 resulted in a significant dose-dependent induction of CAMP mRNA (Fig 2A). At all concentrations of 25D3, the CAMP mRNA

expression was more robust in IL-15 MΦ relative to IL-10 MΦ. We observed a ~315-fold induction of CAMP mRNA in SFM supplemented with 10^{-8}M 25D3 as compared to media without 25D3 in IL-15 MΦ, and ~500-fold induction of CAMP mRNA in SFM containing 10^{-7}M 25D3 (Fig 2A). In comparison, we observed a ~80-fold induction of CAMP mRNA in SFM containing 10^{-8}M 25D3 in IL-10 MΦ and a ~100-fold induction of CAMP mRNA in SFM containing 10^{-7}M 25D3 (Fig 2A). The baseline values of CYP27B1 mRNA expression was not significant between IL-15 MΦ and IL-10 MΦ (Supplemental Figure 1).

We determined whether the induction of CAMP mRNA was associated with expression of cathelicidin protein using intracellular flow cytometry. The CAMP mRNA expression levels in IL-15 MΦ correlated with both the frequency of cathelicidin and the cathelicidin protein abundance as measured by ΔMFI (Fig 2B,C). The average frequency of cathelicidin was ~13% in IL-15 MΦ derived in 10^{-8}M 25D3 and ~30% in 10^{-7}M 25D3 supplemented SFM (Fig 2B). The ΔMFI was ~45 AU in IL-15 MΦ derived in 10^{-7}M 25D3 and ~80 AU in 10^{-8}M 25D3 supplemented SFM (Fig 2C).

Representative fluorescence microscopy images of IL-15 MΦ conditioned in 25D3 indicates that cathelicidin protein accumulates in the intracellular vesicles proximal to the host nucleus, but not in IL-15 MΦ differentiated in no 25D3 (Fig 2D). These data collectively indicate that cathelicidin mRNA and protein expression directly correlate with 25D3 status during IL-15 induced MΦ differentiation.

Vitamin D status does not alter IL15-MΦ phagocytic function

An important function of antimicrobial MΦ is the phagocytosis of pathogens to contain microbes in the host *in vivo*. However, it is unclear how vitamin D status may alter the phagocytic function of the MΦ during *M. leprae* infection. To assess phagocytic function, IL-15 MΦ were conditioned with or without 25D3, infected with PE labeled-*M. leprae* for 24 hours, stained for the MΦ specific marker CD14 and phagocytosis was analyzed by flow cytometry and image stream flow cytometry. The efficiency of *M. leprae* infection in IL-15 MΦ differentiated in the absence of vitamin D or in the presence of either 10^{-8}M 25D3 or 10^{-7}M 25D3, was not statistically different, although somewhat greater in culture in which no 25D3 was present (Fig 3A). Image stream flow cytometry analysis of the same samples demonstrated a frequency of infection of $CD14^{+}mLEP^{+}$ cells ranging from 30%, 35%, to 25%, when conditioned with no vitamin D, 10^{-8}M 25D3 or 10^{-7}M 25D3, respectively (Fig 3B). Using an unsupervised spot counting function of image stream flow cytometry, we determined the frequency of $CD14^{+}$ cells containing varying numbers of intracellular *M. leprae* and no effect of 25D3 was observed (Fig 3C). Images from image flow cytometry analysis show the number of bacteria per MΦ (Fig 3D). Cells that contained either 7 or 8 bacteria all showed large clumps of bacteria in which were difficult to interpret as an accurate number of bacteria. Overall no significant difference was observed in the number of bacteria per cell. These data indicate that vitamin D status does not alter the phagocytic capacity of IL-15 MΦ.

Vitamin D status in IL-15 MΦ triggers antimicrobial response against *M. leprae*

After the phagocytosis of invading pathogens, a major function of MΦ is to effectively mount an antimicrobial response to defend the host. However, it is unclear whether sufficient levels of 25D3 will provide MΦ with the capacity to mount an antimicrobial response. To investigate whether 25D3 status during MΦ differentiation affects the antimicrobial response, we simultaneously measured the kinetics of CAMP mRNA induction and antimicrobial activity against *M. leprae* in IL-15 MΦ. IL-15 MΦ were conditioned with or without 25D3, infected with *M. leprae* for 24, 48, and 120 hours, at which time both RNA and DNA were harvested.

The levels of CAMP mRNA in *M. leprae* infected IL-15 MΦ at 24 hours were relatively low as compared to the previous experiments in which CAMP mRNA was measured in uninfected MΦ, to the extent that CAMP mRNA was not detectable in some donors at this time point. However, the cathelicidin protein colocalized with *M. leprae* in IL-15 MΦ differentiated in 25D3, but not in IL-15 MΦ differentiated in no 25D3 24 hours post *M. leprae* infection (Fig 4A). The low level of CAMP mRNA expression was not different whether the MΦ were differentiated in the presence or absence of 25D3 (Fig 4B). One possibility for the absence of CAMP mRNA but presence of cathelicidin protein at 24 hrs post infection is that upon infection with *M. leprae* the CAMP mRNA is downregulated yet the protein was already synthesized during differentiation.

At 48 hours after *M. leprae* infection, CAMP mRNA expression was approximately 1000 fold in the IL-15 MΦ differentiated in 25D3, at either 10^{-8}M 25D3 or 10^{-7}M 25D3 (Fig 4C). At 120-hours post infection, the relative CAMP mRNA remained significantly increased in the MΦ differentiated in 25D3, approximately 200-330 fold greater than in MΦ differentiated in the absence of 25D3 (Fig 4D).

The *M. leprae* burden was measured in the infected IL-15 MΦ according to the level of bacterial DNA. The *M. leprae* burden in infected IL-15 MΦ was not affected by the presence of 25D3 during differentiation as assessed at 24 or 48 hours (Fig 4E,F). In one of the five donors, we noted a reduction in bacterial burden at 48 hours. However at 120 hours post infection the relative bacteria burden significantly decreased to 0.67 and 0.44 in IL-15 MΦ differentiated in 10^{-8}M and 10^{-7}M 25D3 compared to no 25D3, respectively (Fig 4G). The decrease in viability of *M.leprae* at 120 hours was not due to differences in macrophage number, as H36B4 levels remained constant. Antimicrobial activity against *M. leprae* was detected in IL-15 MΦ differentiated in 25D3 in all five donors. These data indicate that the presence of 25D3 during the IL-15 MΦ differentiation program and throughout *M.leprae* infection contributes to the vitamin D-dependent antimicrobial response against by *M. leprae*.

Discussion

The ability of human MΦ to mount an effective response against intracellular mycobacteria depends in part upon their ability to induce the vitamin D-dependent antimicrobial pathway [1,2,5,22]. Although sufficient levels of vitamin D are required for optimal MΦ effector function, previous studies have indicated that myeloid cell differentiation and function can be altered by vitamin D bioavailability. Here, we investigated whether the level of 25D influences MΦ differentiation and programming of an antimicrobial response against *M. leprae*. The distinct phenotypes of IL-15 MΦ and IL-10 MΦ were largely sustained during differentiation from monocytes regardless of 25D3 status, yet only IL-15 MΦ differentiated in the presence 25D3 robustly triggered the expression of CAMP mRNA and cathelicidin protein levels in a dose-dependent manner. Vitamin D status did not alter the phagocytic function of IL-15 MΦ, but a significant decrease in bacteria burden against *M. leprae* was observed at 120 hours post-infection. These data indicate that 25D3 status during IL-15 MΦ differentiation permits the induction of an antimicrobial response against intracellular *M. leprae*.

It is important for the host to mount an antimicrobial response against intracellular mycobacteria before the bacteria employ evasion mechanisms that help establish infection and progress to clinical disease [23,24]. A key finding of the present study was that the addition of 25D3 during the IL-15 induced differentiation of monocytes into MΦ led to a robust induction of the vitamin D-dependent antimicrobial pathway, including the induction of cathelicidin and an antimicrobial response against *M. leprae*. We detected a 315-fold induction of CAMP mRNA in IL-15 MΦ differentiated in the presence 10^{-8}M 25D3 as compared to SFM without 25D3 and a 1/3 reduction in the *M. leprae* burden in

infected cells. Previously we have shown that IL-15 MΦ supplemented with 10^{-8}M 25D3 post-differentiation demonstrated a 5-fold increase in CAMP mRNA and a ~50% reduction in avirulent *M. tuberculosis* (H37ra) viability [4]. However, these IL-15 MΦ were differentiated in 10% 25D insufficient FCS (16nM). These data collectively suggest that 25D levels during IL-15 MΦ differentiation facilitate their antimicrobial function as part of the innate immune response. There are situations that allow the pathogen to escape the vitamin D antimicrobial response. For example, genetic polymorphisms in the VDR have been associated with increased susceptibility to mycobacterial infection [25]. *M. leprae* evades the vitamin D antimicrobial response via the induction of a microRNA that targets the pathway [23], and by induction of type 1 interferon leading to IL-10 and subsequent suppression of the vitamin D pathway [24]. These data imply that upon the onset of microbial challenge, monocytes that are recruited to the site of infection are dependent on the presence of sufficient levels of 25D to differentiate into powerful IL-15 MΦ that fend of *M. leprae* evasion mechanisms and effectively reduce bacterial viability [1,5,26].

The addition of 25D3 during the IL-15 induced differentiation of monocytes into MΦ affected antimicrobial function, but we observed little change in cell phenotype. Regardless if the MΦ were differentiated with or without 25D3, we found that the distinct phenotypes of IL-15 MΦ and IL-10 MΦ were largely not affected. In particular, the IL-15 MΦ were $CD209^{+}CD163^{-}$ and the IL-10 MΦ were $CD209^{+}CD163^{+}$. Only IL-15 MΦ differentiated in 25D3 demonstrated both a significant increase in CD14 frequency and cellular abundance. Although CD14 is a marker that identifies VDR-activated MΦ [27], we have no evidence that the differences in CD14 expression directly affected function as

phagocytic capacity was not affected. In contrast to our findings, the addition of 1,25D3 during differentiation of monocytes into MΦ by macrophage colony-stimulating factor (M-CSF) decreased phagocytic function and the release of pro-inflammatory cytokines [18]. Similarly, the addition of 25D3 or 1,25D3 during differentiation of monocytes into dendritic cells by granulocyte-macrophage colony-stimulating factor (GM-CSF) plus IL-4 decreased the expression of DC-specific surface markers CD1a, CD80, CD86, and MHC class-II, as well as antigen presentation capacity [16,17]. In these experiments the levels of 1,25D3 were supraphysiologic, although 25D3 was added at physiologic levels. Taken together with our findings, these findings suggest that although physiologic levels of 25D may alter the differentiation of DC, it permits MΦ differentiation and enhances MΦ antimicrobial function.

In the present study we determined that clinically sufficient levels of 25D3 led to a functional difference in IL-15 MΦ, relative to MΦ differentiated in the absence of 25D3. In humans, there is a range of 25D levels that can be classified from deficient (45nM) to sufficient (98nM) [2]. Previously, we compared the ability of African American sera and Caucasian sera to induce the expression of the mRNAs encoding the antimicrobial peptides cathelicidin and beta-defensin 2 and found that African American sera was less capable to induce the antimicrobial peptides *ex vivo* due to the relatively lower 25D sera levels [1,2]. Both exogenous 25D supplementation to African American sera *ex vivo* and 25D supplementation to vitamin D deficient individuals *in vivo* significantly enhanced CAMP mRNA expression in activated monocytes and MΦ *in vitro* [1,2,28].

Our data suggest that people with higher levels of vitamin D will derive MΦ with more antimicrobial function that could prevent the establishment of infection; however, testing the effects of vitamin D status on the prevention of infection by *M. tuberculosis* is challenging. The ability to acquire a large enough population with differential 25D levels randomly will be difficult as 25D status strongly correlates with season [29], as such there are few studies that investigate the interaction of 25D status with infection by the pathogen. Deficient levels of 25D in household contacts of TB patients demonstrated either increased latent TB incidence or positive tuberculoid skin tests [29,30]; however the number of patients that acquire active TB is unclear. [31-33]. These data support continued and more thorough investigation into whether vitamin D supplementation of deficient and insufficient individuals *in vivo* can enhance the MΦ antimicrobial response against mycobacterial infections and contain the spread and outcome of disease.

In conclusion, we found that vitamin D-dependent antimicrobial MΦ differentiated in the presence of sufficient levels of 25D3 sustain a MΦ phenotype and exhibit an antimicrobial response against *M. leprae*. Our model indicates that vitamin D-dependent antimicrobial MΦ differentiated in the presence of sufficient 25D are capable of intrinsic microbicidal activity against infection. In contrast, the same MΦ differentiated in the low levels of 25D require the addition of exogenous 25D to induce activity [1,2,5,28]. These data suggest that sufficient levels of 25D at the site of microbial infection allow recruited monocytes to differentiate into vitamin D-dependent antimicrobial MΦ with the capacity to effectively reduce the viability of intracellular bacteria. Future clinical trials that study the relationship between vitamin D

supplementation and susceptibility to microbial infection will determine if the prophylactic effects of vitamin D are therapeutically beneficial.

Methods

Statistical analysis

Experiments with three or more measurements were analyzed using One Way ANOVA or with Student-Newman-Keuls Method (*P<0.05, **P<0.01, ***P<0.005, ****P<0.001) for pairwise analyses using GraphPad Prism 7 software. Error bars represent the standard error of the mean between individual donor values. A two-tailed student's t-test was used to compare two different experimental conditions.

Ethics Statement

This study was conducted according to the principles expressed in the Declaration of Helsinki and was approved by the Institutional Review Board (IRB) of the University of California at Los Angeles (UCLA). Human peripheral blood from healthy donors was acquired with informed consent (UCLA Institutional Review Board #11-001927). All adult subjects provided written informed consent. Peripheral blood mononuclear cells (PBMCs) *were isolated from the blood of healthy donors using Ficoll-Paque (GE healthcare) and monocytes were purified with plastic adherence as previously described* [34].

Macrophage differentiation

Adherent monocytes were cultured in the presence of IL-15 (R&D Systems, 200ng/ml) or IL-10 (R&D Systems, 10ng/ml) for 48 hours using Serum Free MΦ media (SFM) (Gibco) at 37^{o}C and 5% CO_2. Cell phenotypes were consistent with previously published data [10].

Flow Cytometry

The following antibody clones were used per manufacturers' protocol for flow cytometry: CD209 (DCN46), CD163 (GHI/61), CD16 (3G8), CD14 (M5E2), and CAMP/LL37/FALL39/Cathelicidin Antibody (OSX12). Differentiated MΦ were harvested and stained as previously described [1,4,5,34].

Quantitative real-time PCR (qPCR)

RNA was harvested using TRIzol reagent (Life Technologies) via phenol-chloroform extraction, followed by RNA cleanup and DNase digestion using the RNeasy Miniprep Kit (Qiagen) as previously described [35]. cDNA was synthesized using iScript cDNA synthesis kit (Bio-Rad) and stored at -80^{o}C. Primer sequences were used as follows: CYP27B1 F: ACC CGA CAC GGA GAC CTT C, CYP27B1 R: ATG GTC AAC AGC GTG GAC AC; CAMP F: TGG GCC TGG TGA TGC CT, CAMP R: CGA AGG ACA GCT TCC TTG TAG C H36B4 F: CCA CGC TGC TGA ACA TGC T, H36B4 R: TCG AAC ACC TGC TGG ATG AC. Real-time PCR was performed using SYBR Green (Kapa Biosystems) according to the manufacturers' protocol. cDNA levels were normalized with H36B4 as the housekeeping gene. Relative CAMP mRNA levels were normalized to IL-15 MΦ differentiated in the absence of vitamin D and shown as fold-change (FC). Relative CYP27B1 mRNA levels were normalized to IL-15 MΦ baseline levels and shown as fold-change (FC) as previously described [1,6,10,35].

Cathelicidin protein levels in IL-15 MΦ (microscopy)

Primary human monocytes were seeded onto chamber slides (BD falcon) and treated with IL-15 with or without the presence of vitamin D. The cells were fixed and permeabilized using fixation/permeabilization solution kit (BD Bioscience) as indicated by the manufacturer. Cells were blocked with 10% human serum for 20 minutes and stained with CAMP/LL37/FALL39/Cathelicidin Antibody (OSX12) antibody at 10µg/mL overnight. The monolayers were washed three times with cold-PBS and stained with a biotinylated-horse anti-mouse antibody (Bio-Rad) at 10µg/mL at room temperature for one-hour. The monolayers were washed again three times with cold-PBS and stained with streptavidin-conjugated to Alexa Fluor™ 488 (Invitrogen) protected from light as previously described [1,5]. The cells were washed with PBS and sealed with ProLong™ Gold antifade reagent with DAPI (Invitrogen). Microscopy images were analyzed with the SP8-SMD confocal microscope (Leica) at the Advanced Microscopy Laboratory Macro-Scale Imaging Laboratory, California Nanosystems Institute, UCLA [24].

Cathelicidin protein levels in IL-15 MΦ (flow cytometry)

IL-15 MΦ were differentiated in the presence or absence of vitamin D in a 24-well tissue culture plate (Corning). The cells were harvested and fixed with 4% paraformaldehyde for 15 minutes at room temperature in a V-bottom plate (Corning). After fixation, the MΦ were permeabilized with 0.5% saponin (Sigma) in PBS and quickly washed with a series of PBS washes. The cells were then stained using same staining protocol as described above. The cells were acquired with a BD LSRII in the Janis V. Gorgi Flow Cytometry Core Laboratory at UCLA. All analysis was done using FlowJo 10.4.2 software.

IL-15 MΦ phagocytosis (flow cytometry)

Cells were infected with PE-labeled *M. leprae* and harvested 24 hours post infection (PI). The cells were blocked with 10% human serum for 20 minutes at room temperature and stained with an anti-CD14 antibody as indicated by the manufacturer for 30 minutes on ice. The cells were then fixed with 4% paraformaldehyde for 15 minutes and analyzed by flow cytometry as previously described [4,34]. The cells were acquired with a BD LSRII in the Janis V. Gorgi Flow Cytometry Core Laboratory at UCLA. All analysis was done using FlowJo 10.4.2 software. The same samples were also analyzed using IdEAS Software, ImageStream (Amnis) as explained below.

ImageStream

The ImageStreamX MarkII imaging flow cytometer from Amnis Corporation was used for acquisition at 60X magnification. Anti-human CD14 antibody conjugated to PacBlue channel 1 was detected on the 405 nm laser at 30.00 mW, and PE labeled *M. leprae* channel 3 was detected off the 488 nm laser set at 70.00 mW. Acquisition was set to collect 5000 objects from the single cell population (Aspect Ratio Bright Field channel 4 vs. Area Bright Field channel 4).

Data was analyzed using the Amnis IDEAS software. A compensation matrix was first created using single-stained CD14 labeled macrophages and PE calibrite beads (BD). Compensated data was then applied to a template with a gating hierarchy. Focused cells were first selected from the higher population of the Gradient RMS histogram; single cells were then chosen using the same gating strategy applied during acquisition and

lastly, PE and PacBlue double positive cells were then applied to the Spot Count Wizard. Two populations containing 10 or more cells, each expressing high or low values of spots (single PE labeled *M.leprae* bacterium) were manually selected. The Spot Count Wizard has the ability to measure uptake and count spots, thus providing individual bacterial counts per cell.

M. leprae and the assay of antimicrobial assay activity

IL-15 MΦ were differentiated with or without the indicated amount of 25D for 48 hours. The MΦ were then infected with *M.leprae* overnight at an MOI of 10. The cells were washed with SFM to remove extracellular bacteria and treated with IL-15 and the indicated amounts of 25D. The infection progressed for 24 hours, 48 hours and 120 hours and all the material in the well was harvested into a 15mL conical tube. To ensure that all the material in the well was harvested, each well was washed with a series of cold PBS-EDTA washes and accumulated into their respective 15mL conical tube. Each 15mL conical tube was placed into a centrifuge for 300xg for 10 mins at 4^{o}C. The supernatants were carefully removed and the genomic DNA was isolated as previously described. [23,35] We compared RLEP DNA levels of *M.leprae* with the H36B4 levels of the IL-15 MΦ to measure bacterial burden using real-time PCR using SYBR Green as indicated by the manufacturer (Kapa Biosystems) [36,37]. The following primers sequences were used: RLEP F: GCA GCA GTA TCG TGT TAG TGA A, RLEP R: CGC TAG AAG GTT GCC GTA T; H36B4 F: CCA CGC TGC TGA ACA TGC T, H36B4 R: TCG AAC ACC TGC TGG ATG AC. The bacteria burden at each time point was normalized to IL-15 MΦ differentiated without vitamin D to quantify relative bacteria burden.

Figure Legends

Fig 1. Phenotype of IL-15 MΦ and IL-10 MΦ differentiated in 25D3. A) IL-15 MΦ (left) or IL-10 MΦ (right) were differentiated with or without the presence of 10^{-8}M 25D3 for 48 hours. Cells were stained with indicated markers and analyzed by flow cytometry. Data is represented as average frequency (%) +/- SEM relative to isotype control (n=3-4). **B)** Data is represented as the change in mean fluorescence intensity of CD14 (CD14 ΔMFI) +/- SEM relative to isotype control (n=4). *P<0.05, **P<0.01.

Fig 2. CAMP mRNA and cathelicidin protein expression in IL-15 MΦ is dependent on 25D3 status. A) IL-15 MΦ and IL-10 MΦ were differentiated in increasing concentrations of 25D3 (0 to 10^{-7}M) for 48 hours and CAMP mRNA levels were determined by qPCR. Fold change was calculated relative to IL-15 MΦ differentiated in no 25D3. Data is represented as average fold change +/- SEM (n=4-7). **B)** The frequency (%) of cathelicidin protein expression of IL-15 MΦ differentiated in increasing concentrations of 25D3 (0 to 10^{-7}M) for 48 hours. Data is represented as average frequency +/- SEM (n=6) relative to isotype control. **C)** The change in cathelicidin mean fluorescence intensity (cathelicidin ΔMFI) in IL-15 MΦ differentiated in increasing concentrations of 25D3 (0 to 10^{-7}M) for 48 hours. The data is represented as the average cathelicidin ΔMFI +/- SEM (n=6) relative to no 25D3. **D)** Monocytes were treated with IL-15 in the presence of increasing concentrations of 25D3 (0 to 10^{-7}M) for 48 hours. Cells were harvested and stained with either an anti-cathelicidin antibody or IgG1 isotype control antibody and analyzed by confocal microscopy. (Original magnification, 400x

(top row)); (6.5x zoom of original magnification (bottom row)). Scale bar = 5μm. (n=3) *P<0.05, **P<0.01, ***P<0.005, ****P<0.001.

Fig 3. IL-15 MΦ phagocytose *M. leprae*. IL-15 MΦ were differentiated in the presence of increasing concentrations of 25D3 (0 to 10^{-7}M) for 48 hours and infected with PE-labeled *M. leprae* (mLEP) for 24 hours and analyzed with either **A)** flow cytometry or **B)** image stream flow cytometry. Data is represented as average frequency of IL-15 MΦ that are positive for both CD14 and mLEP +/- SEM relative to uninfected and isotype controls (n=3). **C)** The number of $CD14^+$ IL-15 MΦ that contained 1-8 bacteria was analyzed with an unsupervised spot counting function Ideas software. Data is represented as an average number of $CD14^+mLEP^+$ for each bacterium count +/- SEM (n=3). **D)** Representative microscopy images from image stream flow cytometry analysis (1-6 bacteria per cell). Scale bar = 7μm. (n=3).

Fig 4. 25D3 status contributes to IL-15 MΦ antimicrobial response. A) Colocalization of *M. leprae* (mLEP = red) and cathelicidin (CATH=green) 24 hours PI in IL-15 MΦ differentiated in the presence of 25D3 for 48 hours. (Original magnification, 400); (6.5x zoom of original magnification). Scale bar = 5μm. IL-15 MΦ were differentiated in increasing concentrations of 25D3 (0 to 10^{-7}M) for 48 hours and infected with *M. leprae* for **B)** 24 hours (n=3), **C)** 48 hours (n=5) or **D)** 120 hours (n=5) and CAMP mRNA expression was assessed by qPCR. Data is represented as the average fold change in CAMP mRNA +/- SEM relative to IL-15 MΦ differentiated in no 25D3. IL-15 MΦ were differentiated in increasing concentrations of 25D3 (0 to 10^{-7}M) for 48

hours and infected with *M. leprae* for **E)** 24 hours (n=3), **F)** 48 hours (n=5) or **G)** 120 hours (n=5) and bacteria burden was assessed by qPCR. Data is represented as the average change in bacteria burden +/- SEM relative to IL-15 MΦ differentiated in no 25D3. *P<0.05, **P<0.01, ***P<0.005, ****P<0.001.

S1 Fig. CYP27B1 mRNA expression in IL-15 MΦ and IL-10 MΦ. Primary human monocytes were treated with either IL-15 or IL-10 for 48 hours in SFM. No significant difference is observed between CYP27B1 mRNA expression levels between IL-15 MΦ and IL-10 MΦ.

References

1 Liu, P. T. *et al.* Toll-like receptor triggering of a vitamin D-mediated human antimicrobial response. *Science* **311**, 1770-1773, doi:10.1126/science.1123933 (2006).

2 Fabri, M. *et al.* Vitamin D is required for IFN-gamma-mediated antimicrobial activity of human macrophages. *Sci Transl Med* **3**, 104ra102, doi:10.1126/scitranslmed.3003045 (2011).

3 Fabri, M. & Modlin, R. L. A vitamin for autophagy. *Cell Host Microbe* **6**, 201-203, doi:10.1016/j.chom.2009.08.008 (2009).

4 Krutzik, S. R. *et al.* IL-15 links TLR2/1-induced macrophage differentiation to the vitamin D-dependent antimicrobial pathway. *J Immunol* **181**, 7115-7120 (2008).

5 Liu, P. T., Stenger, S., Tang, D. H. & Modlin, R. L. Cutting edge: vitamin D-mediated human antimicrobial activity against Mycobacterium tuberculosis is dependent on the induction of cathelicidin. *J Immunol* **179**, 2060-2063 (2007).

6 Montoya, D. *et al.* IL-32 is a molecular marker of a host defense network in human tuberculosis. *Sci Transl Med* **6**, 250ra114, doi:10.1126/scitranslmed.3009546 (2014).

7 White, J. H. Vitamin D signaling, infectious diseases, and regulation of innate immunity. *Infect Immun* **76**, 3837-3843, doi:10.1128/IAI.00353-08 (2008).

8 White, J. H. Vitamin D as an inducer of cathelicidin antimicrobial peptide expression: past, present and future. *J Steroid Biochem Mol Biol* **121**, 234-238, doi:10.1016/j.jsbmb.2010.03.034 (2010).

9 Bursuker, I. & Goldman, R. On the origin of macrophage heterogeneity: a hypothesis. *J Reticuloendothel Soc* **33**, 207-220 (1983).

10 Montoya, D. *et al.* Divergence of macrophage phagocytic and antimicrobial programs in leprosy. *Cell Host Microbe* **6**, 343-353, doi:10.1016/j.chom.2009.09.002 (2009).

11 Koeffler, H. P., Amatruda, T., Ikekawa, N., Kobayashi, Y. & DeLuca, H. F. Induction of macrophage differentiation of human normal and leukemic myeloid stem cells by 1,25-dihydroxyvitamin D3 and its fluorinated analogues. *Cancer Res* **44**, 5624-5628 (1984).

12 Taimi, M., Chateau, M. T., Cabane, S. & Marti, J. Synergistic effect of retinoic acid and 1,25-dihydroxyvitamin D3 on the differentiation of the human monocytic cell line U937. *Leuk Res* **15**, 1145-1152 (1991).

13 Jensen, S. S., Madsen, M. W., Lukas, J., Binderup, L. & Bartek, J. Inhibitory effects of 1alpha,25-dihydroxyvitamin D(3) on the G(1)-S phase-controlling machinery. *Mol Endocrinol* **15**, 1370-1380, doi:10.1210/mend.15.8.0673 (2001).

14 Studzinski, G. P., Garay, E., Patel, R., Zhang, J. & Wang, X. Vitamin D receptor signaling of monocytic differentiation in human leukemia cells: role of MAPK pathways in transcription factor activation. *Curr Top Med Chem* **6**, 1267-1271 (2006).

15 Samuel, S. & Sitrin, M. D. Vitamin D's role in cell proliferation and differentiation. *Nutr Rev* **66**, S116-124, doi:10.1111/j.1753-4887.2008.00094.x (2008).

16 Hewison, M. *et al.* Differential regulation of vitamin D receptor and its ligand in human monocyte-derived dendritic cells. *J Immunol* **170**, 5382-5390 (2003).

17 Piemonti, L. *et al.* Vitamin D3 affects differentiation, maturation, and function of human monocyte-derived dendritic cells. *J Immunol* **164**, 4443-4451 (2000).

18 Arboleda Alzate, J. F., Rodenhuis-Zybert, I. A., Hernandez, J. C., Smit, J. M. & Urcuqui-Inchima, S. Human macrophages differentiated in the presence of vitamin D3 restrict dengue virus infection and innate responses by downregulating mannose receptor expression. *PLoS Negl Trop Dis* **11**, e0005904, doi:10.1371/journal.pntd.0005904 (2017).

19 Holick, M. F. *et al.* Evaluation, treatment, and prevention of vitamin D deficiency: an Endocrine Society clinical practice guideline. *J Clin Endocrinol Metab* **96**, 1911-1930, doi:10.1210/jc.2011-0385 (2011).

20 Bruns, H. *et al.* Vitamin D-dependent induction of cathelicidin in human macrophages results in cytotoxicity against high-grade B cell lymphoma. *Sci Transl Med* **7**, 282ra247, doi:10.1126/scitranslmed.aaa3230 (2015).

21 Adams, J. S. & Hewison, M. Update in vitamin D. *J Clin Endocrinol Metab* **95**, 471-478, doi:10.1210/jc.2009-1773 (2010).

22 Martineau, A. R. *et al.* IFN-gamma- and TNF-independent vitamin D-inducible human suppression of mycobacteria: the role of cathelicidin LL-37. *J Immunol* **178**, 7190-7198 (2007).

23 Liu, P. T. *et al.* MicroRNA-21 targets the vitamin D-dependent antimicrobial pathway in leprosy. *Nat Med* **18**, 267-273, doi:10.1038/nm.2584 (2012).

24 Teles, R. M. *et al.* Type I interferon suppresses type II interferon-triggered human anti-mycobacterial responses. *Science* **339**, 1448-1453, doi:10.1126/science.1233665 (2013).

25 Bornman, L. *et al.* Vitamin D receptor polymorphisms and susceptibility to tuberculosis in West Africa: a case-control and family study. *J Infect Dis* **190**, 1631-1641, doi:10.1086/424462 (2004).

26 Liu, P. T. *et al.* Convergence of IL-1beta and VDR activation pathways in human TLR2/1-induced antimicrobial responses. *PLoS One* **4**, e5810, doi:10.1371/journal.pone.0005810 (2009).

27 Zamani, F., Zare Shahneh, F., Aghebati-Maleki, L. & Baradaran, B. Induction of CD14 Expression and Differentiation to Monocytes or Mature Macrophages in Promyelocytic Cell Lines: New Approach. *Adv Pharm Bull* **3**, 329-332, doi:10.5681/apb.2013.053 (2013).

28 Adams, J. S. *et al.* Vitamin d-directed rheostatic regulation of monocyte antibacterial responses. *J Immunol* **182**, 4289-4295, doi:10.4049/jimmunol.0803736 (2009).

29 Balcells, M. E. *et al.* Association of vitamin D deficiency, season of the year, and latent tuberculosis infection among household contacts. *PLoS One* **12**, e0175400, doi:10.1371/journal.pone.0175400 (2017).

30 Ganmaa, D. *et al.* Vitamin D, tuberculin skin test conversion, and latent tuberculosis in Mongolian school-age children: a randomized, double-blind,

placebo-controlled feasibility trial. *Am J Clin Nutr* **96**, 391-396, doi:10.3945/ajcn.112.034967 (2012).

31 LoBue, P. A. & Castro, K. G. Is it time to replace the tuberculin skin test with a blood test? *JAMA* **308**, 241-242, doi:10.1001/jama.2012.7511 (2012).

32 Esmail, H., Barry, C. E., 3rd, Young, D. B. & Wilkinson, R. J. The ongoing challenge of latent tuberculosis. *Philos Trans R Soc Lond B Biol Sci* **369**, 20130437, doi:10.1098/rstb.2013.0437 (2014).

33 Hornum, M., Mortensen, K. L., Kamper, A. L. & Andersen, A. B. Limitations of the QuantiFERON-TB Gold test in detecting Mycobacterium tuberculosis infection in immunocompromised patients. *Eur J Intern Med* **19**, 137-139, doi:10.1016/j.ejim.2007.03.020 (2008).

34 Krutzik, S. R. *et al.* TLR activation triggers the rapid differentiation of monocytes into macrophages and dendritic cells. *Nat Med* **11**, 653-660, doi:10.1038/nm1246 (2005).

35 Wheelwright, M. *et al.* All-trans retinoic acid-triggered antimicrobial activity against Mycobacterium tuberculosis is dependent on NPC2. *J Immunol* **192**, 2280-2290, doi:10.4049/jimmunol.1301686 (2014).

36 Kim, E. W. *et al.* The Rhoptry Pseudokinase ROP54 Modulates Toxoplasma gondii Virulence and Host GBP2 Loading. *mSphere* **1**, doi:10.1128/mSphere.00045-16 (2016).

37 Martinez, A. N. *et al.* Molecular determination of Mycobacterium leprae viability by use of real-time PCR. *J Clin Microbiol* **47**, 2124-2130, doi:10.1128/JCM.00512-09 (2009).

Fig 1

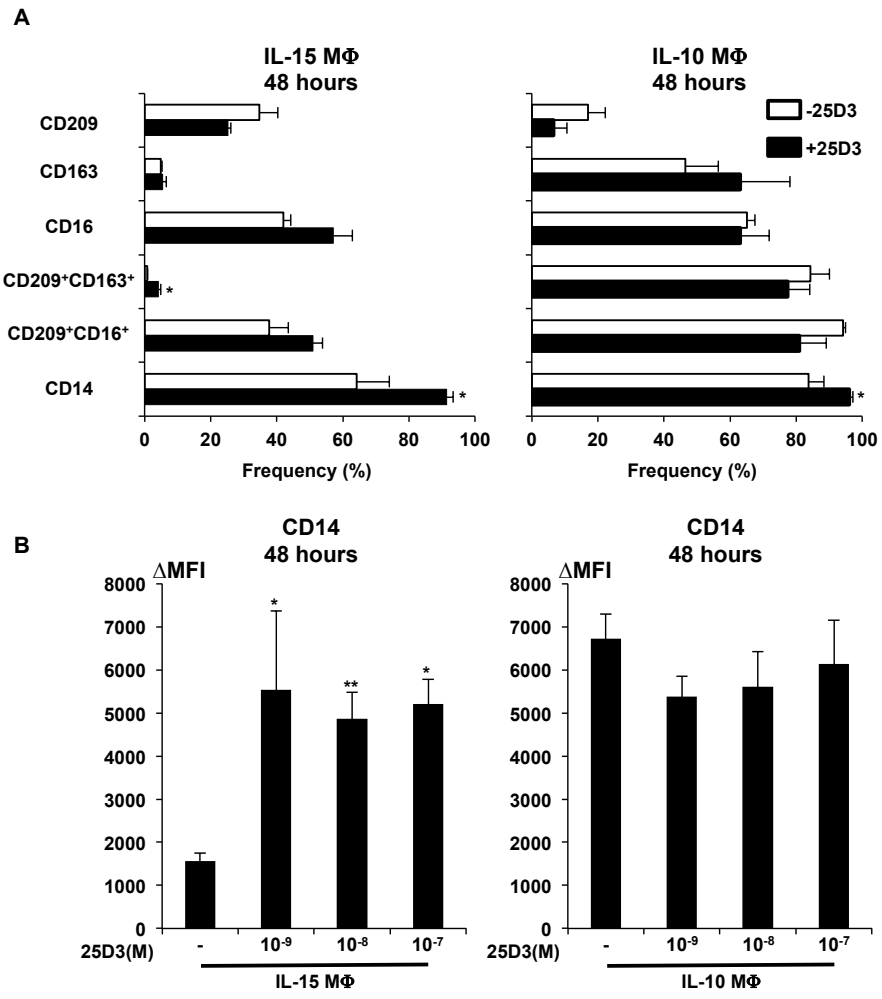
A
IL-15 MΦ
48 hours
IL-10 MΦ
48 hours
-25D3
+25D3
CD209
CD163
CD16
CD209+CD163+
CD209+CD16+
CD14
*
0
20
40
60
80
100
Frequency (%)
B
CD14
48 hours
ΔMFI
8000
7000
6000
5000
4000
3000
2000
1000
0
**
25D3(M)
-
10-9
10-8
10-7
IL-15 MΦ
IL-10 MΦ

Fig 2

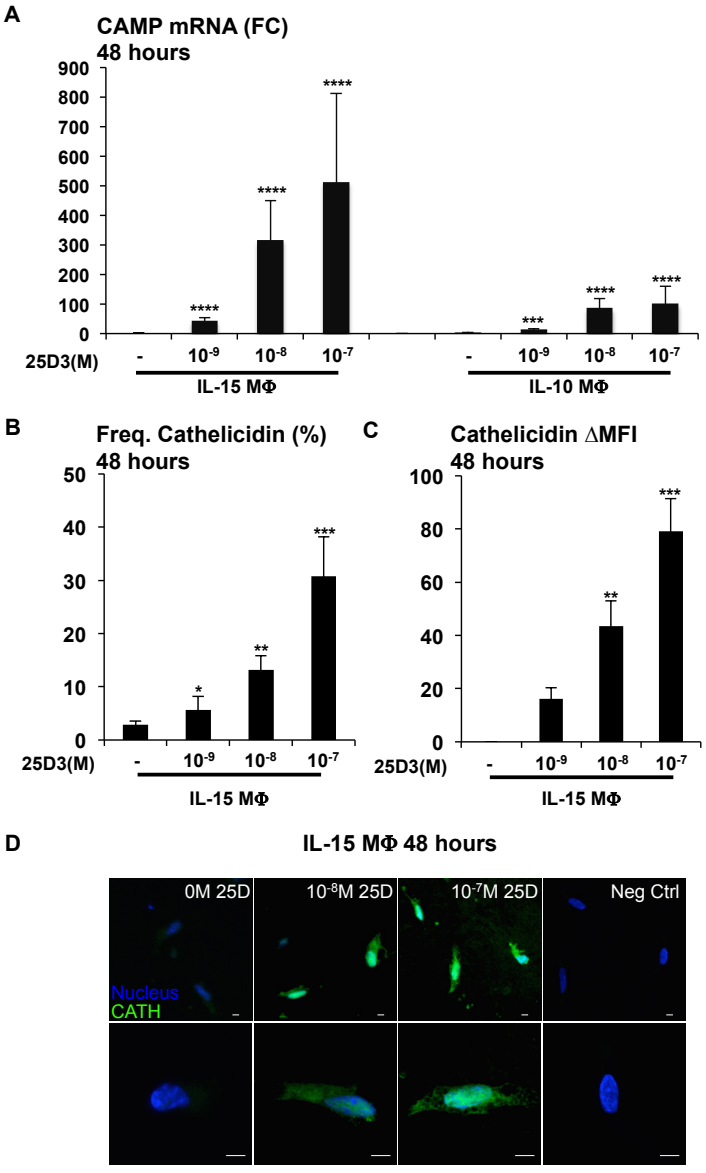
A
CAMP mRNA (FC)
48 hours
900
800
700
600
500
400
300
200
100
0
****
****
****
***
****
****
25D3(M)
-
10-9
10-8
10-7
-
10-9
10-8
10-7
IL-15 MΦ
IL-10 MΦ
B
Freq. Cathelicidin (%)
48 hours
50
40
30
20
10
0
*
**
***
25D3(M)
-
10-9
10-8
10-7
IL-15 MΦ
C
Cathelicidin ΔMFI
48 hours
100
80
60
40
20
0
**
***
25D3(M)
-
10-9
10-8
10-7
IL-15 MΦ
D
IL-15 MΦ 48 hours
0M 25D
10-8M 25D
10-7M 25D
Neg Ctrl
Nucleus
CATH

Fig 3

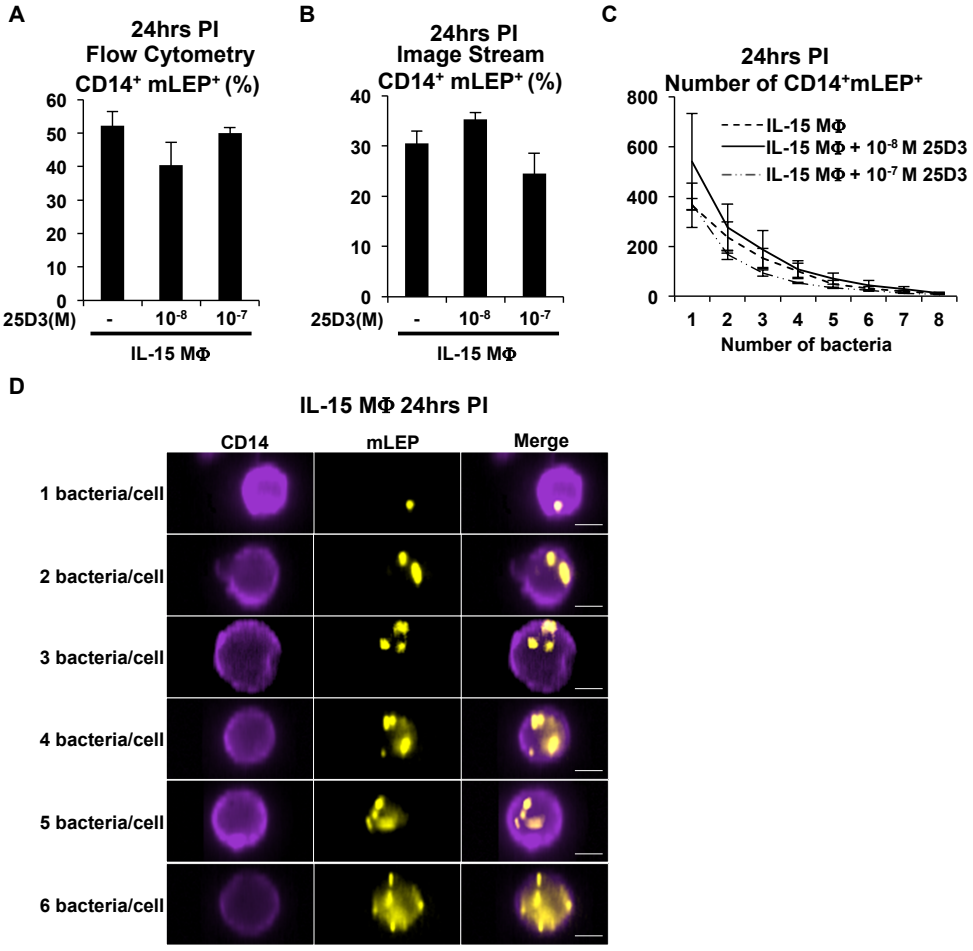
A
24hrs PI
Flow Cytometry
CD14+ mLEP+ (%)
60
50
40
30
20
10
0
25D3(M)
-
10-8
10-7
IL-15 MΦ
B
24hrs PI
Image Stream
CD14+ mLEP+ (%)
40
30
20
10
0
25D3(M)
-
10-8
10-7
IL-15 MΦ
C
24hrs PI
Number of CD14+mLEP+
800
600
400
200
0
IL-15 MΦ
IL-15 MΦ + 10-8 M 25D3
IL-15 MΦ + 10-7 M 25D3
1 2 3 4 5 6 7 8
Number of bacteria
D
IL-15 MΦ 24hrs PI
CD14
mLEP
Merge
1 bacteria/cell
2 bacteria/cell
3 bacteria/cell
4 bacteria/cell
5 bacteria/cell
6 bacteria/cell

Fig 4

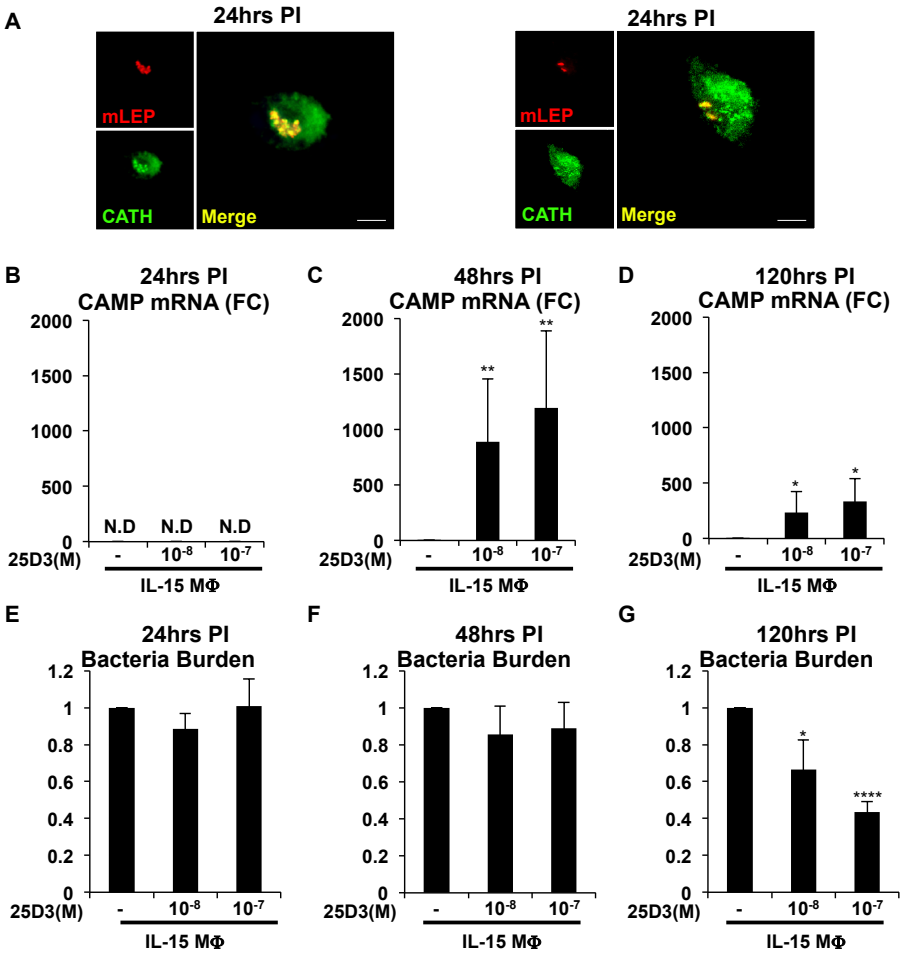
A
24hrs PI
mLEP
CATH
Merge
24hrs PI
mLEP
CATH
Merge
B
24hrs PI
CAMP mRNA (FC)
2000
1500
1000
500
0
N.D
N.D
N.D
25D3(M)
-
10-8
10-7
IL-15 MΦ
C
48hrs PI
CAMP mRNA (FC)
**
**
D
120hrs PI
CAMP mRNA (FC)
*
*
E
24hrs PI
Bacteria Burden
1.2
1
0.8
0.6
0.4
0.2
0
F
48hrs PI
Bacteria Burden
G
120hrs PI
Bacteria Burden
*
****

S1 Fig

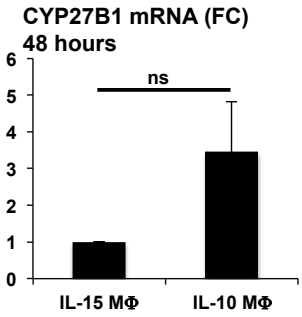

CHAPTER 3

Dendritic cell metabolism of vitamin A triggers an innate antimicrobial response in *Mycobacterium tuberculosis*-infected macrophages

Abstract

Epidemiological evidence correlates low serum vitamin A (retinol) levels with increased susceptibility to active tuberculosis (TB); however, retinol is biologically inactive and must be converted into its bioactive form all-*trans* retinoic acid (ATRA). Given that ATRA triggers an (Niemann-Pick Type C2) NPC2-dependent antimicrobial response against *M. tuberculosis*, we investigated the mechanism by which the immune system converts retinol into ATRA at the site of infection. We demonstrate that GM-CSF-derived dendritic cells (GM-DCs) but not macrophages express enzymes in the vitamin A metabolic pathway, including aldehyde dehydrogenase 1 family, member a2 (ALDH1A2) and short-chain dehydrogenase/reductase family, member 9 (DHRS9), catalysts capable of the two-step conversion of retinol into ATRA, which is subsequently released from the cell. The conditioned medium from DCs cultured with retinol stimulated antimicrobial activity from *M. tuberculosis*-infected monocytes and macrophages, as well as the expression of NPC2 in monocytes, which was blocked by specific inhibitors, including retinoic acid receptor inhibitor (RARi) or N,N-diethylaminobenzaldehyde (DEAB), an ALDH1A2 inhibitor. Additionally, mRNA and protein expression levels of ALDH1A2 are lower in tuberculosis lung tissues compared to normal lung. These results indicate that transcellular metabolism of vitamin A by DC activates macrophage antimicrobial responses.

Introduction

Globally, there are 1.7 billion people infected with *M. tuberculosis,* the etiological agent of tuberculosis (TB), of whom about 10% will progress to develop the active disease [1]. TB is prominent in low-income areas where people suffer from malnutrition, resulting in a lack of critical immunomodulatory vitamins. Epidemiological studies have correlated low serum levels of retinol, the circulating form of vitamin A, with a 10-fold increased risk and susceptibility to TB [2-4]. In addition, laboratory studies have demonstrated that the addition of ATRA, the bioactive hormonal form of vitamin A, to *M. tuberculosis*-infected macrophages induced antimicrobial activity against the pathogen *in vitro* [5-8]. Collectively these studies indicate an important role for the vitamin A system in the immune response against *M. tuberculosis* infection. However, for systemic retinol to influence immune responses at the site of infection, it must first be metabolized into ATRA.

To produce ATRA, retinol is first converted into all-*trans* retinaldehyde (ATRH), a step catalyzed by several enzymes, including DHRS9, DHRS3 and retinol dehydrogenase 10 (RDH10) [9]. ATRH is then converted into ATRA, which can be catalyzed by the ALHD1 (aldehyde dehydrogenase 1) family of enzymes, including ALDH1A1, ALDH1A2 and ALHD1A3 [10]. Several of these enzymes are expressed in DCs, an innate immune cell type which is correlated to host immune control of mycobacterial infection [11-18]. Although lung resident DCs exist in normal healthy lung, whether the immune microenvironment in the lung of a TB patient includes DCs or

vitamin A metabolic system is unclear.

We and others have previously shown that treatment of *M. tuberculosis*-infected macrophages with ATRA results in antimicrobial activity [5,6,8]. Our previous study demonstrates that at least one of the mechanisms driving the ATRA-triggered antimicrobial activity is the expression of the lipid transporter protein Niemann-Pick Type C2 (NPC2), which mediated both reduction in cellular cholesterol and antimicrobial activity [8]. Other studies have demonstrated the ability of ATRA to restrict infection as well as reduce survival of *M. tuberculosis* in macrophages by down-regulating the expression of tryptophan-aspartate containing coat protein (TACO), a cytoskeletal protein that prevents phagosome-lysosome fusion [19]. This ability of ATRA to induce these antimicrobial mechanisms suggests that the generation of ATRA from retinol may be an important factor in host defense against *M. tuberculosis* infection. Therefore, we investigated the potential of innate immune cells to metabolize and activate retinol to elicit vitamin A-driven antimicrobial responses.

Results

Activation of innate immune cells by vitamin A metabolites

To determine the vitamin A status in tuberculosis disease, we measured serum retinol levels from active tuberculosis patients and compared the levels to healthy household contacts from previously completed studies [20,21]. The serum retinol levels were significantly lower in tuberculosis patients compared to healthy household contacts (Fig. 1A). To determine if retinol or other vitamin A metabolites can directly stimulate monocytes, we stimulated primary human monocytes with equimolar concentrations (10^{-8}M) of retinol, all-*trans* retinaldahyde (ATRH), or all-*trans* retinoic acid (ATRA) for 18 hours. Following incubation, total RNA was harvested and mRNA expression levels of two ATRA response genes, NPC2 and CYP27A1 [8], were measured by qPCR. Only ATRA stimulation resulted in significant induction of NPC2 mRNA (Fig. 1B), which is a required gene for ATRA-induced antimicrobial activity against *M. tuberculosis* [8]. Similarly, CYP27A1 mRNA expression was significantly induced by ATRA but not by ATRH or retinol (Fig. 1C). Based on these results, we posit that local metabolism of retinol into ATRA at the site of infection by immune cells will be crucial to vitamin A-driven host defense.

GM-DCs express the retinol metabolism pathway

Since fetal calf serum (FCS) used for cell culture typically contains relatively high levels (~128 ng/ml) of retinol, immune cells cultured in FCS that metabolize retinol to ATRA will subsequently demonstrate an autocrine activation of the retinoic acid receptor (RAR) gene program [22]. Therefore, we sought to interrogate the gene expression profiles of human monocyte-derived macrophages and DCs for a RAR activation signature. Gene signatures of macrophages were determined from our previously published gene microarrays [15] of primary human monocytes stimulated with cytokines that drive macrophage differentiation and polarization: IL-10 (M2a), IL-15 (M1), and IL-4 (M2a). A signature for DCs was determined from a new gene microarray data of primary human monocytes stimulated with the DC differentiation driving cytokine, granulocyte-macrophage colony-stimulating factor (GM-CSF). Induction of the DC phenotype by GM-CSF was confirmed by the increase in cell surface expression of DC specific markers [23], CD206, CD86 and CD1b measured via flow cytometry as change in mean fluorescent intensity (MFI) (Fig. S1). Next, Ingenuity Pathways Analysis (IPA) of the macrophage and DC gene signatures demonstrated that the canonical pathway 'RAR activation' was significantly enriched in only the GM-CSF induced gene profile (Bonferroni's corrected P value = 0.024, Fig. S2) but none of the macrophage signatures (Bonferroni's corrected P value $\geq$ 0.32, for all macrophage signatures).

Further investigation of the retinol metabolism pathway was investigated in the GM-CSF dendritic cell expression profile. The mRNA expression of enzymes that metabolize retinol into ATRH (DHSR3, DHRS9 and RDH10) as well as ATRH into ATRA (ALDH1A1, ALDH1A2 and ALDH1A3) were examined using the gene

expression microarray. For the enzymes that metabolize retinol into ATRH, DHSR9 was significantly induced by GM-CSF; however, DHSR3 and RDH10 did not show any significant regulation by GM-CSF (Fig. 2A). As for the enzymes that metabolize ATRH into ATRA, one of two ALDH1A2 probes present on the array was significantly up-regulated, ALDH1A1 was significantly down-regulated and ALDH1A3 showed no significant regulation by GM-CSF (Fig. 2A). To confirm the microarray results, primary human monocytes were isolated from whole blood and stimulated for 24 hours with a titration of GM-CSF (0 ng/ml, 1 ng/ml, 10 ng/ml or 100 ng/ml) compared to a titration of IL-15 (40 ng/ml, 80 ng/ml). The cells were stimulated with IL-15 as a control given that the IPA did not identify a RAR activation signal by IL-15 (Fig. S2), but is known to induce vitamin D metabolism in human monocytes [23]. Following the incubation, total RNA was isolated and the expression of DHRS9 and ALDH1A2 were measured by qPCR. GM-CSF at concentrations of 1 ng/ml, 10 ng/ml and 100 ng/ml induced DHRS9 mRNA levels by 9.43-, 16.8- and 16.3- fold respectively, compared to unstimulated control (Fig. 2B). In the same experiment, 1 ng/ml, 10 ng/ml and 100 ng/ml of GM-CSF induced ALDH1A2 mRNA levels to 22.0-, 21.9- and 57.4- fold respectively, compared to unstimulated control (Fig. 2C). Since IL-15 did not induce expression of DHRS9 or ALDH1A2, we assayed CYP27B1 levels to verify that the IL-15 was active, finding that IL-15 induced significant CYP27B1 expression (Fig. 2D) as previously described [23]. Concurrent induction of DHRS9 and ALDH1A2 by GM-CSF suggests that the capacity to metabolize retinol into ATRA is part of the GM-CSF-derived DC gene program.

GM-DCs demonstrate transcellular metabolism of retinol

To establish that the induction of DHRS9 and ALDH1A2 in GM-CSF-derived DCs leads to the two-step bioconversion of retinol into ATRA, GM-CSF-derived DCs were cultured in serum-free conditions with or without retinol for six hours and retinol metabolites were measured in the cellular and supernatant fractions via high performance liquid chromatography (HPLC). The GM-CSF-derived DCs were treated with control, 1 ng/ml, or 10 ng/ml of retinol and the total levels of ATRA were measured from the cellular fraction at an average of 9.8, 150.4 and 121.0 mean arbitrary units (mAU), respectively (Fig. 3A). The ATRA contained in the supernatants from the same experiment was also quantified at 16.6, 251.2 and 2131.2 mAUs, respectively. Although ATRA was significantly higher in both the cellular and supernatant fractions when retinol was present, GM-DCs treated with 10 ng/ml of retinol demonstrated significantly higher (17.6 fold) ATRA mAUs in the supernatant compared to the cellular fraction, suggesting that the majority of ATRA produced is released into the extracellular space.

To determine whether GM-DCs-produced ATRA can transactivate innate immune cells to trigger an antimicrobial response, media with or without retinol (10 ng/ml) was conditioned by GM-DCs for 18 hours (CM). Primary human monocytes or M-CSF-derived macrophages (MDMs) were infected with either H37Ra or H37Rv, respectively, and recultured with CM from DCs with or without retinol for three days. Following the incubation, bacterial viability was assessed using our previously described PCR-based method [8]. When the infected monocytes and MDMs were cultured using CM with retinol, the resulting bacterial viability was significantly lower than cells cultured with

CM with no retinol (Fig. 3B). These data suggest that DCs are capable of triggering a retinol-dependent antimicrobial response in neighboring cells.

To ascertain the role of vitamin A metabolism in the ability of DCs to elicit antimicrobial responses *in trans*, we used two chemical inhibitors of the vitamin A pathway. DCs were cultured for 18 hours in serum free conditions with or without retinol, as well as N,N-diethylaminobenzaldehyde (DEAB), a known inhibitor of ALDH1A2 activity. The CM supernatants were collected and supplemented with FCS and used to culture fresh primary human monocytes pre-incubated for 20 minutes with or without a RAR antagonist (RARi). The RARi inhibited ATRA-induced NPC2 and CYP27A1 gene expression in monocytes at a ten-fold excess (Fig. S3A). Monocytes cultured using CM with retinol demonstrated a significant 3.8-fold increase in expression of NPC2 and a significant 3.3-fold increase in CYP27A1 mRNA compared to the CM without retinol (Fig. 3C). Concurrent treatment of the DCs with retinol and DEAB inhibited the ability of the CM to induce NPC2 and CYP27A1 in monocytes (Fig. 3C); however, DEAB had no direct effect on ATRA induction of NPC2 and CYP27A1 (Fig. S3B). Furthermore, pretreatment of monocytes with RARi prior to addition of CM also ablated the induction of NPC2 and CYP27A1 (Fig. 3C). Taken together these results indicate that DCs are able to produce ATRA from retinol and stimulate the RAR in neighboring cells.

Transcriptional profiling of retinol metabolism in TB infected lung

We hypothesize that vitamin A metabolism is suppressed at the site of infection in TB, leading to disease pathogenesis. To establish the *in vivo* relevance of vitamin A metabolism in TB, we extended our previously published analysis of microarray data, comparing the gene expression profile of human caseous TB lung tissue to unaffected lung [24]. The expanded analysis indicates that the expression of ALDH1A2, DHRS9, as well as the DC marker CD1B, was significantly less in TB as compared to unaffected lung tissue (Fig. 4A). In contrast, the IL-10-derived macrophage marker, CD163, was more highly expressed in TB tissue compared to unaffected lung [25]. These results suggest a lack of a significant vitamin A metabolic gene profile in the chronic and late state of TB disease. To investigate the early stages of infection, we utilized a previously published expression data set comparing rabbit lung after *M. tuberculosis* infection to uninfected lung tissue [26]. This analysis indicates that ALDH1A2 is significantly down-regulated at two-weeks after infection, but shows no change after 16 weeks (Fig. 4B). DHRS9 was significantly up-regulated at two weeks shown by one of two probes present on the array, but no significant change is detected otherwise (Fig. 4B). NPC2 is significantly down regulated at both two and 16 weeks, whereas CYP27A1 is significantly down-regulated only at 16 weeks (Fig. 4B). CD1b is significantly up regulated at two weeks, but becomes significantly down-regulated at 16 weeks (Fig. 4B). Lastly, CD163 is significantly up regulated at both two and 16 weeks (Fig. 4B). Taken together, with the caveat that the human and rabbit disease pathology is likely different [27], these data suggest DCs and the vitamin A metabolic pathway are down-regulated or absent in the course of tuberculosis infection.

DC-mediated retinol metabolism is absent in TB lung

To confirm the microarray findings, surgically resected lung tissue from five active TB patients were compared to normal lung tissue obtained by the UCLA Translational Pathology Core Laboratory (TPCL) by immunohistochemistry. The lung tissues were formalin-fixed, paraffin embedded, cut into sections and mounted onto slides. Lung sections from two TB patients (TB1 and TB2) patients showed little to no ALDH1A2 protein expression, whereas normal lung tissue showed positive cells dispersed throughout the lung tissue and in clusters (Fig. 5A). In terms of cellular composition, both human TB lung and human normal lung tissues contain macrophages as detected by CD163 expression (Fig. 5B), but DCs as detected by CD1B were predominately found in the normal lung (Fig. 5C). Corresponding isotype control antibodies for ALDH1a2, CD163 and CD1B show that IHC staining is specific with limited background signal (Fig. S4). Using Immunoratio, we quantified the number of ALDH1A2, CD163 and CD1B positive cells compared to nuclear staining in 4-5 sections per normal lung and 8-10 sections per TB lung. The decreased mRNA expression levels of ALDH1A2 in TB lung from the microarray data correlate with the decreased protein expression of ALDH1A2 in TB lung relative to normal lung (Fig. 5D). In contrast, we found that TB lung expressed significantly higher CD163 protein levels relative to normal lung (Fig. 5E). Lastly, the decreased CD1B mRNA expression in TB lung also correlated with the decreased protein expression of CD1B in TB lung relative to normal lung (Fig. 5F). Taken together, the decrease in ALDH1A2 and CD1B in the TB lung

indicates that the DC-mediated vitamin A metabolism is attenuated in TB lung, thus preventing ATRA mediated immune responses.

Discussion

Vitamin A metabolites have been implicated in the pathogenesis of TB in humans. Low levels of the circulating form of vitamin A, retinol, correlate with susceptibility to disease [3,4,28], whereas the bioactive form of vitamin A, ATRA, induces antimicrobial activity in *M. tuberculosis*-infected macrophages [5,6,8,19]. Given that retinol is biologically inactive, our work sought to explore the mechanism by which retinol can influence the immune response; specifically, to understand how retinol is metabolized into a bioactive form by immune cells. A bioinformatics survey of macrophage- and DC-differentiating cytokines indicated that the DC-differentiating cytokine, GM-CSF, induces expression of the vitamin A metabolism genes, DHRS9 and ALDH1A2 in primary human monocytes. GM-CSF-derived DCs, by producing ATRA from retinol and releasing it, can elicit a response *in trans* from neighboring macrophages, including induction of NPC2 and an antimicrobial response. Examining human and rabbit TB lung *in situ*, we found that expression of vitamin A metabolism genes and the DC marker CD1B were largely down regulated in lung tissue from TB patients compared to controls. Taken together, the present results indicate that DCs, through metabolism of retinol, may play a critical role of supplying a bioactive form of vitamin A to neighboring infected macrophages, eliciting antimicrobial responses in TB.

The canonical function of DCs is to regulate the adaptive immune response through antigen presentation and cytokine secretion; our results indicate that DCs can also regulate the immune response through metabolic activity. Here we provide evidence

that transcellular metabolism of vitamin A by DC leads to the release of ATRA and uptake by macrophages. Previously, prostaglandins have been metabolized by one cell and then delivered to monocytes and macrophages [29,30]. In contrast, our results provide novel evidence that transcellular metabolism contributes to host defense as DC conversion of retinol to ATRA led to an antimicrobial activity against *M. tuberculosis* in macrophages. The transcellular metabolism of retinol by DC to activate a macrophage antimicrobial pathway complements intracellular metabolism of vitamin D in macrophages leading to a distinct antimicrobial response [31].

The role of DCs in TB pathogenesis is not well defined due to the lack of an accessible experimental animal system that accurately models the human disease as well as the difficulty in acquiring lung tissue samples from active and latent TB patients. Many of the immune paradigms described for the host immune response to mycobacterial infections have, therefore, been established by studying other human mycobacterial diseases, especially leprosy, which is caused by dermal infection with *M. leprae*. $CD1b^{+}$ DCs were found in the granulomas derived from patients with the self-limiting form of leprosy (tuberculoid); in contrast, DCs were absent in the lesions derived from patients with the disseminated form of leprosy (lepromatous) [32]. Examination of resected lung tissue from patients with active TB confirmed similar results, indicating that expression of the DC specific marker, CD1b, as well as ALDH1A2 are significantly diminished relative to normal lung. However, it is unclear whether the decrease in CD1b and ALDH1A2 is due to DC cell death [33], transmigration away from the lung [34] or defective DC differentiation [35]. Since DC status and function correlate with favorable outcome to

disease, factors that regulate DCs during infection in the complex microenvironment of granulomas will warrant further investigation.

We demonstrate here that generation of ATRA by DCs can elicit antimicrobial activity from infected monocytes/macrophages; however, due to the pleiotropic effects of ATRA on the immune system, ATRA modulates other cellular innate and adaptive immune responses that are beneficial to the host at the site of *M. tuberculosis* infection, such as autophagy [36]. For example, ATRA has been shown to drive monocyte differentiation into $CD209^+$ macrophages with antimicrobial properties [37], or macrophages with tissue-preservation/wound-healing functions [38]. ATRA can also regulate the adaptive immune response through inducing differentiation of $Foxp3^+$ regulatory T-cells, as well as preserving Th1 inflammatory responses [39]. In combination, $CD209^+$ macrophages and the Th1 inflammatory response are critical to the clearance of mycobacterium from the host [40-42], whereas tissue-like macrophages are critical to sustaining granulomas thus preventing the spread of disease within the host *in vivo* [43]. Studies have also indicated that ATRA regulates the composition of the extracellular matrix through induction of a gene expression profile that drives tissue preservation and wound healing. Active TB lung show an increase of MMP-1, MMP-8 and MMP-9 protein expression and decrease in TIMP-1 protein expression, which results in pulmonary cavitation [44-46]. In contrast, stimulation of monocytes with ATRA decreases mRNA expression of MMP-1/MMP-9, and increases the expression of TIMP-1, leading to tissue preservation and wound healing [38]. On the other hand, since sustained inflammation in the lung can lead to severe lung tissue damage or mortality, regulation of

chronic inflammation by FoxP3^{+} regulatory T-cells can be important in disease outcome and reduction of mortality [47]. The diverse roles of ATRA-mediated immunological pathways suggest that regulating vitamin A metabolism at the site of infection can play a critical role in balancing the antimicrobial response and mitigate inflammation-triggered tissue damage in TB.

Clinical studies have shown that patients with active TB have lower circulating retinol levels compared to healthy individuals [2-4]; however, retinol supplementation has demonstrated mixed results [48-52]. Yet, Omowunmi *et al* demonstrate that household contacts who are vitamin A deficient have a 10-fold increased risk in acquiring tuberculosis disease [2], and active TB patients treated with chemotherapy exhibit increased circulating retinol levels [4]. These studies indicate that the vitamin A system plays an important role in mitigating TB; however, the mechanism by which retinol influences the immune response is not a direct effect. Our results here demonstrate that for retinol to trigger an antimicrobial response, it must first be metabolized into ATRA; therefore, since TB lung has lower expression of ALDH1A2 systemic restoration of retinol levels will have minimal effects at the site of infection with a lack of local transcellular metabolism. Therefore, further studies are needed to enhance metabolism of retinol as an adjuvant to therapy of TB. Alternatively, given that normal lung expresses the vitamin A metabolic machinery, supplementation of retinol deficient individuals prior to exposure to *M. tuberculosis* could provide a strategy to prevent the spread of disease.

Materials and Methods

Statistical analysis

A two-tailed student's t-test was used to compare two different experimental conditions. Experiments with three or more measurements were analyzed using One Way ANOVA or Kruskal-Wallis One Way ANOVA on Ranks as appropriate with Student-Newman-Keuls Method for pairwise analyses using GraphPad Prism 7 software. Error bars represent the standard error of the mean between individual donor values. The p values are either precisely indicated in the text or noted in the figures using the following convention: * = $p < 0.05$, ** = $p < 0.01$, *** = $p < 0.001$.

Reagents

Retinol, ATRA, and ATRH were purchased (Sigma-Aldrich), dissolved in DMSO and stored at −80°C in small aliquots protected from light. Unless stated, the retinol, ATRH, and ATRA were utilized at 10^{-8}M. Recombinant IL-15 (R&D systems) and GM-CSF (R&D systems) were cultured with monocytes in RPMI 1640 (Gibco) and 10% fetal calf serum (FCS) (Omega Scientific). Macrophage-colony stimulating factor (M-CSF) (R&D systems) differentiated monocytes into macrophages as described as previously described [8]. Immunohistochemistry was performed with the following antibodies: purified-CD1b (MT101, BD biosciences), purified-ALDH1a2 (ab75674, ABcam), and purified-CD163 (EDHu-1, Biorad).

Retinol measurements of clinical samples

Adult TB contacts (n=202) and adult patients with smear-positive pulmonary TB (n=145) were recruited from TB clinics in London, UK, as previously described [20,21]. Serum concentrations of retinol were determined by high performance liquid chromatography (HPLC) in the clinical biochemistry departments of Northwick Park Hospital (TB contacts) and the Royal London Hospital (TB patients). The studies were approved by the Research Ethics Committees of North East London, Harrow and East London and The City Research Ethics Committee (REC refs. P/02/146, EC 2759 and 06/Q0605/83), and written informed consent to participate was obtained from all participants.

Cell Culture

This study was conducted according to the principles expressed in the Declaration of Helsinki, and was approved by the Institutional Review Board of the University of California at Los Angeles. Whole blood from healthy donors were acquired from two sources: 1) through the UCLA CFAR Virology Core and 2) UCLA IRB #92-10-591-31 with informed consent. Peripheral Blood Mononuclear Cells (PBMCs) were isolated from the peripheral blood of healthy donors using Ficoll-Paque (GE healthcare) density gradient, and monocytes were purified by plastic adherence as previously described [8,16,23].

Monocyte-derived macrophages (MDMs) and granulocyte-macrophage colony-stimulating factor (GM-CSF)-derived DCs were produced as previously described [16,23].

Flow Cytometry

The following antibodies (BD Biosciences) were used for flow cytometry: CD1b-FITC (MT101), CD86-APC (FUN-1), and CD206-PE (19.2). DCs were harvested and subsequently stained as previously described [16].

Quantitative real-time PCR

Gene expression of CYP27B1, CYP27A1, NPC2, DHRS9 and ALDH1a2 were analyzed by quantitative real-time RT-PCR (qPCR) as described previously described [8]. The primers are as follows: ALDH1a2 Forward 5'-TTG GTT CAG TGT GGA GAA GG-3', ALDH1a2 Reverse 5'-AAA GCT TGC AGG AAT GGT TTG -3', DHRS9 Forward 5'-CTT GCA ATC GTT GGA GGG GGC T -3', DHRS9 Reverse 5'-AGA CAG CTG CTC CCA AAT GGC G-3'.

Bioconversion of retinol to all-trans retinoic acid (ATRA)

Dendritic cells were differentiated as described above and treated with or without retinol for 6-hours in serum free conditions. The cultures were harvested and the supernatants and cellular fractions were separated by centrifugation (300g). Retinoids

were extracted in hexane and samples were analyzed by high performance liquid chromatography as previously described [53]. ATRA levels were expressed as milli absorbance units (mAU).

Conditioned media

DCs were generated from primary human monocytes treated with GM-CSF for 2 days. The DCs were harvested, washed, enumerated, and a portion was pre-treated with DEAB (STEMCELL Tech.) for 20 minutes, and the all DCs were treated with or without retinol for 18 hours at 37^{o}C and 5% CO_2. The conditioned media was harvested, filtered with a 0.2um filter, aliquoted, and frozen in an -80^{o}C freezer. Fresh monocytes were then isolated by plastic adherence, and a portion were pre-treated with RARi (Sigma) for 20 minutes at 37^{o}C and 5%CO_2, then 900uL of conditioned media and 100uL of fresh FCS were added to the culture. The cells were incubated for 18 hours and the gene expression of NPC2 was measured as explained above.

M. tuberculosis and antimicrobial assay

H37ra and H37rv were cultured, harvested, and enumerated as previously described [8]. Monocytes and macrophages were isolated as explained above and infected with either H37ra or H37rv, respectively for 24 hours. Extracellular bacteria were vigorously washed out of the tissue culture well, the cells were treated with 90% of conditioned media and 10% of fresh FCS and incubated for 3 days. The monolayers

were harvested and bacteria viability was calculated with a PCR based method as previously described [8], which compares 16S RNA levels to a genomic DNA (IS6110) levels as an indicator of bacterial viability. Following the incubation, the cells are harvested and divided. Half of the cells were lysed by boiling at 100°C for 5 minutes then snap frozen at -80°C. Total RNA was isolated from the remaining half using Trizol (Life Technologies) according to the manufacturer's recommended protocol, followed by RNA cleanup and on column DNAse digestion using RNeasy Miniprep Kit (Qiagen, Valencia, CA). cDNA was synthesized from the total RNA using the iScript cDNA Synthesis kit (BioRad, Hercules, CA) according to the manufacturer's recommended protocol. The bacterial 16S rRNA, and genomic element DNA levels were then assessed from the cDNA and cellular lysate, respectively, using real time PCR using iQ SYBR Green (BioRad). Comparison of the bacterial DNA to the mammalian genomic 36B4 levels was used to monitor infectivity between all the conditions in the assay as well as PCR quality. The 16S and DNA values were calculated using the DDCT analysis, with the mammalian bacterial DNA value serving as the housekeeping gene.

Caseous vs human lung microarray data

For the caseous tuberculosis granuloma and WGCNA validation microarray analysis, data files were obtained from the Gene Expression Omnibus database (http://www.ncbi.nlm.nih.gov/geo/, accession numbers GSE20050, GSE23073, GSE13762, and GSE28995) [54]. Gene expression levels were normalized to G3PDH.

Since there are multiple G3PDH probes represented on the microarray, the NPC2 and IL6 probe values were normalized to every G3PDH probe and averaged.

Microarray analysis of macrophage and DC profiles

Expression profiles of IL-10-, IL-15-, and IL-4-derived macrophages were analyzed from previous data deposited in the Gene Expression Omnibus database (http://www.ncbi.nlm.nih.gov/geo/) in series entity GSE59184 [15]. Briefly, adherent PBMC from four healthy individuals were stimulated with indicated cytokine and $CD14^+$ cells were harvested at 0h, 6h, or 24h after stimulation. RNA expression analyzed by Affymetrix Human U133 Plus 2.0 array. DC expression profiles were derived from $CD14^+$ purified monocytes from three healthy individuals then stimulated with recombinant GM-CSF (100U/ml) for 0, 3h, or 12h. Total RNA was isolated and then processed by the University of California Los Angeles Clinical Microarray Core Facility using Affymetrix Human U133 Plus 2.0 array and normalized as previously described [8,31]. Expression gene signatures of DC and macrophage were determined by analyzing genes with ≥ 1.5 fold-change, P value ≤ 0.05, and experimental minus baseline intensity ≤ 100 across all time points versus time 0. Gene signatures were then analyzed by Ingenuity Pathways Analysis (Qiagen) using the canonical pathways comparison function for nuclear receptor activation. Microarray data from rabbit lung was downloaded from GSE33094 [26]. Briefly, New Zealand White rabbits infected via aerosol with *M. tuberculosis* HN878 and total RNA isolated from rabbit lungs at indicated times. Agilent-020908 Oryctolagus cuniculus two-color Oligo Microarray was utilized using

one channel for infected and the other color channel for uninfected per sample. Gene expression represented as the fold-change between Mtb-HN878 infected and uninfected animals at indicated times post infection.

Figure Legends

Fig. 1. Activation of innate immune cells by vitamin A metabolites. (**A**) Black dots represent the serum retinol levels of TB household contact (TB contacts) or active TB patients. The red line indicates the average retinol sera levels in each group $\pm$ SEM. *P* value by Student's *t* test; *** = $p < 0.001$. Primary human monocytes were treated with either vehicle alone (CTRL), retinol (10^{-8}M), retinaldehyde (ATRH) (10^{-8}M), or all-trans retinoic acid (ATRA) (10^{-8}M) for 18 hours and the mRNA expression levels of (**B**) NPC2 and (**C**) CYP27A1 were measured via qPCR. Data shown is fold change (FC) vs CTRL, n = 3-7. *P* value by one-way ANOVA; * = $p < 0.05$, ** = $p < 0.01$, *** = $p < 0.001$.

Fig. 2. GM-DCs express the retinol metabolism pathway. (**A**) Primary human monocytes stimulated with GM-CSF for zero, three and 12 hours, then gene expression was profiled using microarrays. Expression data of vitamin A pathway genes, DHRS3, DHRS9, RHD10, ALDH1A1, ALDH1A2, and ALDH1A3 are displayed as mean expression in arbitrary units (AU) of three independent donors $\pm$ SEM. Primary human monocytes stimulated with a titration of GM-CSF or IL-15 for 18 hours and mRNA expression of (**B**) DHRS9 (n = 3-5) and (**C**) ALDH1A2 (n=3-6) were measured by qPCR. (**D**) Induction of CYP27B1 mRNA expression in monocytes by IL-15 was measured by

qPCR (n = 3). *P* value by one-way ANOVA; * = $p < 0.05$, ** = $p < 0.01$, *** = $p < 0.001$.

Fig. 3. GM-DCs demonstrate transcellular metabolism of retinol. (**A**) GM-CSF-derived DCs were treated with the indicated amount of retinol for six hours in serum free conditions and the amount of ATRA in the cellular (Cell) and supernatant (Supe) fractions were analyzed via HPLC. Data represent the mean ± SEM of the average area of ATRA peak from HPLC plots of four independent donors. (**B**) Primary human monocytes were infected with *M. tuberculosis* H37ra and MDMs were infected with *M. tuberculosis* H37rv, then cultured with media conditioned by DCs with or without retinol for three days. Following incubation, bacteria viability is measured by qPCR. Data shown is mean bacterial viability comparing the CM with retinol to without retinol ± SEM (n = 4-5). (**C**) Primary human monocytes preteated with or without RARi, were cultured in DC conditioned media generated as described above with or without DEAB, for 18 hours. NPC2 and CYP27A1 expression levels were measured by qPCR. Data shown is mean fold change vs. control ± SEM (n = 3-7). *P* value by one-way ANOVA; * = $p < 0.05$, ** = $p < 0.01$, *** = $p < 0.001$.

Fig. 4. Transcriptional profiling of retinol metabolism in TB infected lung. Expression of vitamin A metabolism (ALDH1A2 and DHRS9) and activation (NPC2 and CYP27A1) genes as well as DC (CD1b) and macrophage (CD163) markers in (**A**) human caseous TB vs. normal lung tissue and (**B**) rabbit lung two and 16 weeks post *M. tuberculosis*

infection as measured by gene microarray. *P* value by one-way ANOVA; * = $p < 0.05$, ** = $p < 0.01$, *** = $p < 0.001$.

Fig. 5. DC-mediated retinol metabolism is absent in TB lung. TB patient lung tissue and normal lung protein expression of (**A**) ALDH1A2, (**B**) CD163 and (**C**) CD1B by immunohistochemistry. Data shown is representative images (TB n = 8-10, normal n = 4-5). Scale bar = 40μm. Expression of (**D**) ALDH1A2, (**E**) CD163 and (**F**) CD1B in TB vs. normal lung was quantified per nucleated cell using Immunoratio. Data shown is mean %+ cells/nucleus + SEM. *P* value by Student's *t* test; * = $p < 0.05$, ** = $p < 0.01$, *** = $p < 0.001$.

Fig. S1. GM-CSF induces DC phenotype. Primary human monocytes were differentiated into DCs by stimulation with GM-CSF for 48 hours. Cell surface markers CD206, CD86 and CD1B were assessed by flow cytometry using monoclonal antibodies (mAB) and their corresponding isotype controls (Iso). Data shown is average of the mean fluorescence intensity (MFI) $\pm$ SEM (n = 4). *P* value by Student's *t* test; * = $p < 0.05$, ** = $p < 0.01$, *** = $p < 0.001$.

Fig. S2. IPA predicts GM-DCs are cellular source of retinol metabolism. Ingenuity analysis of RAR activation gene signature in GM-CSF, IL-10, IL-15 and IL-4 stimulated primary human monocytes.

Fig. S3. RARi blocked ATRA induced genes, but not DEAB. Primary human monocytes are pretreated with (**A**) RARi or (**B**) DEAB at the indicated concentrations then stimulated with 10^{-8}M ATRA for 18 hours. Expression of NPC2 and CYP27A1 was

measured by qPCR. Data shown is mean FC ± SEM (n = 4). *P* value by one-way ANOVA; * = $p < 0.05$, ** = $p < 0.01$, *** = $p < 0.001$.

Fig. S4. Representative isotype control stains for normal and TB lung. Corresponding isotype controls for immunohistochemistry comparing TB lung tissue vs normal lung. (**A**) Rb IgG isotype control antibody for ALDH1A2 (**B**) mouse IgG1 isotype control antibody for CD163 and CD1b. Scale bar = 40μm.

References and notes

1 Houben, R. M. & Dodd, P. J. The Global Burden of Latent Tuberculosis Infection: A Re-estimation Using Mathematical Modelling. *PLoS Med* **13**, e1002152, doi:10.1371/journal.pmed.1002152 (2016).

2 Aibana, O. *et al.* Impact of Vitamin A and Carotenoids on the Risk of Tuberculosis Progression. *Clin Infect Dis* **65**, 900-909, doi:10.1093/cid/cix476 (2017).

3 Mugusi, F. M., Rusizoka, O., Habib, N. & Fawzi, W. Vitamin A status of patients presenting with pulmonary tuberculosis and asymptomatic HIV-infected individuals, Dar es Salaam, Tanzania. *Int J Tuberc Lung Dis* **7**, 804-807 (2003).

4 Ramachandran, G. *et al.* Vitamin A levels in sputum-positive pulmonary tuberculosis patients in comparison with household contacts and healthy 'normals'. *Int J Tuberc Lung Dis* **8**, 1130-1133 (2004).

5 Anand, P. K., Kaul, D. & Sharma, M. Synergistic action of vitamin D and retinoic acid restricts invasion of macrophages by pathogenic mycobacteria. *J Microbiol Immunol Infect* **41**, 17-25 (2008).

6 Crowle, A. J. & Ross, E. J. Inhibition by retinoic acid of multiplication of virulent tubercle bacilli in cultured human macrophages. *Infect Immun* **57**, 840-844 (1989).

7 Costet, P. *et al.* Retinoic acid receptor-mediated induction of ABCA1 in macrophages. *Mol Cell Biol* **23**, 7756-7766 (2003).

8 Wheelwright, M. *et al.* All-trans retinoic acid-triggered antimicrobial activity against Mycobacterium tuberculosis is dependent on NPC2. *J Immunol* **192**, 2280-2290, doi:10.4049/jimmunol.1301686 (2014).

9 Adams, M. K., Belyaeva, O. V., Wu, L. & Kedishvili, N. Y. The retinaldehyde reductase activity of DHRS3 is reciprocally activated by retinol dehydrogenase 10 to control retinoid homeostasis. *The Journal of biological chemistry* **289**, 14868-14880, doi:10.1074/jbc.M114.552257 (2014).

10 Black, W. J. *et al.* Human aldehyde dehydrogenase genes: alternatively spliced transcriptional variants and their suggested nomenclature. *Pharmacogenet Genomics* **19**, 893-902, doi:10.1097/FPC.0b013e3283329023 (2009).

11 Sato, T. *et al.* Human CD1c(+) myeloid dendritic cells acquire a high level of retinoic acid-producing capacity in response to vitamin D(3). *J Immunol* **191**, 3152-3160, doi:10.4049/jimmunol.1203517 (2013).

12 Coombes, J. L. *et al.* A functionally specialized population of mucosal CD103+ DCs induces Foxp3+ regulatory T cells via a TGF-beta and retinoic acid-dependent mechanism. *J Exp Med* **204**, 1757-1764, doi:10.1084/jem.20070590 (2007).

13 Villablanca, E. J. *et al.* MyD88 and retinoic acid signaling pathways interact to modulate gastrointestinal activities of dendritic cells. *Gastroenterology* **141**, 176-185, doi:10.1053/j.gastro.2011.04.010 (2011).

14 Feng, T., Cong, Y., Qin, H., Benveniste, E. N. & Elson, C. O. Generation of mucosal dendritic cells from bone marrow reveals a critical role of retinoic acid. *Journal of immunology* **185**, 5915-5925, doi:10.4049/jimmunol.1001233 (2010).

15 Montoya, D. *et al.* IL-32 is a molecular marker of a host defense network in human tuberculosis. *Sci Transl Med* **6**, 250ra114, doi:10.1126/scitranslmed.3009546 (2014).

16 Krutzik, S. R. *et al.* TLR activation triggers the rapid differentiation of monocytes into macrophages and dendritic cells. *Nat Med* **11**, 653-660, doi:10.1038/nm1246 (2005).

17 Molenaar, R. *et al.* Expression of retinaldehyde dehydrogenase enzymes in mucosal dendritic cells and gut-draining lymph node stromal cells is controlled by dietary vitamin A. *J Immunol* **186**, 1934-1942, doi:10.4049/jimmunol.1001672 (2011).

18 Jaensson-Gyllenback, E. *et al.* Bile retinoids imprint intestinal CD103+ dendritic cells with the ability to generate gut-tropic T cells. *Mucosal Immunol* **4**, 438-447, doi:10.1038/mi.2010.91 (2011).

19 Anand, P. K. & Kaul, D. Downregulation of TACO gene transcription restricts mycobacterial entry/survival within human macrophages. *FEMS Microbiol Lett* **250**, 137-144, doi:10.1016/j.femsle.2005.06.056 (2005).

20 Martineau, A. R. *et al.* High-dose vitamin D(3) during intensive-phase antimicrobial treatment of pulmonary tuberculosis: a double-blind randomised controlled trial. *Lancet* **377**, 242-250, doi:10.1016/S0140-6736(10)61889-2 (2011).

21 Martineau, A. R. *et al.* A single dose of vitamin D enhances immunity to mycobacteria. *Am J Respir Crit Care Med* **176**, 208-213, doi:10.1164/rccm.200701-007OC (2007).

22 Hengesbach, L. M. & Hoag, K. A. Physiological concentrations of retinoic acid favor myeloid dendritic cell development over granulocyte development in cultures of bone marrow cells from mice. *J Nutr* **134**, 2653-2659 (2004).

23 Krutzik, S. R. *et al.* IL-15 links TLR2/1-induced macrophage differentiation to the vitamin D-dependent antimicrobial pathway. *J Immunol* **181**, 7115-7120 (2008).

24 Kim, M. J. *et al.* Caseation of human tuberculosis granulomas correlates with elevated host lipid metabolism. *EMBO Mol Med* **2**, 258-274, doi:10.1002/emmm.201000079 (2010).

25 Montoya, D. *et al.* Divergence of macrophage phagocytic and antimicrobial programs in leprosy. *Cell Host Microbe* **6**, 343-353, doi:10.1016/j.chom.2009.09.002 (2009).

26 Subbian, S. *et al.* Chronic pulmonary cavitary tuberculosis in rabbits: a failed host immune response. *Open Biol* **1**, 110016, doi:10.1098/rsob.110016 (2011).

27 Kruml, J., Trnka, L., Urbancik, R. & Kuska, J. Histological Differences between Experimental Cavernous Tuberculosis in Rabbits and Human Cavitary Disease. *Am Rev Respir Dis* **92**, 299-302, doi:10.1164/arrd.1965.92.2.299 (1965).

28 Aibana, O. *et al.* Nutritional Status and Tuberculosis Risk in Adult and Pediatric Household Contacts. *PloS one* **11**, e0166333, doi:10.1371/journal.pone.0166333 (2016).

29 Bigby, T. D. & Meslier, N. Transcellular lipoxygenase metabolism between monocytes and platelets. *J Immunol* **143**, 1948-1954 (1989).

30 Folco, G. & Murphy, R. C. Eicosanoid transcellular biosynthesis: from cell-cell interactions to in vivo tissue responses. *Pharmacol Rev* **58**, 375-388, doi:10.1124/pr.58.3.8 (2006).

31 Liu, P. T. *et al.* Toll-like receptor triggering of a vitamin D-mediated human antimicrobial response. *Science* **311**, 1770-1773, doi:10.1126/science.1123933 (2006).

32 Ridley, D. S. & Jopling, W. H. Classification of leprosy according to immunity. A five-group system. *Int J Lepr Other Mycobact Dis* **34**, 255-273 (1966).

33 Ryan, R. C., O'Sullivan, M. P. & Keane, J. Mycobacterium tuberculosis infection induces non-apoptotic cell death of human dendritic cells. *BMC Microbiol* **11**, 237, doi:10.1186/1471-2180-11-237 (2011).

34 Darmanin, S. *et al.* All-trans retinoic acid enhances murine dendritic cell migration to draining lymph nodes via the balance of matrix metalloproteinases and their inhibitors. *Journal of immunology* **179**, 4616-4625 (2007).

35 Stenger, S., Niazi, K. R. & Modlin, R. L. Down-regulation of CD1 on antigen-presenting cells by infection with Mycobacterium tuberculosis. *Journal of immunology* **161**, 3582-3588 (1998).

36 Coleman, M. M. *et al.* All-trans Retinoic Acid Augments Autophagy during Intracellular Bacterial Infection. *Am J Respir Cell Mol Biol*, doi:10.1165/rcmb.2017-0382OC (2018).

37 Liu, P. T. *et al.* CD209(+) macrophages mediate host defense against Propionibacterium acnes. *Journal of immunology* **180**, 4919-4923 (2008).

38 Jalian, H. R. *et al.* All-trans retinoic acid shifts Propionibacterium acnes-induced matrix degradation expression profile toward matrix preservation in human monocytes. *J Invest Dermatol* **128**, 2777-2782, doi:10.1038/jid.2008.155 (2008).

39 Brown, C. C. *et al.* Retinoic acid is essential for Th1 cell lineage stability and prevents transition to a Th17 cell program. *Immunity* **42**, 499-511, doi:10.1016/j.immuni.2015.02.003 (2015).

40 Fabri, M. *et al.* Vitamin D is required for IFN-gamma-mediated antimicrobial activity of human macrophages. *Sci Transl Med* **3**, 104ra102, doi:10.1126/scitranslmed.3003045 (2011).

41 Krutzik, S. R. *et al.* Activation and regulation of Toll-like receptors 2 and 1 in human leprosy. *Nat Med* **9**, 525-532, doi:10.1038/nm864 (2003).

42 Realegeno, S. *et al.* S100A12 Is Part of the Antimicrobial Network against Mycobacterium leprae in Human Macrophages. *PLoS Pathog* **12**, e1005705, doi:10.1371/journal.ppat.1005705 (2016).

43 Gundra, U. M. *et al.* Vitamin A mediates conversion of monocyte-derived macrophages into tissue-resident macrophages during alternative activation. *Nat Immunol* **18**, 642-653, doi:10.1038/ni.3734 (2017).

44 Al Shammari, B. *et al.* The Extracellular Matrix Regulates Granuloma Necrosis in Tuberculosis. *J Infect Dis* **212**, 463-473, doi:10.1093/infdis/jiv076 (2015).

45 Elkington, P. *et al.* MMP-1 drives immunopathology in human tuberculosis and transgenic mice. *The Journal of clinical investigation* **121**, 1827-1833, doi:10.1172/JCI45666 (2011).

46 Taylor, J. L. *et al.* Role for matrix metalloproteinase 9 in granuloma formation during pulmonary Mycobacterium tuberculosis infection. *Infect Immun* **74**, 6135-6144, doi:10.1128/IAI.02048-05 (2006).

47 Boer, M. C., Joosten, S. A. & Ottenhoff, T. H. Regulatory T-Cells at the Interface between Human Host and Pathogens in Infectious Diseases and Vaccination. *Front Immunol* **6**, 217, doi:10.3389/fimmu.2015.00217 (2015).

48 Karyadi, E. *et al.* A double-blind, placebo-controlled study of vitamin A and zinc supplementation in persons with tuberculosis in Indonesia: effects on clinical response and nutritional status. *Am J Clin Nutr* **75**, 720-727 (2002).

49 Mathur, M. L. Role of vitamin A supplementation in the treatment of tuberculosis. *Natl Med J India* **20**, 16-21 (2007).

50 Pakasi, T. A. *et al.* Zinc and vitamin A supplementation fails to reduce sputum conversion time in severely malnourished pulmonary tuberculosis patients in Indonesia. *Nutr J* **9**, 41, doi:10.1186/1475-2891-9-41 (2010).

51 Range, N. *et al.* The effect of multi-vitamin/mineral supplementation on mortality during treatment of pulmonary tuberculosis: a randomised two-by-two factorial trial in Mwanza, Tanzania. *Br J Nutr* **95**, 762-770 (2006).

52 Visser, M. E. *et al.* The effect of vitamin A and zinc supplementation on treatment outcomes in pulmonary tuberculosis: a randomized controlled trial. *Am J Clin Nutr* **93**, 93-100, doi:10.3945/ajcn.110.001784 (2011).

53 Radu, R. A. *et al.* Retinal pigment epithelium-retinal G protein receptor-opsin mediates light-dependent translocation of all-trans-retinyl esters for synthesis of

visual chromophore in retinal pigment epithelial cells. *The Journal of biological chemistry* **283**, 19730-19738, doi:10.1074/jbc.M801288200 (2008).

54 Edgar, R., Domrachev, M. & Lash, A. E. Gene Expression Omnibus: NCBI gene expression and hybridization array data repository. *Nucleic acids research* **30**, 207-210 (2002).

Fig. 1

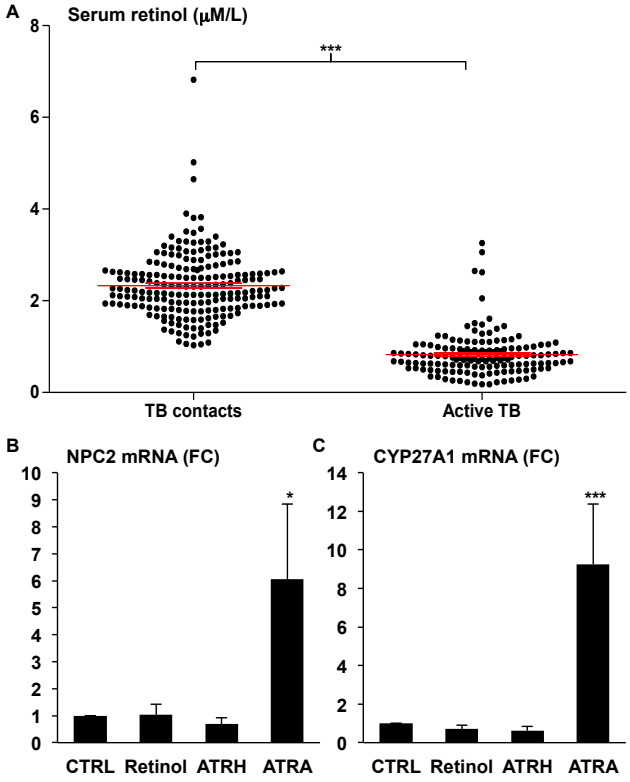
A
Serum retinol (μM/L)
***
8
6
4
2
0
TB contacts
Active TB
B
NPC2 mRNA (FC)
*
10
9
8
7
6
5
4
3
2
1
0
CTRL
Retinol
ATRH
ATRA
C
CYP27A1 mRNA (FC)
***
14
12
10
8
6
4
2
0
CTRL
Retinol
ATRH
ATRA

Fig. 2

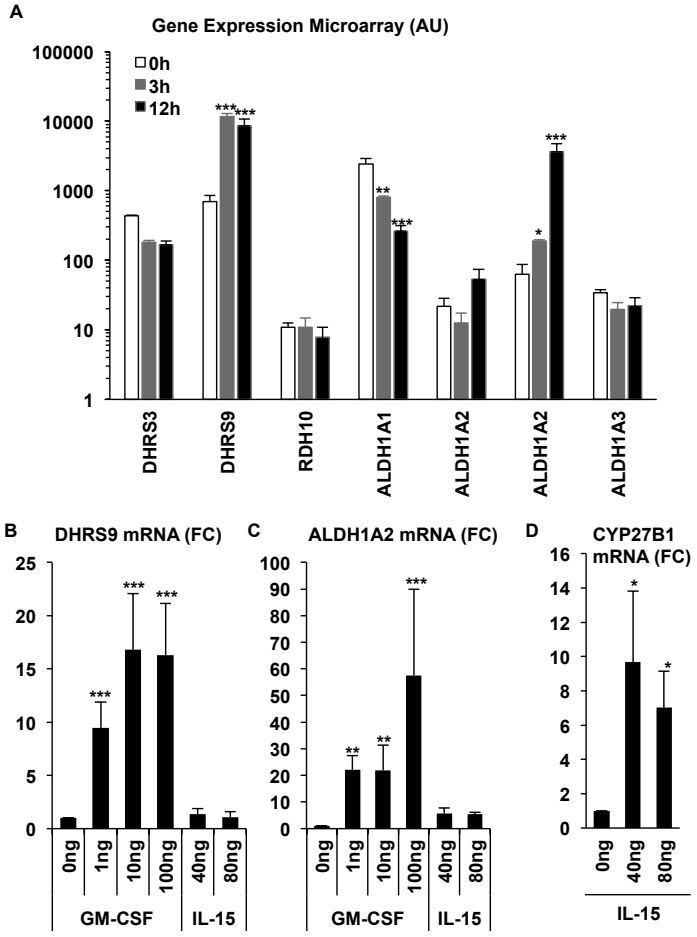
A
Gene Expression Microarray (AU)
0h
3h
12h
DHRS3
DHRS9
RDH10
ALDH1A1
ALDH1A2
ALDH1A2
ALDH1A3
B
DHRS9 mRNA (FC)
C
ALDH1A2 mRNA (FC)
D
CYP27B1 mRNA (FC)
0ng
1ng
10ng
100ng
40ng
80ng
GM-CSF
IL-15

Fig. 3

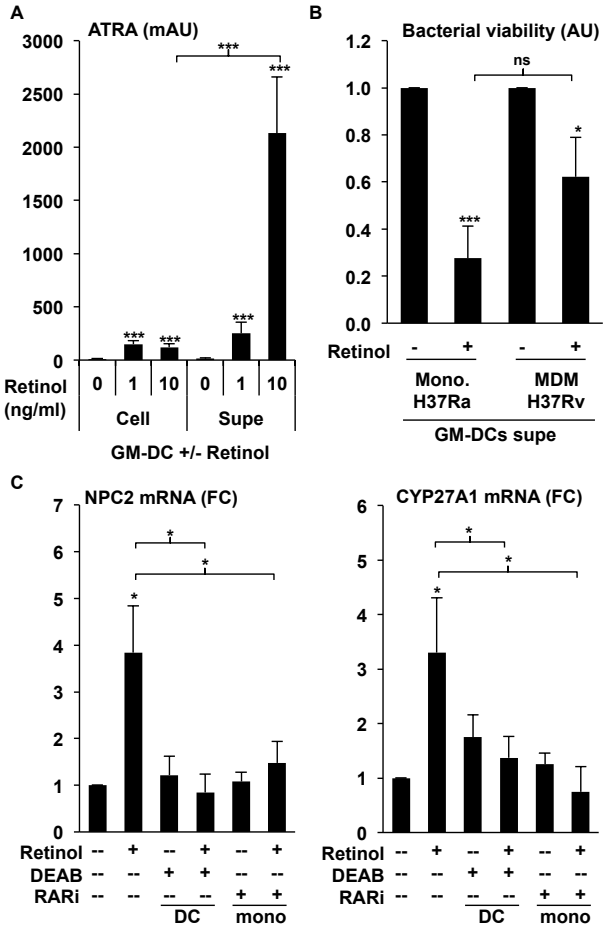
A
ATRA (mAU)
3000
2500
2000
1500
1000
500
0
***
***
***
***
***
Retinol (ng/ml)
0
1
10
0
1
10
Cell
Supe
GM-DC +/- Retinol
B
Bacterial viability (AU)
1.2
1.0
0.8
0.6
0.4
0.2
0.0
ns
*
***
Retinol
-
+
-
+
Mono. H37Ra
MDM H37Rv
GM-DCs supe
C
NPC2 mRNA (FC)
7
6
5
4
3
2
1
0
*
*
*
Retinol -- + -- + -- +
DEAB -- -- + + -- --
RARi -- -- -- -- + +
DC
mono
CYP27A1 mRNA (FC)
6
5
4
3
2
1
0
*
*
*
Retinol -- + -- + -- +
DEAB -- -- + + -- --
RARi -- -- -- -- + +
DC
mono

Fig. 4

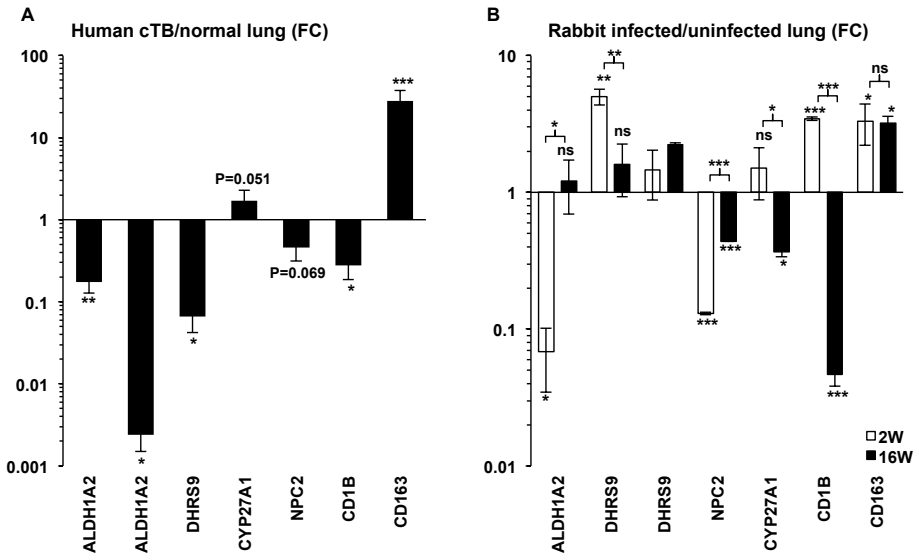
A
Human cTB/normal lung (FC)
100
10
1
0.1
0.01
0.001
P=0.051
P=0.069
ALDH1A2
ALDH1A2
DHRS9
CYP27A1
NPC2
CD1B
CD163
B
Rabbit infected/uninfected lung (FC)
10
1
0.1
0.01
ns
2W
16W
ALDH1A2
DHRS9
DHRS9
NPC2
CYP27A1
CD1B
CD163

Fig. 5

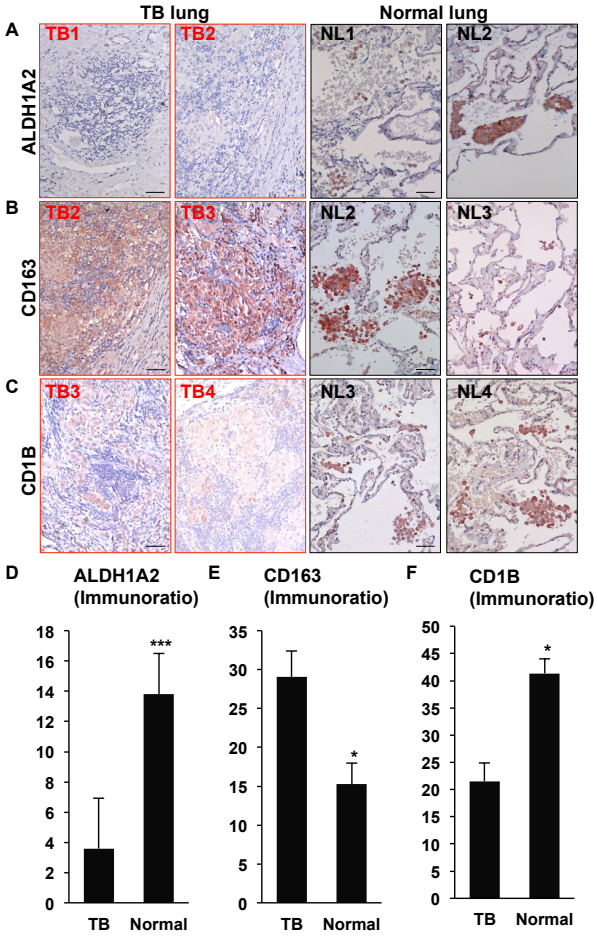
TB lung
Normal lung
A
ALDH1A2
TB1
TB2
NL1
NL2
B
CD163
TB2
TB3
NL2
NL3
C
CD1B
TB3
TB4
NL3
NL4
D
ALDH1A2
(Immunoratio)
***
TB
Normal
E
CD163
(Immunoratio)
*
TB
Normal
F
CD1B
(Immunoratio)
*
TB
Normal

Fig. S1

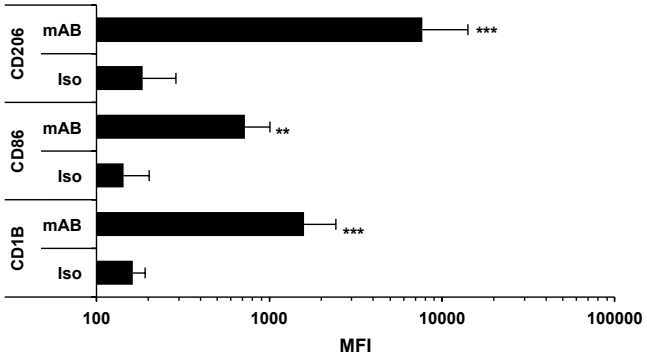
CD206
mAB
Iso
CD86
mAB
Iso
CD1B
mAB
Iso
***
**
***
100
1000
10000
100000
MFI

Fig. S2

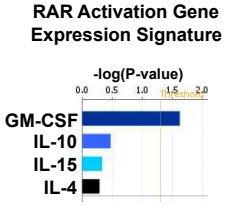
RAR Activation Gene
Expression Signature
-log(P-value)
0.0
0.5
1.0
1.5
2.0
GM-CSF
IL-10
IL-15
IL-4

Fig. S3

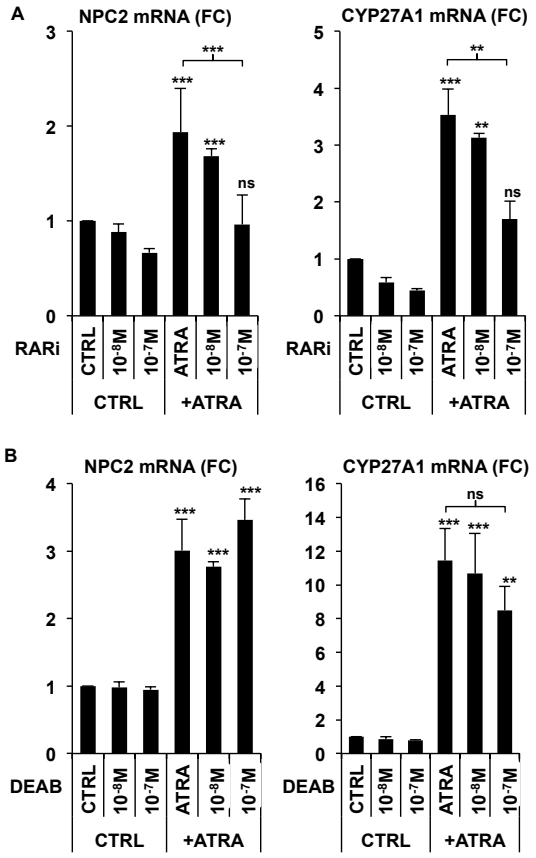
A
NPC2 mRNA (FC)
CYP27A1 mRNA (FC)
RARi
CTRL
10-8M
10-7M
ATRA
CTRL
+ATRA
B
NPC2 mRNA (FC)
CYP27A1 mRNA (FC)
DEAB
ns

Fig. S4

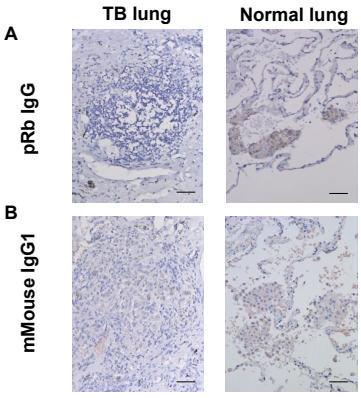

CHAPTER 4

The Rhoptry Pseudokinase ROP54 Modulates *Toxoplasma gondii* Virulence and Host GBP2 Loading

RESEARCH ARTICLE
Host-Microbe Biology

The Rhoptry Pseudokinase ROP54 Modulates *Toxoplasma gondii* Virulence and Host GBP2 Loading

Elliot W. Kim,[a,b] Santhosh M. Nadipuram,[a] Ashley L. Tetlow,[a] William D. Barshop,[c] Philip T. Liu,[d,e] James A. Wohlschlegel,[b,c] Peter J. Bradley[a,b]

Department of Microbiology, Immunology and Molecular Genetics,[a] Molecular Biology Institute,[b] Department of Biological Chemistry,[c] and Division of Dermatology, Department of Medicine, David Geffen School of Medicine,[d] University of California Los Angeles, Los Angeles, California, USA; University of California Los Angeles and Orthopaedic Hospital Department of Orthopaedic Surgery and the Orthopaedic Hospital Research Center, Los Angeles, California, USA[e]

ABSTRACT *Toxoplasma gondii* uses unique secretory organelles called rhoptries to inject an array of effector proteins into the host cytoplasm that hijack host cell functions. We have discovered a novel rhoptry pseudokinase effector, ROP54, which is injected into the host cell upon invasion and traffics to the cytoplasmic face of the parasitophorous vacuole membrane (PVM). Disruption of *ROP54* in a type II strain of *T. gondii* does not affect growth *in vitro* but results in a 100-fold decrease in virulence *in vivo*, suggesting that ROP54 modulates some aspect of the host immune response. We show that parasites lacking ROP54 are more susceptible to macrophage-dependent clearance, further suggesting that ROP54 is involved in evasion of innate immunity. To determine how ROP54 modulates parasite virulence, we examined the loading of two known innate immune effectors, immunity-related GTPase b6 (IRGb6) and guanylate binding protein 2 (GBP2), in wild-type and $\Delta rop54_{II}$ mutant parasites. While no difference in IRGb6 loading was seen, we observed a substantial increase in GBP2 loading on the parasitophorous vacuole (PV) of *ROP54*-disrupted parasites. These results demonstrate that ROP54 is a novel rhoptry effector protein that promotes *Toxoplasma* infections by modulating GBP2 loading onto parasite-containing vacuoles.

IMPORTANCE The interactions between intracellular microbes and their host cells can lead to the discovery of novel drug targets. During *Toxoplasma* infections, host cells express an array of immunity-related GTPases (IRGs) and guanylate binding proteins (GBPs) that load onto the parasite-containing vacuole to clear the parasite. To counter this mechanism, the parasite secretes effector proteins that traffic to the vacuole to disarm the immunity-related loading proteins and evade the immune response. While the interplay between host IRGs and *Toxoplasma* effector proteins is well understood, little is known about how *Toxoplasma* neutralizes the GBP response. We describe here a *T. gondii* pseudokinase effector, ROP54, that localizes to the vacuole upon invasion and is critical for parasite virulence. *Toxoplasma* vacuoles lacking ROP54 display an increased loading of the host immune factor GBP2, but not IRGb6, indicating that ROP54 plays a distinct role in immune evasion.

KEYWORDS: *Toxoplasma gondii*, guanylate binding proteins, immunity-related GTPases, pseudokinase, rhoptry, virulence

Received 24 February 2016 **Accepted** 29 February 2016 **Published** 23 March 2016

Citation Kim EW, Nadipuram SM, Tetlow AL, Barshop WD, Liu PT, Wohlschlegel JA, Bradley PJ. 2016. The rhoptry pseudokinase ROP54 modulates *Toxoplasma gondii* virulence and host GBP2 loading. mSphere 1(2):e00045-16. doi:10.1128/mSphere.00045-16.

Editor Ira J. Blader, University at Buffalo

Address correspondence to Peter J. Bradley, pbradley@ucla.edu.

Toxoplasma gondii is an obligate intracellular parasite that infects approximately one-third of the human population and causes disease in immunocompromised individuals and neonates (1). *Toxoplasma* has the ability to infect a wide range of host cells and has evolved unique secretory organelles to help it to establish infection. One

of these organelles is the rhoptries, which secrete proteins that form a tight junction interface between the parasite and host cell and thus mediate invasion (2, 3). In addition, the rhoptries secrete effector proteins called ROPs that are delivered into the host cytosol, which then traffic to the host nucleus or parasitophorous vacuole membrane (PVM) to coopt host signaling and innate immune pathways (4, 5). The ROP2 superfamily is the best-characterized of the ROP effector proteins and consists of more than ~40 kinases and pseudokinases, whose functions are largely unknown.

The most notable ROP kinases and pseudokinases described thus far have been shown to function in disarming the host innate immune response during infection. For example, the ROP16 kinase is injected into the host cytosol and transits to the host nucleus. ROP16 phosphorylates STAT-3 and STAT-6, which results in a decrease in production of the proinflammatory cytokine the interleukin-12–p40 (IL-12p40), thereby dampening the Th1 response against the parasite (6–8). One effector in the ROP2 superfamily whose mechanism is understood is the ROP5/17/18 complex (9–12). In contrast to ROP16, this complex of effectors traffics to the cytoplasmic face of the PVM upon injection into the host cytoplasm (10, 13). Upon reaching the PVM, they collaborate to disarm a class of cell-autonomous proteins called immunity-related GTPases (IRGs), which load onto the PVM and serve as the first line of defense against intracellular pathogens (14, 15). The IRGs are a large family of GTP-binding proteins (GBPs) that oligomerize on the PVM and cause membrane blebbing, ultimately disrupting vacuolar integrity and clearing the parasite (16). Phosphorylation of the IRGs by the ROP5/17/18 complex releases the IRGs from the PVM and protects the parasite from clearance (17). Several other ROP pseudokinases, such as ROP2 and ROP4, also associate with the PVM; however, their functions at the vacuolar membrane are unknown (18, 19). While this basic mechanism of defense against the parasite is understood, the large families of IRGs and rhoptry kinase/pseudokinases suggest that additional players are involved in a complex process of modulating cell-autonomous immunity at the PVM.

Another class of gamma interferon (IFN-γ)-dependent immunity-related loading proteins that have been shown to be important during a *Toxoplasma* infection is the GBPs (20). The GBPs have been the focus of particular interest, as the IRGs are largely absent or unlikely to play a role in human infections (e.g., there are 23 IRGs in mice but only 2 in humans, 1 of which is only expressed in testes and the other of which appears to lack GTPase activity) (21). There are 11 GBPs in mice (7 in humans), several of which have been shown to load onto the PVM during infection and are important for parasite clearance (21–23). For example, the presence of GBP1 on parasite vacuoles has been linked with membrane vesiculation and vacuole rupture (24). In addition, GBP2 has been implicated in controlling the replication of the parasites (24, 25). While type I alleles of ROP5 and ROP18 are able to diffuse GBP1 loading onto the PVM, the parasite-derived virulence factors that modulate GBP2 are unknown (22, 24).

In this report, we have identified a novel rhoptry pseudokinase, ROP54. Like other ROP effectors, ROP54 localizes to the body portion of the rhoptries and is secreted into the host cell during invasion. Upon delivery into the host cell, ROP54 traffics to the cytoplasmic face of the PVM. While disruption of *ROP54* in type I parasites shows no apparent phenotype *in vitro* and *in vivo*, *ROP54* knockouts in type II parasites grow normally *in vitro* but display a dramatic decrease in virulence *in vivo*, suggesting that ROP54 modulates some aspect of innate immunity. ROP54 does not appear to interact with the ROP5/17/18 complex and does not affect loading of IRGb6, but instead it appears to modulate the innate immune loading of GBP2 (6, 14, 26, 27). Together, the discovery and functional analyses of ROP54 provide new insight into the complex interplay between *Toxoplasma* and the interferon-inducible GTPases that regulate innate immunity.

RESULTS

TgME49_210370 is a novel rhoptry protein pseudokinase. In examining the *T. gondii* genome for potential novel rhoptry effector proteins, we discovered a gene, designated TgME49_210370, that contained a predicted signal peptide for secretion as

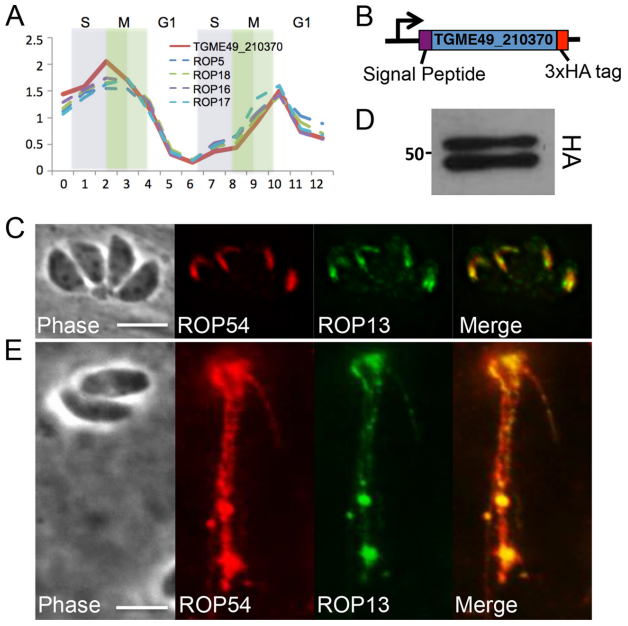

FIG 1 TGME49_210370 is a novel rhoptry protein. (A) The cell cycle expression profile of TGME49_210370 is similar to known *Toxoplasma* effectors. (B) Illustration of TGME49_210370 with an HA tag at its endogenous locus. (C) IFA results showing HA-tagged TGME49_210370 colocalizes with ROP13 in the rhoptries. TGME49_210370 was thus designated ROP54HA. (D) Western blot analysis demonstrated ROP54 migrates as a doublet at its predicted size (53.6 kDa). (E) Results of the evacuole assay, demonstrating that ROP54HA$_{II}$ is secreted into the host cell, similar to the known rhoptry protein ROP13.

well as a cell cycle expression profile that was similar to known rhoptry proteins (Fig. 1A) (28). While this locus was annotated as a putative RNA helicase-1 type protein in the *T gondii* genome (or a hypothetical protein, depending on strain type), BLAST analysis did not reveal homology to any known proteins (http://www.toxodb.org) (29). We examined the amino acid sequence further by using DELTA-BLAST and Phyre-2 searches, which surprisingly indicated that TgME49_210370 was instead related to the ROP family of kinases and pseudokinases, indicating that this protein may be a more divergent member of the ROP kinase family (30, 31). The amino acid sequence for TgME49_210370 is identical between type II and III strains, with 1 amino acid change at position 112 in type I parasites. Alignment with the known rhoptry kinase ROP18 demonstrated that TgME49_210370 is missing key catalytic residues, which suggests that it functions as a ROP pseudokinase effector protein rather than a true kinase (see Fig. S1 in the supplemental material) (32).

To determine if TgME49_210370 is a rhoptry protein, we used endogenous gene tagging to introduce sequences encoding a 3× hemagglutinin (3×HA) epitope tag at the 3′ end of the gene of both highly virulent type I (RHΔ*ku80*) and intermediate-virulence type II (PruΔ*ku80*) parasites (Fig. 1B). Evaluation in immunofluorescence assays (IFA) with anti-HA antibodies showed that TgME49_210370 localized to apical structures resembling the body portion of the rhoptries (Fig. 1C; see also Fig. S2A in the supplemental material) and colocalized with known rhoptry body proteins ROP13 and ROP7. We therefore designated TgME49_210370 rhoptry protein 54 (ROP54). Western

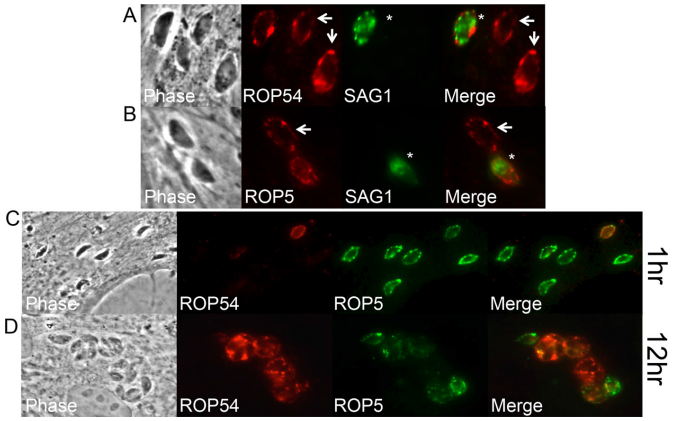

FIG 2 Selective permeabilization demonstrated that ROP54 localizes to the PVM. (A) Digitonin permeabilization of HFFs infected with ROP54HA$_{II}$ parasites for 12 h showed that ROP54 is present on the cytoplasmic face of the PVM (arrow). Overpermeabilized vacuoles were SAG1 positive and are annotated with an asterisk. (B) ROP5 control for vacuolar membrane localization under digitonin treatment conditions. (C and D) HFF monolayers were infected with ROP54HA$_{II}$ parasites and then fixed and selectively permeabilized with digitonin 1 h postinfection (C) or 12 h postinfection (D). Whereas ROP5 localized relatively early on the PVM, ROP54 was more frequently found at later time points.

blot analysis of ROP54HA$_{II}$ parasites showed a reproducible doublet migrating at approximately the predicted mass of the protein lacking its signal peptide (Fig. 1D).

For ROP54 to be a potential effector protein, it must be secreted into the host cell, as typically seen with other ROP effectors (5, 33). To evaluate whether ROP54 is an injected effector, we carried out "evacuole" assays, in which parasites are unable to invade due to inhibition by cytochalasin D (CytoD) treatment but still able to release streams of rhoptry proteins into the cytosol of the host cell (10, 33). Using ROP54HA$_{II}$ parasites, we were able to observe classic "strings" of HA-positive evacuoles emanating from CytoD-arrested parasites (Fig. 1E). These evacuoles were also positive for ROP13, which is known to be secreted into the host cell in evacuoles (33). Similar results were obtained when an evacuole assay was performed with ROP54HA$_{I}$ parasites (data not shown). Thus, we conclude that ROP54 is injected from the rhoptry body into the host cell.

ROP54 associates with the PVM after being injected into the host cell. Once they reach the host cytoplasm, rhoptry effectors are known to target specific intracellular compartments, including the cytoplasm, nucleus, or the PVM (6, 10, 13, 26, 33). As some of the best-studied rhoptry kinases and pseudokinases traffic to the PVM and anchor to it using amphipathic α-helices in the N-terminal region of the proteins, we examined the ROP54 sequence for putative α-helices that could mediate PV association (13). We identified two such regions, from residues 83 to 120 and 123 to 155 (see Fig. S3A in the supplemental material) that might form amphipathic α-helices when plotted on a helical wheel predictor (see Fig. S3B). To assess whether ROP54 traffics to the cytoplasmic face of the vacuolar membrane, similar to other rhoptry effectors (i.e., ROPs 2/4/5/7/17/18), we examined ROP54HA$_{II}$ in early invasion and digitonin semipermeabilization assays (Fig. 2A) (10, 26, 34). Digitonin treatment is able to selectively permeabilize the host plasma membrane but not the vacuolar membrane or parasite membranes, enabling detection of the vacuolar membrane effectors that face the host cytoplasm. As controls, we similarly examined the rhoptry pseudokinase ROP5, which is known to traffic to the PVM, and we also utilized staining for the parasite surface antigen SAG1 to show that the vacuoles being evaluated were not breached by

digitonin treatment, as the degree of permeabilization varied within individual cells on the coverslip in these experiments (Fig. 2A and B) (13).

Using these assays, we were able to demonstrate that ROP54 traffics to the cytoplasmic face of the PVM (Fig. 2A and B). We also observed that ROP54 is less frequently detected on the PVM relative to ROP5 at 1 h postinfection (Fig. 2C). The differences seen between the effectors may be due to fewer vacuoles being targeted by ROP54 than ROP5, although we cannot exclude the possibility that these differences are merely due to levels of detection, since ROP5 is encoded in a multicopy gene and *ROP54* appears to be present in a single copy and is likely expressed at lower levels. However, at 12 h postinfection, ROP54 can be detected on the PVM, similar to ROP5 (Fig. 2D). This suggests that ROP54 may load onto the PVM later than that seen for ROP5, perhaps requiring another partner to traffic to the PVM.

To further examine trafficking of ROP54 to the PVM, we exogenously expressed the protein in human cells with an HA epitope tag and assessed its localization to the PVM following *T. gondii* infection (see Fig. S4A in the supplemental material). Whereas ROP5 is targeted to the PVM under these conditions (33), ROP54 remained diffuse in the cytoplasm and was not detected in significant amounts on the PVM (see Fig. S4B). Because we could not be certain of the precise N terminus of ROP54 following cleavage of its signal peptide and any potential prodomains, we constructed two deletions that might expose the charged regions present in the N terminus of the protein (Fig. S4C and D), but these truncated proteins also failed to traffic to the PVM (data not shown).

ROP54SF$_{II}$ immunoprecipitation suggests it functions independently from the ROP5/17/18 complex. To identify the binding partners of ROP54, we engineered an endogenous tagging construct that would add sequences encoding a 2×Strep 3×Flag epitope tag at the C-terminal end of the ROP54 gene (Fig. 3A). The tagged ROP54 properly localized to the rhoptry body, and therefore the strain was designated ROP54SF$_{II}$ (Fig. 3B). We additionally analyzed ROP54SF$_{II}$ by Western blotting, which revealed a doublet that was enriched for the slower-migrating band (Fig. 3C), suggesting that this is the primary product of ROP54. To determine if ROP54 interacted with the ROP5/17/18 complex or other members of the ROP kinase family, we purified ROP54 by using a Strep-Tactin column and eluted the ROP54 complex with desthiobiotin (10). Western blot analysis of the precolumn (pre) and elution (E) fractions with an anti-Flag antibody demonstrated a significant enrichment of ROP54 relative to the untagged control (Fig. 3D). The fractions were evaluated for known ROP kinases or pseudokinases (ROPs 5/18 as well ROPs 2/3/4 and ROP7), and none was enriched in our immunoprecipitation (IP)-Western blotting or mass spectrometry data (Fig. 3E; see Table S2 in the supplemental material). These results suggest that ROP54 functions independently of the ROP5/17/18 complex and ROPs 2/4/7 on the PVM, although we cannot exclude more transient interactions that would have been disrupted during isolation. Mass spectrometric analysis of the ROP54 pulldown product did not identify any other known active kinases that may work in conjunction with ROP54. We did identify the small amounts of the inactive kinase ROP24 as well as another hypothetical protein with a predicted signal peptide (TGME49_237180), but tagging of these proteins suggested dense granule localization, and thus they were not pursued further (data not shown).

Disruption of ROP54 in type I parasites does not affect growth *in vitro* or virulence *in vivo*. To determine the function of ROP54, we disrupted its gene in ROP54HA$_{I}$ parasites by homologous recombination. To do this, we utilized a knockout construct consisting of the ROP54 flanking regions surrounding the selectable marker dihydrofolate reductase (DHFR). The linearized construct was transfected into ROP54HA$_{I}$ parasites, and knockouts were screened for loss of the HA tag. Parasite clones that lacked HA staining were isolated and verified by IFA and Western blot analysis (the resulting strain was designated Δ*rop54*$_{I}$ [see Fig. S2B and C in the supplemental material]). No gross defects were observed in parasite intracellular growth, as evaluated in plaque assays over a 6-day period of the lytic cycle (data not shown). To determine if this disruption affected virulence *in vivo*, a small number of the

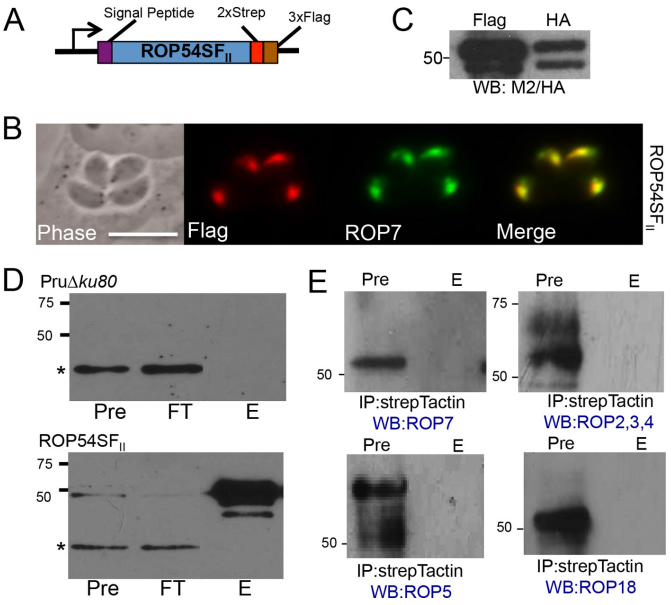

FIG 3 Purification of ROP54 indicated that there is no robust interaction with other known ROP effector proteins. (A) Illustration showing the endogenously tagged ROP54 with predicted signal peptide, coding region, and C-terminal 2×Strep 3×Flag epitope tags. (B) IFA with anti-Flag antibody showed colocalization with the rhoptry protein ROP7. (C) Western blot assay results for ROP54SF$_{II}$ and ROP54HA$_{II}$ parasite lines demonstrated that the slower-migrating band was the main band of ROP54. (D) Western blotting results with precolumn (Pre), flowthrough (FT), and elution (E) fractions of the Pru*Δku80* (top) and ROP54SF (bottom) StrepTactin pulldown product probed with mouse anti-Flag antibody. A nonspecific band is represented by the asterisk. (E) IP-Western blot probing for known ROP kinases and pseudokinase after ROP54SF pulldown.

Δ*rop54*$_{I}$ parasites (~10 parasites) was injected into mice, and all of the mice died at 11 days postinfection, similar to that seen with control parasites (data not shown). Thus, loss of ROP54 does not appear to impact growth or virulence in type I parasites.

ROP54 is not required for normal *in vitro* growth of type II parasites. The hypervirulence of type I parasites is largely due to the robust activity of the ROP5/17/18 complex, which inactivates IRGs that would otherwise load onto the PVM, disrupt the vacuolar membrane, and clear the parasite (10, 26). Since the effects of type I ROPs 5/17/18 may mask the importance of ROP54 in parasite virulence, we assessed the function of ROP54 as an intermediate virulence type II strain (10, 14, 26). To do this, we disrupted ROP54 in Pru*Δku80* parasites and confirmed the knockout by IFA and Western blotting (Fig. 4A and C). A *ROP54*-complemented strain (ROP54c$_{II}$) was generated by expressing *ROP54HA*$_{II}$ driven from its endogenous promoter (Fig. 4B). The complementation construct was observed to target the *Ku80* locus, thereby excluding potential polar effects in the Δ*rop54*$_{II}$ strain. A clonal isolate of ROP54c$_{II}$ was evaluated by IFA, and it showed apical staining of the 3×HA epitope tag that colocalized with ROP13. The strain was also assessed by Western blot analysis, which demonstrated expression levels nearly identical to those of the parental ROP54HA$_{II}$ parasites (Fig. 4C). To examine the role of ROP54 in *in vitro* growth, the ROP54HA$_{II}$, Δ*rop54*$_{II}$, and ROP54c$_{II}$ lines of parasites were evaluated by plaque assay, and no apparent differences in growth rate were detected between the three strains (Fig. 4D and E).

Disruption of ROP54 in type II parasites dramatically decreases virulence *in vivo*. To evaluate the effect of the knockout *in vivo*, mice were infected with doses of

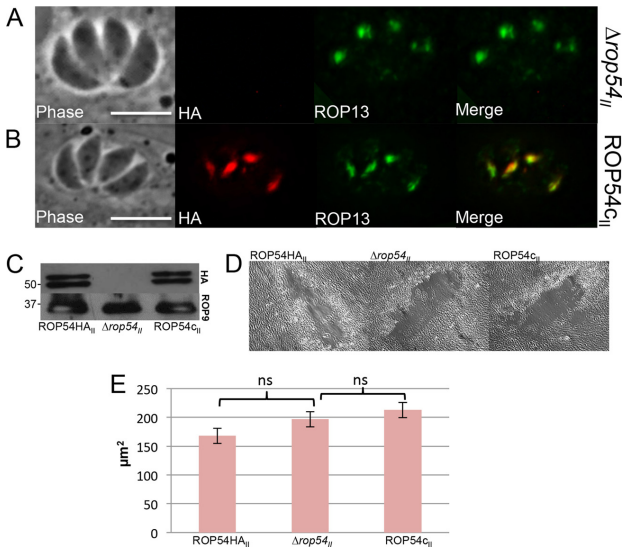

FIG 4 Disruption of *ROP54* in type II parasites does not affect growth *in vitro*. (A) IFA results, demonstrating the loss of ROP54HA$_{II}$ staining in a Δ*rop54*$_{II}$ clone. (B) IFA results for Δ*rop54*$_{II}$ parasites complemented with *ROP54HA*$_{II}$ at the *ku80* locus (designated ROP54c$_{II}$). Proper localization of ROP54 in the ROP54c$_{II}$ parasite clone was assessed by colocalization with ROP13. (C) Western blot assay results, demonstrating loss of HA signal in Δ*rop54*$_{II}$ parasites and restoration of HA signal for ROP54c$_{II}$ parasites. ROP9 is shown as a loading control. (D and E) HFF monolayers were infected with ROP54HA$_{II}$, Δ*rop54*, or ROP54c$_{II}$ parasites, and plaques were visualized after 10 days. All strains exhibited similar overall fitness *in vitro* (representative plaques are shown in panel D). The area of 30 plaques from each parasite line was measured, and no significant difference ($P > 0.05$) was determined by one-way ANOVA. ns, not significant (E).

500, 5,000, and 50,000 parasites of the ROP54HA$_{II}$, Δ*rop54*$_{II}$, or ROP54c$_{II}$ strain. To ensure that any attenuation of virulence was not due to viability of the knockout or counting errors, plaque assays were performed on the parasites used for the infections, which demonstrated comparable amounts of parental and complemented strains but ~2-fold higher numbers of plaques with the knockout, demonstrating that even more knockout parasites were injected than wild-type or complemented strain parasites (Fig. 5A). Interestingly, Δ*rop54*$_{II}$ parasites exhibited a 2-log reduction in virulence compared to the parental line (Fig. 5B to D). This defect was mostly restored in the complemented strain, showing that ROP54 plays an important role in virulence *in vivo* in type II strain parasites. Finally, we evaluated whether Δ*rop54*$_{II}$-infected mice were protected against a lethal challenge with 10,000 RHΔ*ku80* parasites, and all mice survived the challenge (data not shown).

Δ*rop54*$_{II}$ parasites are more susceptible to innate immune clearance. To determine the kinetics of Δ*rop54*$_{II}$ clearance *in vivo*, we performed an *in vivo* competition assay. We intraperitoneally (i.p.) injected a mixture of ROP54HA$_{II}$ and strain Δ*rop54*$_{II}$ parasites into C57BL/6 mice at a dose of 50,000 parasites per mouse (~40/60 ratio of ROP54HA$_{II}$/Δ*rop54*$_{II}$). At days 4 and 7 postinfection, we euthanized mice and performed a peritoneal lavage to collect the parasites from the peritoneum and assess the ratio of ROP54HA$_{II}$ to Δ*rop54*$_{II}$ parasites by IFA. The Δ*rop54*$_{II}$ parasites were outcompeted by the ROP54HA$_{II}$ parasites *in vivo* as the infection progressed (Fig. 6A). In parallel to peritoneal lavage, spleens were harvested from animals euthanized on day 7, and ROP54HA$_{II}$ versus Δ*rop54*$_{II}$ parasite burdens were quantitated by IFA; the results showed similar parasite vacuole ratios to those found in the peritoneal lavage exper-

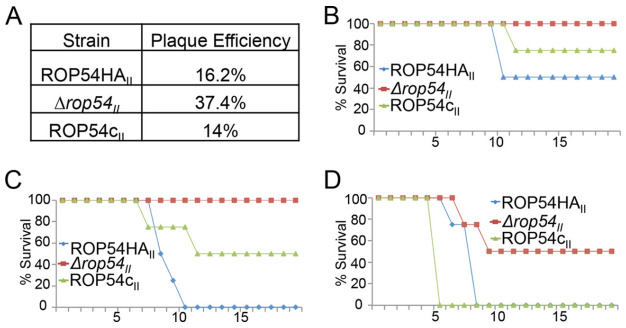

FIG 5 Disruption of ROP54 results in a dramatic decrease in virulence *in vivo*. (A) A plaque assay was used to verify viability of parasites injected into mice. More viable Δ*rop54*$_{II}$ parasites were injected into the mice than into the controls. A total of 500 (A), 5,000 (B), or 50,000 (C) ROP54HA$_{II}$, Δ*rop54*$_{II}$, or ROP54c$_{II}$ parasites were i.p. injected into C57BL/6 mice. An ~100-fold decrease in virulence was observed between ROP54HA$_{II}$ (50% lethal dose [LD$_{50}$] of 500 parasites) and Δ*rop54*$_{II}$ (LD$_{50}$ of 50,000 parasites). Virulence was mostly restored with complementation of ROP54.

iment (see Fig. S5 in the supplemental material). The decrease in relative amounts of Δ*rop54*$_{II}$ parasites suggests that Δ*rop54*$_{II}$ parasites either grow poorly *in vivo* or are cleared by the innate immune response.

To resolve these two possibilities, we examined the virulence of ROP54HA$_{II}$ and Δ*rop54*$_{II}$ parasites in IFN-γ receptor-deficient (IFN-γR$^{-/-}$) mice. We predicted that the

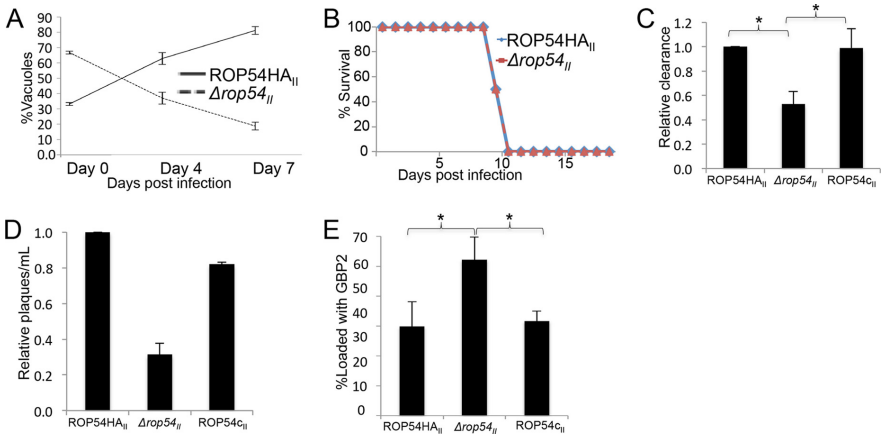

FIG 6 ROP54 modulates IFN-γ-dependent parasite clearance through the interference of GBP2 loading on the PV. (A) *In vivo* competition assay results for ROP54HA$_{II}$ and Δ*rop54*$_{II}$ parasite lines, showing a steady increase in the percentage of ROP54HA$_{II}$ vacuoles and a steady decrease in the percentage of Δ*rop54*$_{II}$ vacuoles as the coinfection progressed ($n = 6$, from two independent experiments). (B) IFN-γR$^{-/-}$ mice were injected with 5,000 parasites of ROP54HA$_{II}$ or Δ*rop54*$_{II}$ and became moribund with the same kinetics, suggesting that ROP54 modulates an IFN-γ-dependent response ($n = 4$). (C) RAW 267.4 cells were activated with IFN-γ and LPS for 24 h. The parasite strains ROP54HA$_{II}$, Δ*rop54*$_{II}$, and ROP54c$_{II}$ were used to infect the cells for 20 h at an MOI of 1. qPCR demonstrated an ~50% decrease of Δ*rop54*$_{II}$ parasites relative to levels with the parental and complemented strains. Significance was determined by a one-way ANOVA. *, $P < 0.05$ ($n = 3$). (D) Primary BMDMs were activated with IFN-γ and LPS for 24 h. The strains ROP54HA$_{II}$, Δ*rop54*$_{II}$, and ROP54c$_{II}$ were used to infect the cells for 20 h at an MOI of 1. Parasites were liberated by manual disruption and quantitated in a plaque assay. Values were normalized to ROP54HA$_{II}$, and a decrease in Δ*rop54*$_{II}$ viability was demonstrated ($n = 2$). (E) MEFs were primed with IFN-γ and LPS. The ROP54HA$_{II}$, Δ*rop54*$_{II}$, and ROP54c$_{II}$ parasite lines were used to infect the cells for 12 h. The proportion of GBP2 loading on the vacuoles of Δ*rop54*$_{II}$-infected cells was significantly increased, based on a one-way ANOVA. *, $P < 0.05$ ($n = 3$). The decrease in loading was restored to wild-type levels upon complementation.

virulence of Δ*rop54*$_{II}$ parasites would mimic that of the parental line if virulence were dependent on an IFN-γ-mediated immune response (but would still be dramatically lower if merely due to a reduction in growth *in vivo*). To test this, we i.p. injected 5,000 ROP54HA$_{II}$ or Δ*rop54*$_{II}$ parasites separately in IFN-γR$^{-/-}$ mice and observed their morbidity. The IFN-γR$^{-/-}$ mice demonstrated identical morbidity kinetics when infected with either ROP54HA$_{II}$ or Δ*rop54*$_{II}$ parasites (Fig. 6B). These data demonstrated that IFN-γ signaling is necessary for the difference in virulence of ROP54HA$_{II}$ and Δ*rop54*$_{II}$ parasites and suggest that ROP54 enables parasites to evade an IFN-γ-mediated immune response (14).

To determine whether Δ*rop54*$_{II}$ parasites are deficient in the avoidance of the host innate immune response, we examined ROP54HA$_{II}$, Δ*rop54*$_{II}$, and ROP54c$_{II}$ parasites in primed macrophages, which are the primary immune cell type infected *in vivo* (14, 35). To assess macrophage-mediated clearance *in vitro*, we infected activated murine macrophages with ROP54HA$_{II}$, Δ*rop54*$_{II}$, and ROP54c$_{II}$ parasites, isolated genomic DNA, and calculated the relative amount of parasite genomic DNA via quantitative PCR (qPCR) at 20 h postinfection. We observed a 2-fold decrease in the relative amount of Δ*rop54*$_{II}$ genomic DNA compared to the ROP54HA$_{II}$ and ROP54c$_{II}$ parasite lines (Fig. 6C) (36–38). To determine if the decrease in Δ*rop54*$_{II}$ genomic DNA correlated with a decrease in Δ*rop54*$_{II}$ parasite viability, we similarly assessed the viability of ROP54HA$_{II}$, Δ*rop54*$_{II}$, and ROP54c$_{II}$ parasites within activated macrophages under the same conditions. We mechanically disrupted the macrophages to liberate the parasites from the cells and measured parasite viability in plaque assays (38). In agreement with the PCR results, we observed a substantial decrease in the Δ*rop54*$_{II}$ parasite viability relative to the controls (Fig. 6D), indicating that ROP54 enhances the ability of the parasite to avoid macrophage clearance.

The loss of virulence in Δ*rop54*$_{II}$ parasites correlates with GBP2 loading. Since ROP54 localizes to the PVM upon invasion (Fig. 2A) and aids in the avoidance of an innate immune response, we investigated whether ROP54 potentially interfered with the function of IRGs (10, 14, 27, 39). We first wanted to determine if IRGb6 and ROP54 were both present on the PVM during the course of a *Toxoplasma* infection. To test this, ROP54HA$_{II}$ parasites were used to infect activated macrophages for 1 h and 12 h. The cells were assessed by IFA, and colocalization of ROP54 and IRGb6 was observed at both time points (see Fig. S6A in the supplemental material). To determine whether ROP54 disrupted IRGb6 loading, we quantified the loading events between ROP54HA$_{II}$ and Δ*rop54*$_{II}$ parasites in activated macrophages (14). However, no difference was observed with the loading of IRGb6 between ROP54HA$_{II}$ and Δ*rop54*$_{II}$ parasites (see Fig. S5B in the supplemental material).

We also investigated a different family of immune loading proteins called p65 GBPs. To determine if ROP54 enables parasites to evade the antimicrobial effects of GBP2, we compared the immune loading of GBP2 on ROP54HA$_{II}$, Δ*rop54*$_{II}$, and ROP54c$_{II}$ parasites. We predicted that if ROP54 modulated GBP2 loading, we would observe a difference in loading between the Δ*rop54*$_{II}$ parasites and the controls. To examine loading of GBP2, we activated mouse embryonic fibroblasts (MEFs) and infected the cells with ROP54HA$_{II}$, Δ*rop54*$_{II}$, or ROP54c$_{II}$ parasites. IFA analysis with anti-GBP2 antibodies showed a substantial increase in the percentage of Δ*rop54*$_{II}$ vacuoles loaded with GBP2 compared to that in the ROP54HA$_{II}$, and ROP54c$_{II}$ vacuoles (Fig. 6E). These data indicate that ROP54 is a virulence factor that plays a role in evading the cell-autonomous immune mechanism of GBP2.

DISCUSSION

The family of *Toxoplasma* ROP kinases and pseudokinases has largely been identified by traditional organelle isolation and antibody production strategies, as well as more recent proteomic and bioinformatics approaches (4, 40, 41). Together, these studies have determined that the ROP2 superfamily consists of more than 40 rhoptry kinases and pseudokinases (41). While the functions of most of these proteins are unknown, analyses of just a few of these family members have shown that they are key players

in *T. gondii*'s ability to hijack host functions and evade innate immunity (9). In this work, we identified ROP54 by screening the *T. gondii* genome to find potential rhoptry proteins based on the criteria of the presence of a predicted signal peptide and a cell cycle expression profile similar to that of other known ROPs (9, 42). ROP54 appears to be a member of the ROP kinase family, as it contains a predicted ROP2-like kinase fold, based on DELTA-BLAST and Phyre-2 analyses, and it is most likely a pseudokinase, as it lacks the key amino acids of the kinase catalytic pocket (see Fig. S1 in the supplemental material) (30, 31). We were unable to find other divergent ROP kinase family members using this approach or by BLAST searches with ROP54, but it is possible that other proteins have diverged even further and were thus unrecognized by these searches.

We verified rhoptry localization for ROP54 by C-terminal endogenous gene tagging, and the results were consistent with those for other ROP kinases that are generally amenable to epitope tagging at this terminus (Fig. 1C and 3B; see also Fig. S2A in the supplemental material). The tagged protein migrates as a doublet on Western blots, although this doublet was diminished in the 2×Strep 3×Flag-tagged protein (Fig. 3C). The doublet is not likely due to processing of a prodomain, as seen with other ROPs, as there are no predicted processing sites that are apparent in the N-terminal region of the protein that could give rise to the observed banding pattern (43, 44). In addition, the ratio of the two bands was not consistent with the pattern seen for other rhoptry prodomain processing events (32, 33).

We were able to show that ROP54 is injected into the host cytosol in a evacuole assay, indicating that it is a rhoptry effector protein (as opposed to a resident rhoptry protein that is not secreted) (Fig. 1E). Upon injection into the host cytoplasm, ROP54 appears to associate with the vacuolar membrane (Fig. 2A). Interestingly, ROP54 staining is observed on fewer vacuoles than ROP5 at early time points in invasion (~1 h), but ROP54 staining is more prevalent at later time points (12 h) (Fig. 2C and D). We were unable to accurately quantitate these differences in ROP5 and ROP54 staining at early time points due to the difficulties in detection of low levels of ROP54 on the PVM in these experiments. One possible reason for these differences is that ROP5 is highly expressed with 9 to 10 tandem copies of the gene in type II parasites and thus is more readily detected than a single copy of ROP54 (12). ROP5 is also likely present at a high frequency on the PVM at early time points, because it protects the parasite from the early loading IRGs and clearance (12, 17). The better detection of ROP54 at later time points may also be due to cooperative loading with parasite or host binding partners (e.g., other ROPs, GBPs, or IRGs) that may be important for ROP54 function or may simply reflect detection of the protein.

In spite of having arginine-rich regions in the N-terminal portion of the protein that might function similar to RAH (arginine-rich amphipathic helix) domains (see Fig. S3 in the supplemental material), exogenously expressed ROP54 appears to remain cytosolic and does not traffic to the PVM upon infection (see Fig. S4 in the supplemental material) (26). As we could not exclude processing events that would result in correct positioning of the arginine-rich region, we tested various N-terminal truncations, but these also did not result in vacuolar targeting. It is still formally possible that a precise N terminus is required for ROP54 vacuolar association, although other ROP RAH domains appear to be much more robust and tolerate N-terminal fusions as well as deletions of subregions of the key trafficking helices (13). Alternatively, association of ROP54 with the vacuolar membrane may require other parasite- or host-derived partners.

To address whether ROP54 acts by interacting with other ROP kinases, we immunoprecipitated the protein using ROP54SF$_{II}$ strain parasites (Fig. 3). While we anticipated that we might immunoprecipitate an active rhoptry kinase, we did not find detectable amounts of the ROP 5/17/18 complex or other known active ROP kinases. This is in agreement with tandem affinity purification pulldown products of ROP 5/17/18, which also do not coprecipitate with ROP54 (10, 14). We did immunoprecipitate low amounts of ROP24 and TGME49_237180, although the significance of these partners is unclear, as they appear to have localizations reminiscent of GRA proteins

based on epitope gene tagging (data not shown). The localization of these proteins should be taken with some caution, however, as ROP24 and TGME49_237180 have cell cycle expression profiles similar to ROPs, which suggests that the epitope tags are mislocalizing the proteins (28, 45). It is also possible that the interactions of ROP54 and its bona fide partners are transient or weaker than those of the ROP5/17/18 complex and its host substrates. Ultimately, identification of the interactions between ROP54 and its parasite and host partners will best reveal how it functions in *Toxoplasma*.

Disruption of *ROP54* in highly virulent type I parasites leads to no apparent reduction in virulence in laboratory strains of mice *in vivo*. This may be due to the fact that the ROP5/17/18 complex in type I strains is so efficient in disarming the IRGs in mice that it masks the phenotype of the *ROP54* knockout in this context (10, 14, 26). Examination in wild-type strains of mice or other hosts that can resist type I parasites may expose virulence differences with the knockout of *ROP54* (46). In contrast, disruption of *ROP54* in type II parasites resulted in a 2-log decrease in virulence, even though growth in culture was unaffected (Fig. 4E and 5). Whereas the other ROP kinases and pseudokinases tend to be highly polymorphic across strains, the ROP54 amino acid sequences across type I, II, and III strains are nearly identical, with only 1 amino acid change. This suggests that this effector may play the same role in these diverse strains, although it is also possible that ROP54 expression levels may differ or that its activity may be altered by differences in its partners.

We showed that Δ*rop54*$_{II}$ parasites are susceptible to the IFN-γ-mediated antimicrobial response *in vivo* and *in vitro*, suggesting that the Δ*rop54*$_{II}$ parasites lack an immunosuppressive function (Fig. 6A to D). The susceptibility of the Δ*rop54*$_{II}$ parasites correlated with the increased GBP2 loading on the vacuoles of Δ*rop54*$_{II}$ parasites, while IRGb6 loading was sustained (Fig. 6E; see also Fig. S6 in the supplemental material). These data collectively suggest that the virulence defect observed in Δ*rop54*$_{II}$ parasites *in vivo* is due to the GBP2 innate immune response (Fig. 5). GBPs play a significant role in controlling *Toxoplasma* infection, as IFN-γ-primed MEFs lacking GBP^{chr3} are deficient in parasite clearance (23). Multiple GBPs are likely to be important for host resistance, as complementation of GBP^{chr3}-disrupted MEFs with *GBP2* was not sufficient to control parasite burden (23). However, GBP2$^{-/-}$ mice exhibit an increased susceptibility to *Toxoplasma* infection *in vivo*, and GBP2$^{-/-}$ MEFs are unable to limit parasite replication *in vitro* (25). Our data indicate that the pseudokinase ROP54 modulates immune loading of GBP2 (Fig. 6E), suggesting that it may represent a parasite strategy to evade the GBP2-mediated immune response. It is not known whether ROP54 functions in conjunction with an unidentified active ROP kinase to phosphorylate GBP2 (in a manner similar to the ROP5/ROP18 complex). It is also not known whether ROP54 may have potential roles in disarming other members of the IRG or GBP family, which will be the focus of future studies.

MATERIALS AND METHODS

Parasite and host cell culture. *T. gondii* type I RHΔ*ku80* and type II PruΔ*ku80* parental strains and the resulting modified strains were maintained in confluent monolayers of human foreskin fibroblast (HFF) host cells as previously described (47). Immortalized C57BL/6J macrophages were donated by Kenneth Bradley (UCLA). Bone marrow-derived macrophages (BMDMs) were donated by Steven Bensinger (UCLA).

Antibodies used for Western blot assays and IFAs. Hemagglutinin epitope tags were detected with mouse monoclonal antibody (MAb) HA.11 (Covance) and rabbit polyclonal antibody (pAb) anti-HA (Invitrogen). Flag epitope tags were detected with mouse anti-Flag MAb M2 (Sigma). Rabbit anti-ROP5 was received from David Sibley (Washington University, St. Louis, MO). Mouse MAb anti-ROP7, rat pAb anti-ROP9, and rabbit pAb anti-ROP13 antibodies were generated in the Bradley laboratory (33, 48). IRGb6 was detected with a goat pAb antibody (Santa Cruz Biotechnology). Rabbit anti-GBP2 pAb was received from Jorn Coers from Duke University (49). Mouse anti-SAG1 (DG52) MAb and rabbit anti-SAG1 pAb were both obtained from John Boothroyd at Stanford University (50).

Endogenous tagging of TGME49_210370. To endogenously tag TGME49_210370, the C terminus of the gene was PCR amplified with primers P1/P2 (primers are listed in Table S1 in the supplemental material) from PruΔ*ku80* and RHΔ*ku80* genomic DNA, T4 processed, and ligated using ligase-independent cloning (LIC) into 3×HA- or 2×Strep 3×Flag-tagging plasmids which contained the selectable marker *HXGPRT* as previously described (47). Fifty-microgram aliquots of the tagging constructs were linearized with PstI and transfected into PruΔ*ku80* and RHΔ*ku80* parasites. Stably transfected

parasites were selected with MX medium (50 μg/ml mycophenolic acid and 50 μg/ml xanthine) and cloned using the limiting dilution method (51).

IFA. *T. gondii* strains were used to infect coverslips with a confluent monolayer of HFFs under the indicated time constraints for the IFA analyses. The coverslips were fixed in 3.7% formaldehyde–phosphate-buffered saline (PBS) for 15 min and then blocked and permeabilized in 3% bovine serum albumin (BSA)–0.2% Triton X-100–PBS for 30 min. The samples were then incubated with primary antibody diluted in 3% BSA–0.2% Triton X-100–PBS for 1 h at room temperature. The coverslips were then washed in PBS (5 times for 5 min each) and treated with secondary antibodies Alexa 488-conjugated goat anti-mouse and/or Alexa 594-conjugated goat anti-rabbit (Molecular Probes) diluted 1:2,000 in 3% BSA–0.2% Triton X-100–PBS (27, 52).

Evacuole assay. Evacuoles were assessed as previously described (5, 33). Extracellular ROP54HA$_{II}$ parasites were treated with prechilled Dulbecco's modified Eagle's medium containing 1 μM cytochalasin D (Sigma). The parasites were then added to prechilled confluent monolayers of HFFs for 20 min. The coverslips were washed, and warm medium was added for 20 min. The coverslips were then washed with PBS and an IFA was performed as explained above.

Disruption of *ROP54*. To disrupt *ROP54*, the 5′ and 3′ regions flanking the *ROP54* gene were PCR amplified from PruΔ*ku80* and RHΔ*ku80* genomic DNA with primers P3/P4 and P5/P6 and ligated into the pMiniGFP.ht-DHFR knockout plasmid (48). Fifty-microgram amounts of the plasmid were linearized with *XbaI* and transfected into ROP54 HA-tagged parasite lines. The parasites were selected with 1 μM pyrimethamine, and knockouts were cloned via limiting dilution and identified by lack of HA staining in IFA and Western blot assays. The knockouts for type I and type II ROP54 were designated clones Δ*rop54$_I$* and Δ*rop54$_{II}$* (48).

Complementation of *ROP54*. The endogenous locus of *ROP54* was PCR amplified with primers P7 and P8 from genomic DNA from the ROP54HA$_{II}$ strain. The PCR product contained the endogenous promoter, *ROP54* gene, 3×HA tag, and the *HXGPRT* 3′-untranslated region from the tagging construct. The amplicon was ligated into a complementation vector with the 3′ and 5′ flanks of the deleted *Ku80* locus and selectable marker *HXGPRT* (provided by Vern Carruthers, University of Michigan) (53). The plasmid was linearized with BssHII, transfected into the Δ*rop54$_{II}$* clone, and selected with MX medium. A ROP54 complement clone (ROP54c$_{II}$) was generated using limiting dilution, and complementation was assessed by IFA and Western blot analysis (48).

Macrophage clearance assay. For macrophage clearance assays, RAW 267.4 cells were seeded at 1 million cells per T25 flask and activated with 100 units/ml of IFN-γ (Millipore) and 10 ng/ml of lipopolysaccharide (LPS; Sigma). The ROP54HA$_{II}$, Δ*rop54$_{II}$*, and ROP54c$_{II}$ parasite strains were used to infect the RAW 267.4 cells at a multiplicity of infection (MOI) of 1 for 20 h, and the inoculum was confirmed via plaque assay. Total genomic DNA of each flask was isolated by using a DNA isolation kit (Promega). The amount of *Toxoplasma* and RAW 267.4 genomic DNA was quantified by qPCR (BioRad). *TgACT1* was amplified with primers P15 and P16, and BALB/c *actin* was amplified with primers P13 and P14, using 2× SYBR green stain (BioRad). The ΔC_T values were calculated based on the amount of *TgACT1* relative to BALB/c *actin* (36–38). The Δ*rop54$_{II}$* and ROP54c$_{II}$ values were then normalized to the value for ROP54HA$_{II}$ to determine DNA amounts of the strains relative to that in the parental parasite strain.

***In vitro* viability assay.** The *in vitro* viability assays, BMDMs were seeded at 1 million cells per T25 flask and activated as described above. The ROP54HA$_{II}$, Δ*rop54$_{II}$*, and ROP54c$_{II}$ parasite strains were used to infect the BMDMs at an MOI of 1 for 20 h. The inoculum was confirmed via plaque assay. Parasites were mechanically disrupted with syringe lysis via a 17-gauge needle syringe and used to infect HFF monolayers with serial dilutions. Plaques were enumerated at 10 days postinfection, and the average number of live parasites per milliliter was calculated. Averages of Δ*rop54$_{II}$* and ROP54c$_{II}$ parasite plaques were then normalized to the ROP54HA$_{II}$ values to determine the relative fold changes in plaques per milliliter between the parasite strains (38).

Plaque assays. HFF monolayers were seeded onto 24-well plates and allowed to grow to confluence for plaque assays. These host cells were infected with an inoculum of each parasite strain, and plaques were allowed to grow for 6 days for type I parasites and 10 days for type II parasites (54). Each well was fixed with ice-cold methanol for 5 min, and the areas of the individual plaques were measured using the Zen imaging program (Zeiss).

Western blot assay. Extracellular parasites were lysed in Laemmli sample buffer (50 mM Tris-HCl [pH 6.8], 10% glycerol, 2% SDS, 1% 2-mercaptoethanol, 0.1% bromophenol blue) and heated at 95°C for 5 min in preparation for the Western blot assays. Samples were then separated by SDS-PAGE and transferred to nitrocellulose membranes (Maine Manufacturing, LLC). Equivalent loading of protein in each well was confirmed by counting parasites and verified by staining with antibodies against a loading control protein (52).

Light microscopy and image processing. IFA and plaques assay results were visualized on an Axio Imager.Z1 fluorescence microscope (Zeiss) as previously described (55). Images were collected using the AxioCam MRm charge-coupled-device camera and Zeiss Zen imaging software. Image stacks were collected at *z*-increments by using the "optimal slice" tool of the imaging software. The highest-quality images from the stack were deconvolved by using a point-spread function to generate a maximum intensity projection (MIP) (52).

Semipermeabilization of host cell membranes for detection of ROPs on PVM. To detect ROPs on PVM via semipermeabilization, confluent monolayers of HFFs were seeded onto coverslips and infected with ROP54HA$_{II}$ parasites at the indicated time points. The samples were washed quickly with PBS and fixed in 4% formaldehyde (Polysciences) for 10 min at room temperature. The fixed coverslips were quenched with 100 mM glycine–PBS for 5 min at room temperature. The cells were permeabilized with

either 0.002% digitonin–PBS (made fresh for each experiment) for 2.5 min at 4°C or 0.01% saponin–PBS for 30 min at room temperature. The samples were placed in blocking buffer (10% fetal calf serum [FCS]–PBS) for 30 min at room temperature to prevent nonspecific binding of the antibodies. Primary antibodies were diluted in blocking buffer (1:300 for MAb HA.11 [Covance], 1:300 for pAb ROP5 [Sibley], 1:100,000 for mouse SAG1 [DG52], and 1:100,000 for rabbit pAb SAG1) and used to probe the coverslips at room temperature for 1 h. The secondary antibodies Alexa 488-conjugated goat anti-mouse and Alexa 594-conjugated goat anti-rabbit (Invitrogen) were diluted at 1:2,000 in blocking buffer and added to the samples for incubation for 1 h (27). The coverslips were mounted in Vectashield (Vector Labs.) or ProLong Gold (Molecular Probes) and viewed with an Axio Imager.Z1 fluorescence microscope (Zeiss).

***In vivo* virulence assays.** C57BJ/B6 mice (Jackson Laboratory) were injected i.p. with ROP54HA$_{II}$, Δ*rop54*$_{II}$, or ROP54c$_{II}$ parasites at doses of 500, 5,000, and 50,000 parasites (n = 4 mice/dose) (14). IFN-γR$^{-/-}$ mice were acquired from Jane Deng laboratory (UCLA) and i.p. injected with 5,000 parasites. Parasite viability from the injections was verified by plaque assay immediately after infecting the mice. Mice were carefully monitored for 21 days to observe for weight loss and in accordance with institutional guidelines approved by the UCLA Animal Research committee.

***In vivo* competition assay.** A mixed aliquot of ~60% Δ*rop54*$_{II}$ and ~40% ROP54HA$_{II}$ was made at a dose of 50,000 parasites. The mixed dose was i.p. injected into C57BJ/B6 mice, and the ratio of the mixed inoculum was confirmed by IFA. On days 4 and 7, the mice were sacrificed and peritoneal lavage samples were collected with wash buffer (1% FCS–5 mM EDTA in PBS). The cells collected from the lavage fluid were mechanically disrupted to liberate parasites. Confluent HFFs were infected with the parasites for 40 h. The coverslips were fixed and stained for IFA, and the ratios of ROP54HA$_{II}$ and Δ*rop54*$_{II}$ parasite vacuoles were determined. Spleens were also harvested on day 7 and homogenized in 1 ml of PBS. The homogenate was mechanically disrupted with sequential passage through 18-, 25-, and 27.5-gauge needles and used to infect a confluent monolayer of HFFs for 40 h. The monolayer was examined by IFA, and the numbers of ROP54HA$_{II}$ and Δ*rop54*$_{II}$ parasite vacuoles were determined.

Immunoprecipitation. For the immunoprecipitation assays, extracellular ROP54SF$_{II}$ parasites were harvested and lysed in 0.5% NP-40, 150 mM NaCl, and 1× protease inhibitor cocktail (Roche) on ice for 30 min. The lysate was centrifuged at 14,000 × *g* at 4°C for 20 min. The supernatant was incubated with streptactin beads (Iba) for 4 h at room temperature. The beads were washed and eluted with 10 mM desthiobiotin in lysis buffer (56). Ten percent of the eluate was used for Western blot analysis, and the remainder was analyzed by mass spectrometry.

Statistical analysis. All experiments with three or more independent experiments were analyzed using one-way analysis of variance (ANOVA) and the Student-Newman-Keuls method for pairwise analyses.

SUPPLEMENTAL MATERIAL

Supplemental material for this article may be found at http://dx.doi.org/10.1128/mSphere.00045-16.

Table S1, PDF file, 0.1 MB.
Table S2, PDF file, 0.04 MB.
Figure S1, TIF file, 13.7 MB.
Figure S2, TIF file, 10 MB.
Figure S3, TIF file, 8.2 MB.
Figure S4, TIF file, 6.5 MB.
Figure S5, TIF file, 2.2 MB.
Figure S6, TIF file, 6.9 MB.

ACKNOWLEDGMENTS

We acknowledge the following people for their generous gifts: Kenneth Bradley (immortalized macrophages), Steven Bensinger (BMDMs), David Sibley (anti-ROP5 antibodies), Jane Deng (IFN-γR$^{-/-}$ mice), Vern Carruthers (*Ku80* complementation vector), and Jorn Coers (anti-GBP2 antibody). We also thank Amy S. Huang for contributing toward preparing the manuscript. We extend deepest thanks to Jennifer Ngo for her contributions toward the *in vivo* studies.

This work was supported by NIH grant AI064616 to P.J.B. E.W.K. was supported by the Philip Whitcome Predoctoral Fellowship of the Molecular Biology Institute of UCLA.

FUNDING INFORMATION

This work, including the efforts of Peter J. Bradley, was funded by HHS | National Institutes of Health (NIH) (AI064616). This work, including the efforts of James A. Wohlschlegel, was funded by HHS | National Institutes of Health (NIH) (GM089778).

William D. Barshop was supported by the Ruth L. Kirschstein National Research Service (GM007185). Elliot W. Kim was supported by a Philip Whitcome Pre-Doctoral Fellowship.

REFERENCES

1. **Boothroyd JC, Grigg ME**. 2002. Population biology of Toxoplasma gondii and its relevance to human infection: do different strains cause different disease? Curr Opin Microbiol **5:**438–442. http://dx.doi.org/10.1016/S1369-5274(02)00349-1.
2. **Bradley PJ, Sibley LD**. 2007. Rhoptries: an arsenal of secreted virulence factors. Curr Opin Microbiol **10:**582–587. http://dx.doi.org/10.1016/j.mib.2007.09.013.
3. **Boothroyd JC, Dubremetz JF**. 2008. Kiss and spit: the dual roles of Toxoplasma rhoptries. Nat Rev Microbiol **6:**79–88. http://dx.doi.org/10.1038/nrmicro1800.
4. **Bradley PJ, Ward C, Cheng SJ, Alexander DL, Coller S, Coombs GH, Dunn JD, Ferguson DJ, Sanderson SJ, Wastling JM, Boothroyd JC**. 2005. Proteomic analysis of rhoptry organelles reveals many novel constituents for host-parasite interactions in Toxoplasma gondii. J Biol Chem **280:**34245–34258. http://dx.doi.org/10.1074/jbc.M504158200.
5. **Håkansson S, Charron AJ, Sibley LD**. 2001. Toxoplasma evacuoles: a two-step process of secretion and fusion forms the parasitophorous vacuole. EMBO J **20:**3132–3144. http://dx.doi.org/10.1093/emboj/20.12.3132.
6. **Butcher BA, Fox BA, Rommereim LM, Kim SG, Maurer KJ, Yarovinsky F, Herbert DR, Bzik DJ, Denkers EY**. 2011. Toxoplasma gondii rhoptry kinase ROP16 activates STAT3 and STAT6 resulting in cytokine inhibition and arginase-1-dependent growth control. PLoS Pathog **7:**e1002236. http://dx.doi.org/10.1371/journal.ppat.1002236.
7. **Yamamoto M, Standley DM, Takashima S, Saiga H, Okuyama M, Kayama H, Kubo E, Ito H, Takaura M, Matsuda T, Soldati-Favre D, Takeda K**. 2009. A single polymorphic amino acid on Toxoplasma gondii kinase ROP16 determines the direct and strain-specific activation of Stat3. J Exp Med **206:**2747–2760. http://dx.doi.org/10.1084/jem.20091703.
8. **Ong YC, Reese ML, Boothroyd JC**. 2010. Toxoplasma rhoptry protein 16 (ROP16) subverts host function by direct tyrosine phosphorylation of STAT6. J Biol Chem **285:**28731–28740. http://dx.doi.org/10.1074/jbc.M110.112359.
9. **Hunter CA, Sibley LD**. 2012. Modulation of innate immunity by Toxoplasma gondii virulence effectors. Nat Rev Microbiol **10:**766–778. http://dx.doi.org/10.1038/nrmicro2858.
10. **Etheridge RD, Alaganan A, Tang K, Lou HJ, Turk BE, Sibley LD**. 2014. The Toxoplasma pseudokinase ROP5 forms complexes with ROP18 and ROP17 kinases that synergize to control acute virulence in mice. Cell Host Microbe **15:**537–550. http://dx.doi.org/10.1016/j.chom.2014.04.002.
11. **Reese ML, Shah N, Boothroyd JC**. 2014. The Toxoplasma pseudokinase ROP5 is an allosteric inhibitor of the immunity-related GTPases. J Biol Chem **289:**27849–27858. http://dx.doi.org/10.1074/jbc.M114.567057.
12. **Reese ML, Zeiner GM, Saeij JP, Boothroyd JC, Boyle JP**. 2011. Polymorphic family of injected pseudokinases is paramount in Toxoplasma virulence. Proc Natl Acad Sci U S A **108:**9625–9630. http://dx.doi.org/10.1073/pnas.1015980108.
13. **Reese ML, Boothroyd JC**. 2009. A helical membrane-binding domain targets the Toxoplasma ROP2 family to the parasitophorous vacuole. Traffic **10:**1458–1470. http://dx.doi.org/10.1111/j.1600-0854.2009.00958.x.
14. **Behnke MS, Fentress SJ, Mashayekhi M, Li LX, Taylor GA, Sibley LD**. 2012. The polymorphic pseudokinase ROP5 controls virulence in Toxoplasma gondii by regulating the active kinase ROP18. PLoS Pathog **8:**e1002992. http://dx.doi.org/10.1371/journal.ppat.1002992.
15. **Fleckenstein MC, Reese ML, Könen-Waisman S, Boothroyd JC, Howard JC, Steinfeldt T**. 2012. A Toxoplasma gondii pseudokinase inhibits host IRG resistance proteins. PLoS Biol **10:**e1001358. http://dx.doi.org/10.1371/journal.pbio.1001358.
16. **Zhao Z, Fux B, Goodwin M, Dunay IR, Strong D, Miller BC, Cadwell K, Delgado MA, Ponpuak M, Green KG, Schmidt RE, Mizushima N, Deretic V, Sibley LD, Virgin HW**. 2008. Autophagosome-independent essential function for the autophagy protein Atg5 in cellular immunity to intracellular pathogens. Cell Host Microbe **4:**458–469. http://dx.doi.org/10.1016/j.chom.2008.10.003.
17. **Melo MB, Jensen KD, Saeij JP**. 2011. Toxoplasma gondii effectors are master regulators of the inflammatory response. Trends Parasitol **27:**487–495. http://dx.doi.org/10.1016/j.pt.2011.08.001.
18. **Pernas L, Boothroyd JC**. 2010. Association of host mitochondria with the parasitophorous vacuole during Toxoplasma infection is not dependent on rhoptry proteins ROP2/8. Int J Parasitol **40:**1367–1371. http://dx.doi.org/10.1016/j.ijpara.2010.07.002.
19. **Carey KL, Jongco AM, Kim K, Ward GE**. 2004. The Toxoplasma gondii rhoptry protein ROP4 is secreted into the parasitophorous vacuole and becomes phosphorylated in infected cells. Eukaryot Cell **3:**1320–1330. http://dx.doi.org/10.1128/EC.3.5.1320-1330.2004.
20. **Yarovinsky F**. 2014. Innate immunity to Toxoplasma gondii infection. Nat Rev Immunol **14:**109–121. http://dx.doi.org/10.1038/nri3598.
21. **Niedelman W, Gold DA, Rosowski EE, Sprokholt JK, Lim D, Farid Arenas A, Melo MB, Spooner E, Yaffe MB, Saeij JP**. 2012. The rhoptry proteins ROP18 and ROP5 mediate Toxoplasma gondii evasion of the murine, but not the human, interferon-gamma response. PLoS Pathog **8:**e1002784. http://dx.doi.org/10.1371/journal.ppat.1002784.
22. **Degrandi D, Konermann C, Beuter-Gunia C, Kresse A, Würthner J, Kurig S, Beer S, Pfeffer K**. 2007. Extensive characterization of IFN-induced GTPases mGBP1 to mGBP10 involved in host defense. J Immunol **179:**7729–7740. http://dx.doi.org/10.4049/jimmunol.179.11.7729.
23. **Yamamoto M, Okuyama M, Ma JS, Kimura T, Kamiyama N, Saiga H, Ohshima J, Sasai M, Kayama H, Okamoto T, Huang DC, Soldati-Favre D, Horie K, Takeda J, Takeda K**. 2012. A cluster of interferon-gamma-inducible p65 GTPases plays a critical role in host defense against Toxoplasma gondii. Immunity **37:**302–313. http://dx.doi.org/10.1016/j.immuni.2012.06.009.
24. **Selleck EM, Fentress SJ, Beatty WL, Degrandi D, Pfeffer K, Virgin HW, IV, Macmicking JD, Sibley LD**. 2013. Guanylate binding protein 1 (Gbp1) contributes to cell-autonomous immunity against Toxoplasma gondii. PLoS Pathog **9:**e1003320. http://dx.doi.org/10.1371/journal.ppat.1003320.
25. **Degrandi D, Kravets E, Konermann C, Beuter-Gunia C, Klümpers V, Lahme S, Wischmann E, Mausberg AK, Beer-Hammer S, Pfeffer K**. 2013. Murine guanylate binding protein 2 (mGBP2) controls Toxoplasma gondii replication. Proc Natl Acad Sci U S A **110:**294–299. http://dx.doi.org/10.1073/pnas.1205635110.
26. **Reese ML, Boothroyd JC**. 2011. A conserved non-canonical motif in the pseudoactive site of the ROP5 pseudokinase domain mediates its effect on Toxoplasma virulence. J Biol Chem **286:**29366–29375. http://dx.doi.org/10.1074/jbc.M111.253435.
27. **Alaganan A, Fentress SJ, Tang K, Wang Q, Sibley LD**. 2014. Toxoplasma GRA7 effector increases turnover of immunity-related GTPases and contributes to acute virulence in the mouse. Proc Natl Acad Sci U S A **111:**1126–1131. http://dx.doi.org/10.1073/pnas.1313501111.
28. **Behnke MS, Wootton JC, Lehmann MM, Radke JB, Lucas O, Nawas J, Sibley LD, White MW**. 2010. Coordinated progression through two subtranscriptomes underlies the tachyzoite cycle of Toxoplasma gondii. PLoS One **5:**e12354. http://dx.doi.org/10.1371/journal.pone.0012354.
29. **Altschul SF, Gish W, Miller W, Myers EW, Lipman DJ**. 1990. Basic local alignment search tool. J Mol Biol **215:**403–410. http://dx.doi.org/10.1016/S0022-2836(05)80360-2.
30. **Boratyn GM, Schäffer AA, Agarwala R, Altschul SF, Lipman DJ, Madden TL**. 2012. Domain enhanced lookup time accelerated BLAST. Biol Direct **7:**12. http://dx.doi.org/10.1186/1745-6150-7-12.
31. **Kelley LA, Mezulis S, Yates CM, Wass MN, Sternberg MJ**. 2015. The Phyre2 web portal for protein modeling, prediction and analysis. Nat Protoc **10:**845–858. http://dx.doi.org/10.1038/nprot.2015.053.
32. **El Hajj H, Lebrun M, Arold ST, Vial H, Labesse G, Dubremetz JF**. 2007. ROP18 is a rhoptry kinase controlling the intracellular proliferation of Toxoplasma gondii. PLoS Pathog **3:**e14. http://dx.doi.org/10.1371/journal.ppat.0030014.
33. **Turetzky JM, Chu DK, Hajagos BE, Bradley PJ**. 2010. Processing and secretion of ROP13: a unique Toxoplasma effector protein. Int J Parasitol **40:**1037–1044. http://dx.doi.org/10.1016/j.ijpara.2010.02.014.
34. **Sinai AP, Joiner KA**. 2001. The Toxoplasma gondii protein ROP2 mediates host organelle association with the parasitophorous vacuole membrane. J Cell Biol **154:**95–108. http://dx.doi.org/10.1083/jcb.200101073.
35. **Hou B, Benson A, Kuzmich L, DeFranco AL, Yarovinsky F**. 2011. Critical coordination of innate immune defense against Toxoplasma gondii by dendritic cells responding via their Toll-like receptors. Proc Natl Acad Sci U S A **108:**278–283. http://dx.doi.org/10.1073/pnas.1011549108.
36. **Wheelwright M, Kim EW, Inkeles MS, De Leon A, Pellegrini M,**

Krutzik SR, Liu PT. 2014. All-trans retinoic acid-triggered antimicrobial activity against Mycobacterium tuberculosis is dependent on NPC2. J Immunol **192:**2280–2290. http://dx.doi.org/10.4049/jimmunol.1301686.

37. **Liu PT, Wheelwright M, Teles R, Komisopoulou E, Edfeldt K, Ferguson B, Mehta MD, Vazirnia A, Rea TH, Sarno EN, Graeber TG, Modlin RL**. 2012. MicroRNA-21 targets the vitamin D-dependent antimicrobial pathway in leprosy. Nat Med **18:**267–273. http://dx.doi.org/10.1038/nm.2584.
38. **Haldar AK, Foltz C, Finethy R, Piro AS, Feeley EM, Pilla-Moffett DM, Komatsu M, Frickel EM, Coers J**. 2015. Ubiquitin systems mark pathogen-containing vacuoles as targets for host defense by guanylate binding proteins. Proc Natl Acad Sci U S A **112:**E5628–E5637. http://dx.doi.org/10.1073/pnas.1515966112.
39. **Fentress SJ, Behnke MS, Dunay IR, Mashayekhi M, Rommereim LM, Fox BA, Bzik DJ, Taylor GA, Turk BE, Lichti CF, Townsend RR, Qiu W, Hui R, Beatty WL, Sibley LD**. 2010. Phosphorylation of immunity-related GTPases by a Toxoplasma gondii-secreted kinase promotes macrophage survival and virulence. Cell Host Microbe **8:**484–495. http://dx.doi.org/10.1016/j.chom.2010.11.005.
40. **Leriche MA, Dubremetz JF**. 1991. Characterization of the protein contents of rhoptries and dense granules of Toxoplasma gondii tachyzoites by subcellular fractionation and monoclonal antibodies. Mol Biochem Parasitol **45:**249–259. http://dx.doi.org/10.1016/0166-6851(91)90092-K.
41. **Peixoto L, Chen F, Harb OS, Davis PH, Beiting DP, Brownback CS, Ouloguem D, Roos DS**. 2010. Integrative genomic approaches highlight a family of parasite-specific kinases that regulate host responses. Cell Host Microbe **8:**208–218. http://dx.doi.org/10.1016/j.chom.2010.07.004.
42. **Beck JR, Fung C, Straub KW, Coppens I, Vashisht AA, Wohlschlegel JA, Bradley PJ**. 2013. A Toxoplasma palmitoyl acyl transferase and the palmitoylated armadillo repeat protein TgARO govern apical rhoptry tethering and reveal a critical role for the rhoptries in host cell invasion but not egress. PLoS Pathog **9:**e1003162. http://dx.doi.org/10.1371/journal.ppat.1003162.
43. **Lagal V, Binder EM, Huynh MH, Kafsack BF, Harris PK, Diez R, Chen D, Cole RN, Carruthers VB, Kim K**. 2010. Toxoplasma gondii protease TgSUB1 is required for cell surface processing of microneme adhesive complexes and efficient adhesion of tachyzoites. Cell Microbiol **12:**1792–1808. http://dx.doi.org/10.1111/j.1462-5822.2010.01509.x.
44. **Miller SA, Thathy V, Ajioka JW, Blackman MJ, Kim K**. 2003. TgSUB2 is a Toxoplasma gondii rhoptry organelle processing proteinase. Mol Microbiol **49:**883–894. http://dx.doi.org/10.1046/j.1365-2958.2003.03604.x.
45. **Martinez FO, Gordon S, Locati M, Mantovani A**. 2006. Transcriptional profiling of the human monocyte-to-macrophage differentiation and polarization: new molecules and patterns of gene expression. J Immunol **177:**7303–7311. http://dx.doi.org/10.4049/jimmunol.177.10.7303.
46. **Lilue J, Müller UB, Steinfeldt T, Howard JC**. 2013. Reciprocal virulence and resistance polymorphism in the relationship between Toxoplasma gondii and the house mouse. Elife **2:**e01298. http://dx.doi.org/10.7554/eLife.01298.
47. **Huynh MH, Carruthers VB**. 2009. Tagging of endogenous genes in a Toxoplasma gondii strain lacking Ku80. Eukaryot Cell **8:**530–539. http://dx.doi.org/10.1128/EC.00358-08.
48. **Straub KW, Peng ED, Hajagos BE, Tyler JS, Bradley PJ**. 2011. The moving junction protein RON8 facilitates firm attachment and host cell invasion in Toxoplasma gondii. PLoS Pathog **7:**e1002007. http://dx.doi.org/10.1371/journal.ppat.1002007.
49. **Haldar AK, Saka HA, Piro AS, Dunn JD, Henry SC, Taylor GA, Frickel EM, Valdivia RH, Coers J**. 2013. IRG and GBP host resistance factors target aberrant, "non-self" vacuoles characterized by the missing of "self" IRGM proteins. PLoS Pathog **9:**e1003414. http://dx.doi.org/10.1371/journal.ppat.1003414.
50. **Kim K, Bülow R, Kampmeier J, Boothroyd JC**. 1994. Conformationally appropriate expression of the Toxoplasma antigen SAG1 (p30) in CHO cells. Infect Immun **62:**203–209. PubMed.
51. **Donald RG, Roos DS**. 1998. Gene knockouts and allelic replacements in Toxoplasma gondii: HXGPRT as a selectable marker for hit-and-run mutagenesis. Mol Biochem Parasitol **91:**295–305. http://dx.doi.org/10.1016/S0166-6851(97)00210-7.
52. **Beck JR, Chen AL, Kim EW, Bradley PJ**. 2014. RON5 is critical for organization and function of the Toxoplasma moving junction complex. PLoS Pathog **10:**e1004025. http://dx.doi.org/10.1371/journal.ppat.1004025.
53. **Huynh MH, Boulanger MJ, Carruthers VB**. 2014. A conserved apicomplexan microneme protein contributes to Toxoplasma gondii invasion and virulence. Infect Immun **82:**4358–4368. http://dx.doi.org/10.1128/IAI.01877-14.
54. **Hammoudi PM, Jacot D, Mueller C, Di Cristina M, Dogga SK, Marq JB, Romano J, Tosetti N, Dubrot J, Emre Y, Lunghi M, Coppens I, Yamamoto M, Sojka D, Pino P, Soldati-Favre D**. 2015. Fundamental roles of the Golgi-associated Toxoplasma aspartyl protease, ASP5, at the host-parasite interface. PLoS Pathog **11:**e1005211. http://dx.doi.org/10.1371/journal.ppat.1005211.
55. **Beck JR, Rodriguez-Fernandez IA, de Leon JC, Huynh MH, Carruthers VB, Morrissette NS, Bradley PJ**. 2010. A novel family of Toxoplasma IMC proteins displays a hierarchical organization and functions in coordinating parasite division. PLoS Pathog **6:**e1001094. http://dx.doi.org/10.1371/journal.ppat.1001094.
56. **Chen AL, Kim EW, Toh JY, Vashisht AA, Rashoff AQ, Van C, Huang AS, Moon AS, Bell HN, Bentolila LA, Wohlschlegel JA, Bradley PJ**. 2015. Novel components of the Toxoplasma inner membrane complex revealed by BioID. mBio **6:**e02357-02314. http://dx.doi.org/10.1128/mBio.02357-14.

CHAPTER 5

Summary

This dissertation addresses the host-pathogen interactions between the innate immune system of the host and the evasion mechanisms of *Toxoplasma gondii*. From these interactions we have gained insight into the molecular mechanisms by which the innate immune system utilizes to clear microbes from the host. The MΦ is a sentinel of the innate immune system that serves as the first line of host defense during the early stages of infection. Here, we have found that micronutrients contribute to the antimicrobial response of MΦ against mycobacteria. Additionally, we have discovered a novel rhoptry pseudokinase that modulates *Toxoplasma* virulence and evades MΦ clearance by GBP2. Collectively these studies provide insight into the host-pathogen interactions upon the onset of infection, which may help develop novel therapeutics against harmful pathogens.

Previous studies from our laboratory demonstrate that TLR2/1 activation leads to indirect and direct effector pathways by the innate immune system [1,2]. From these immune models we found that primary human monocytes treated with IL-15 differentiate into MΦ that express a vitamin D-dependent antimicrobial pathway against mycobacteria [3]. This specialized MΦ subset has been identified in T-lep lesions, the resistant form of leprosy disease [4]. A caveat from these previous studies is that the IL-15 MΦ was differentiated in vitamin D deficient conditions. Therefore, in Chapter 1 we address how the physiological levels of vitamin D during MΦ differentiation affect phenotype and function. We were interested in how vitamin D status contributed to the immune response prior to the onset of infection because previous reports have demonstrated that vitamin D supplementation to active TB patients had been largely unsuccessful [5,6]. We show that 25D3 status does not alter the phenotype or phagocytic function of IL-15 MΦ,

but armed the MΦ with cathelicidin. Upon microbial challenge, the IL-15 MΦ that were differentiated in the presence of 25D3 demonstrated a powerful antimicrobial response against *M. leprae*. These data suggests that other vitamin D-dependent antimicrobial mechanisms such as autophagy [7], expression of antimicrobial peptides [8,9] (e.g defb4) and inhibition of mycobacteria evasion mechanisms [10,11] may also contribute to the antimicrobial response against *M. tuberculosis*. Taken together, these studies indicate that host vitamin D status is critical to the direct effector function of antimicrobial MΦ.

Due to the lack of an accessible experimental animal model that recapitulates the human immune response and pathogenesis of mycobacterial-mediated diseases, it is difficult to assess the human immune response against *M. tuberculosis* infection in the lung. However, several reports have demonstrated that MΦ packed with high lipid content are associated with the pathogenesis in *M. tuberculosis* [12]. Previous studies from our laboratory demonstrate that ATRA triggers a lipid efflux pathway in monocytes and MΦ, which contributes to the antimicrobial response against *M. tuberculosis in vitro* [13]. ATRA has also been documented to induce several different types immune responses against *M. tuberculosis* such as induce MΦ differentiation [14], sustain granuloma formation [15] and increase phagolysosomal fusion [10]. However, ATRA is the bioactive form of vitamin A, and active TB patients present low sera levels of retinol. These data collectively suggest that retinol must be converted into ATRA in the lung to trigger an antimicrobial response against *M. tuberculosis*.

Active TB patients present low retinol sera levels relative to household contacts [16,17], but *in vitro* studies demonstrate that ATRA triggers direct antimicrobial effects against *M. tuberculosis* [10,13,18]. Therefore, understanding the mechanism by which the

immune system converts retinol to ATRA at the site of infection is critical in understanding how retinol levels influence the immune response against *M. tuberculosis.* We investigated vitamin A metabolism in innate immune subsets in Chapter 2 and found that GM-DCs are the cellular source of retinol bioconversion. The classical function of dendritic cells is to activate the adaptive immune system, but our data provides evidence that transcellular metabolism of retinol by DCs leads to the release of ATRA and triggers an antimicrobial response against *M. tuberculosis* monocytes and MΦ. Transcellular metabolism has also been characterized in monocytes and alveolar MΦ that contain a class of enzymes cyclo-oxygenases (COX), which produce prostaglandin from arachidonic acid (AA) [19,20]. Interestingly, MΦ treated with AA demonstrated a reduced the pH in phagolysosomes containing *M. tuberculosis* and a decrease in bacterial viability [21]. However, during the late stages of TB disease increased levels of prostaglandin and COX-2 protein levels were detected in the lung [22]. Collectively, these studies suggest that understanding the link between lipids and micronutrient transcellular metabolism pathways and how they contribute to resistance or susceptibility to TB disease will warrant further investigation.

The transcellular retinol metabolism pathway by GM-DCs is an *in vitro* immune model that was assessed in the lung of active TB patients. Our data demonstrates that GM-DCs depend on the enzymatic activity of ALDH1A2 to produce ATRA and activate neighboring cells. Microarray analysis and immunohistochemistry data reveal that the mRNA and protein expression levels of ALDH1A2 and CD1b are significantly lower in TB lung tissues compared to normal lung. These observations indicate that DC-mediated vitamin A metabolism is absent in the lung, which implies that ATRA triggered immune

responses against *M. tuberculosis* are attenuated at the site of disease. These results highlight the importance of retinol activation at the site of TB disease and provide a potential mechanism by which retinol supplementation in active TB patients has been unsuccessful [23]. Novel therapeutics that promote retinol metabolism in the lung of active TB patients will support vitamin A adjuvant therapy. Furthermore, given that normal lungs expresses the vitamin A metabolism pathway, retinol supplementation to uninfected and vitamin A deficient individuals that are exposed to active TB patients could be a potential strategy that prevents the spread of disease. Successful containment of the disease may allow for resources to be allocated to the areas that demonstrate the highest rates of TB burden and decrease TB incidence.

Sufficient micronutrient levels are essential to sustaining a fully functional immune system, which protect the host from the onset of microbial infection. However, disease causing microbes have evolved immune evasion mechanisms that block direct effector pathways of the immune system, which promote the survival of the pathogen [24,25]. To understand the mechanisms of evasion against the immune system we studied the parasite *T. gondii*. The rhoptries are secretory organelles that inject effector proteins into the host cell to invade and co-opt host cell functions. There are ~40 pseudokinases and kinases in the ROP effector family, but their functions remain largely unknown. In Chapter 3, we have found a novel rhoptry pseudokinase effector protein, ROP54, which is injected into the host cell upon invasion and traffics to the cytoplasmic face of the parasitophorous vacuole membrane (PVM). Originally, ROP54 was annotated to be a RNA-helicase in the *Toxoplasma* database, but other protein prediction tools suggest that ROP54 is a potential pseudokinase. This observation peaked our interest because

previous studies have demonstrated that peudokinase effector proteins of *Toxoplasma* play a significant role in virulence [26-28]. ROP5 is a known pseudokinase effector protein that also localizes to the PVM and forms a complex with ROP17 and ROP18 to evade clearance from immunity-repated GTPase B6 (IRGB6). During the early stages of infection ROP54 localized to fewer PVM relative to ROP5. At 12 hours post infection ROP54 was detected at similar amounts as ROP5 on the PVM. Additionally, immunoprecipitation of ROP54 revealed that the pseudokinase does not form a complex with ROP5/17/18. These data collectively suggests that ROP54 is a novel rhoptry effector protein that localizes to the PVM, which functions independently from the ROP5/17/18 complex.

Although ROP54 functions independently from the ROP5/17/18 complex, both ROP5 and ROP54 are pseudokinases that localize to the PVM. Since ROP5 has been described as an essential virulence factor of *T. gondii*, we investigated how ROP54 contributed to the virulence of *T. gondii*. Our results show that disruption of ROP54 in type II parasites (Δ*rop54*) did not affect growth *in vitro,* but demonstrated a 100-fold decrease in virulence *in vivo.* Previous studies demonstrate that MΦ and inflammatory monocytes are critical to the clearance of *Toxoplasma* from mice *in vivo* [29]. In addition, the pro-inflammatory cytokine IL-12 and IFN-gamma are critical to the clearance of the parasite in mice [30]. Therefore, we investigated an effector pathway of IFN-gamma activated MΦ in Δ*rop54* parasites. We observed a significant increase of GBP2 loading onto the parasitophorous vacuole (PV) of Δ*rop54* parasites relative to control parasite strains, which suggests that ROP54 plays a role in evading GBP2-mediated clearance. Collectively, these results demonstrate that ROP54 is a pseudokinase effector protein that

promotes virulence by modulating GBP2 loading onto the PVM. Novel therapies that inhibit the immune evasion function of ROP54 could provide an optimal treatment against toxoplasmosis.

In summary, the work in this dissertation describes the host-pathogen interactions between the MΦ and deleterious microbes. Our data shows that the presence of sufficient levels of 25D3 prior to microbial infection contributes to the effective clearance of pathogens in vitamin D-dependent antimicrobial MΦ. This study supports future clinical studies that study the relationship between vitamin D supplementation to the susceptibility to microbial infection and disease. Also, we found that GM-DCs are the cellular source that links host retinol levels to ATRA production at the site of disease. GM-DCs activate retinol and release ATRA, which triggers an antimicrobial response against *M. tuberculosis* in monocytes and MΦ. From this *in vitro* model we demonstrate that transcellular metabolism of vitamin A by DCs is absent in the lung of active TB patients. These data collectively provide insight into TB disease and how transcellular metabolism of vitamin A may be critical to the host defense against *M. tuberculosis* infection at the site of disease. Finally, we identified a novel rhoptry effector protein that modulates GBP2 loading to increase *Toxoplasma* virulence. Further studies that investigate host-pathogen interactions can lead to the discovery of novel drug targets and therapeutic strategies.

References

1 Krutzik, S. R. *et al.* TLR activation triggers the rapid differentiation of monocytes into macrophages and dendritic cells. *Nat Med* **11**, 653-660, doi:10.1038/nm1246 (2005).

2 Liu, P. T. *et al.* Toll-like receptor triggering of a vitamin D-mediated human antimicrobial response. *Science* **311**, 1770-1773, doi:10.1126/science.1123933 (2006).

3 Krutzik, S. R. *et al.* IL-15 links TLR2/1-induced macrophage differentiation to the vitamin D-dependent antimicrobial pathway. *J Immunol* **181**, 7115-7120 (2008).

4 Montoya, D. *et al.* Divergence of macrophage phagocytic and antimicrobial programs in leprosy. *Cell Host Microbe* **6**, 343-353, doi:10.1016/j.chom.2009.09.002 (2009).

5 Martineau, A. R. *et al.* A single dose of vitamin D enhances immunity to mycobacteria. *Am J Respir Crit Care Med* **176**, 208-213, doi:10.1164/rccm.200701-007OC (2007).

6 Daley, P. *et al.* Adjunctive vitamin D for treatment of active tuberculosis in India: a randomised, double-blind, placebo-controlled trial. *Lancet Infect Dis* **15**, 528-534, doi:10.1016/S1473-3099(15)70053-8 (2015).

7 Fabri, M. *et al.* Vitamin D is required for IFN-gamma-mediated antimicrobial activity of human macrophages. *Sci Transl Med* **3**, 104ra102, doi:10.1126/scitranslmed.3003045 (2011).

8 Liu, P. T. *et al.* Convergence of IL-1beta and VDR activation pathways in human TLR2/1-induced antimicrobial responses. *PLoS One* **4**, e5810, doi:10.1371/journal.pone.0005810 (2009).

9 Liu, P. T., Stenger, S., Tang, D. H. & Modlin, R. L. Cutting edge: vitamin D-mediated human antimicrobial activity against Mycobacterium tuberculosis is dependent on the induction of cathelicidin. *J Immunol* **179**, 2060-2063 (2007).

10 Anand, P. K. & Kaul, D. Downregulation of TACO gene transcription restricts mycobacterial entry/survival within human macrophages. *FEMS Microbiol Lett* **250**, 137-144, doi:10.1016/j.femsle.2005.06.056 (2005).

11 Anand, P. K. & Kaul, D. Vitamin D3-dependent pathway regulates TACO gene transcription. *Biochem Biophys Res Commun* **310**, 876-877 (2003).

12 Russell, D. G., Cardona, P. J., Kim, M. J., Allain, S. & Altare, F. Foamy macrophages and the progression of the human tuberculosis granuloma. *Nat Immunol* **10**, 943-948, doi:10.1038/ni.1781 (2009).

13 Wheelwright, M. *et al.* All-trans retinoic acid-triggered antimicrobial activity against Mycobacterium tuberculosis is dependent on NPC2. *J Immunol* **192**, 2280-2290, doi:10.4049/jimmunol.1301686 (2014).

14 Liu, P. T. *et al.* CD209(+) macrophages mediate host defense against Propionibacterium acnes. *J Immunol* **180**, 4919-4923 (2008).

15 Gundra, U. M. *et al.* Vitamin A mediates conversion of monocyte-derived macrophages into tissue-resident macrophages during alternative activation. *Nat Immunol* **18**, 642-653, doi:10.1038/ni.3734 (2017).

16 Mugusi, F. M., Rusizoka, O., Habib, N. & Fawzi, W. Vitamin A status of patients presenting with pulmonary tuberculosis and asymptomatic HIV-infected individuals, Dar es Salaam, Tanzania. *Int J Tuberc Lung Dis* **7**, 804-807 (2003).

17 Ramachandran, G. *et al.* Vitamin A levels in sputum-positive pulmonary tuberculosis patients in comparison with household contacts and healthy 'normals'. *Int J Tuberc Lung Dis* **8**, 1130-1133 (2004).

18 Crowle, A. J. & Ross, E. J. Inhibition by retinoic acid of multiplication of virulent tubercle bacilli in cultured human macrophages. *Infect Immun* **57**, 840-844 (1989).

19 Serhan, C. N., Haeggstrom, J. Z. & Leslie, C. C. Lipid mediator networks in cell signaling: update and impact of cytokines. *FASEB J* **10**, 1147-1158 (1996).

20 Bigby, T. D. & Meslier, N. Transcellular lipoxygenase metabolism between monocytes and platelets. *J Immunol* **143**, 1948-1954 (1989).

21 Anes, E. *et al.* Selected lipids activate phagosome actin assembly and maturation resulting in killing of pathogenic mycobacteria. *Nat Cell Biol* **5**, 793-802, doi:10.1038/ncb1036 (2003).

22 Rangel Moreno, J. *et al.* The role of prostaglandin E2 in the immunopathogenesis of experimental pulmonary tuberculosis. *Immunology* **106**, 257-266 (2002).

23 Pakasi, T. A. *et al.* Zinc and vitamin A supplementation fails to reduce sputum conversion time in severely malnourished pulmonary tuberculosis patients in Indonesia. *Nutr J* **9**, 41, doi:10.1186/1475-2891-9-41 (2010).

24 Liu, P. T. *et al.* MicroRNA-21 targets the vitamin D-dependent antimicrobial pathway in leprosy. *Nat Med* **18**, 267-273, doi:10.1038/nm.2584 (2012).

25 Teles, R. M. *et al.* Type I interferon suppresses type II interferon-triggered human anti-mycobacterial responses. *Science* **339**, 1448-1453, doi:10.1126/science.1233665 (2013).

26 Behnke, M. S. *et al.* The polymorphic pseudokinase ROP5 controls virulence in Toxoplasma gondii by regulating the active kinase ROP18. *PLoS Pathog* **8**, e1002992, doi:10.1371/journal.ppat.1002992 (2012).

27 Reese, M. L. & Boothroyd, J. C. A conserved non-canonical motif in the pseudoactive site of the ROP5 pseudokinase domain mediates its effect on Toxoplasma virulence. *J Biol Chem* **286**, 29366-29375, doi:10.1074/jbc.M111.253435 (2011).

28 Reese, M. L., Zeiner, G. M., Saeij, J. P., Boothroyd, J. C. & Boyle, J. P. Polymorphic family of injected pseudokinases is paramount in Toxoplasma virulence. *Proc Natl Acad Sci U S A* **108**, 9625-9630, doi:10.1073/pnas.1015980108 (2011).

29 Dunay, I. R. *et al.* Gr1(+) inflammatory monocytes are required for mucosal resistance to the pathogen Toxoplasma gondii. *Immunity* **29**, 306-317, doi:10.1016/j.immuni.2008.05.019 (2008).

30 Gazzinelli, R. T. *et al.* Parasite-induced IL-12 stimulates early IFN-gamma synthesis and resistance during acute infection with Toxoplasma gondii. *J Immunol* **153**, 2533-2543 (1994).